General Disclaimer

One or more of the Following Statements may affect this Document

- This document has been reproduced from the best copy furnished by the organizational source. It is being released in the interest of making available as much information as possible.

- This document may contain data, which exceeds the sheet parameters. It was furnished in this condition by the organizational source and is the best copy available.

- This document may contain tone-on-tone or color graphs, charts and/or pictures, which have been reproduced in black and white.

- This document is paginated as submitted by the original source.

- Portions of this document are not fully legible due to the historical nature of some of the material. However, it is the best reproduction available from the original submission.

NASA CR-135025
BBN Report No. 3174

HARDWALL ACOUSTICAL CHARACTERISTICS AND MEASUREMENT CAPABILITIES OF THE NASA LEWIS 9 x 15 FOOT LOW SPEED WIND TUNNEL

by Peter E. Rentz

BOLT BERANEK AND NEWMAN INC.

prepared for

NATIONAL AERONAUTICS AND SPACE ADMINISTRATION

NASA Lewis Research Center
Contract NAS3-19410

1. Report No.	2. Government Accession No.	3. Recipient's Catalog No.
NASA CR-135025		

4. Title and Subtitle	5. Report Date
Hardwall Acoustical Characteristics and Measurement Capabilities of the NASA Lewis 9 x 15 Foot Low Speed Wind Tunnel	June 1976
	6. Performing Organization Code
7. Author(s)	8. Performing Organization Report No.
Peter E. Rentz	3174
	10. Work Unit No.
9. Performing Organization Name and Address	11. Contract or Grant No.
Bolt Beranek and Newman Inc. 21120 Vanowen Street Canoga Park, California 91303	NAS3-19410
	13. Type of Report and Period Covered
12. Sponsoring Agency Name and Address	Contractor Report
National Aeronautics and Space Administration Washington, D. C. 20546	14. Sponsoring Agency Code

15. Supplementary Notes

Project Manager, James A. Diedrich
NASA Lewis Research Center, Cleveland, Ohio

16. Abstract

Experimental evaluations of the acoustical characteristics and source sound power and directionality measurement capabilities of the NASA Lewis 9 x 15 foot low speed wind tunnel in the untreated or hardwall configuration were performed.

The results indicated that source sound power estimates can be made using only settling chamber sound pressure measurements. The accuracy of these estimates, expressed as one standard deviation, can be improved from $\pm$ 4 dB to $\pm$ 1 dB if sound pressure measurements in the preparation room and diffuser are also used and source directivity information is utilized. A simple procedure is presented.

Acceptably accurate measurements of source direct field acoustic radiation were found to be limited by the test section reverberant characteristics to 3.0 feet for omni-directional and highly directional sources. The standard deviation of the measurement reproducibility ranged from 0.6 to 1.7 dB. The source measurement accuracy ranged from - 1.5 to 3.4 dB, but may be due in part to source strength variation.

Wind-on noise measurements in the test section, settling chamber and preparation room were found to depend on the sixth power of tunnel velocity. The levels were compared with various analytic models and it was concluded that:

1. Sound pressure levels measured by test section microphones are due to true acoustic levels, not turbulence induced pseudo-noise.
2. The most likely area of significant noise generation is the transition from the test section to the diffuser.

Numerous procedural recommendations are set forth.

17. Key Words (Suggested by Author(s))	18. Distribution Statement
Acoustic Measurement Wind Tunnel	Unclassified - Unlimited

19. Security Classif. (of this report)	20. Security Classif. (of this page)	21. No. of Pages	22. Price*
Unclassified	Unclassified	99	

* For sale by the National Technical Information Service, Springfield, Virginia 22161

TABLE OF CONTENTS

LIST OF TABLES

LIST OF TABLES (Cont'd)

LIST OF FIGURES

LIST OF FIGURES (Cont'd)

LIST OF FIGURES (Cont'd)

1.0 SUMMARY

Experimental evaluations of the acoustical characteristics and source sound power and directionality measurement capabilities of the NASA Lewis 9 x 15 foot low speed wind tunnel in the untreated or hardwall configuration were performed.

The results indicated that source sound power estimates can be made using only settling chamber sound pressure measurements. The accuracy of these estimates, expressed as one standard deviation, can be improved from $\pm$ 4 dB to $\pm$ 1 dB if sound pressure measurements in the preparation room and diffuser are also used and source directivity information is utilized. A simple procedure is presented.

Acceptably accurate measurements of source direct field acoustic radiation were found to be limited by the test section reverberant characteristics to 3.0 feet for omni-directional and highly directional sources. The standard deviation of the measurement reproducibility ranged from 0.6 to 1.7 dB. The source measurement accuracy ranged from - 1.5 to 3.4 dB, but may be due in part to source strength variation.

Wind-on noise measurements in the test section, settling chamber and preparation room were found to depend on the sixth power of tunnel velocity. The levels were compared with various analytic models and it was concluded that:

1. Sound pressure levels measured by test section microphones are due to true acoustic levels, not turbulence induced pseudo-noise.

2. The most likely area of significant noise generation is the transition from the test section to the diffuser.

Numerous procedural recommendations are set forth.

2.0 INTRODUCTION

The 9 x 15 foot low speed wind tunnel at the NASA Lewis Research Center (LeRC), Cleveland, Ohio (1)*, has been adapted for measurement of the acoustic performance of model propulsion systems. The purpose of the effort reported herein is to evaluate the resulting acoustic measurement capabilities.

2.1 Wind Tunnel Description

The 9 x 15 foot wind tunnel at the NASA Lewis Research Center, Cleveland, Ohio, was built in the return leg of the 8 x 6 foot supersonic wind tunnel, Figure 1 (1). Prior to construction of the subsonic 9 x 15 foot test section, the 8 x 6 foot facility had received acoustic treatment downstream of the test section for the purpose of community noise abatement. The treatment consists of low frequency Helmholtz resonators, a lined duct muffler, wall treatment and acoustic baffles. As a result, noise propagating downstream from the supersonic test section is low relative to community noise standards (2), and subsequently does not affect acoustic measurements in the 9 x 15 foot low speed wind tunnel.

Other aspects of the construction of the facility which relate to acoustic measurement are the presence of flow regulation doors upstream and downstream of the 9 x 15 foot test section, a cooler screen upstream of the settling chamber, and dryer beds between the diffuser leg and the drive fan, Figure 1.

---

*Numbers in parentheses indicate references listed.

The test section is constructed of steel with wood lining on the side walls. The side walls also have four inch slots running the length of the test section, 27 ft (8.2m). Acoustically, the slots provide a window of 67 ft^2 (6.2m^2) between the test section and the surrounding preparation room.

The tunnel flow is induced by a seven stage axial flow compressor. Operation of the 9 x 15 foot low speed wind tunnel is usually conducted at a standard compressor rotational speed which ranges from 800 to 820 rpm. The desired tunnel flow is achieved with the flow control doors. The compressor first stage has 52 blades, preceded by an array of 72 guide vanes. The final stage rotor has 60 blades. This stage is preceded by 66 stator blades and followed by 84 exit blades.

2.2 Acoustic Measurement Approaches

In the hardwall or untreated configuration the approach to acoustic measurement has been limited to the placement of microphones in appropriate locations. Four microphones in the tunnel settling chamber have been used to evaluate relative sound power generation. The signals from microphones placed on rigid supports in a pattern around a model have provided source directivity data. Finally, directional microphones placed outside the tunnel test section have been calibrated and utilized for source directivity evaluation (3).

2.3 Relation to Preceding Work

Increasing interest in performing aero-acoustic measurements has resulted in a number of studies (4-15) similar to this one. Typically, the tunnel ambient noise and reverberant

properties are described with the intended aim of making direct field measurements in an unmodified or a treated closed test section. Sound power measurement calibrations are also performed in open test section tunnels.

Preceding work on this program resulted in a report delineating the wind-on noise characteristics and an omnidirectional source sound power measurement calibration (16). This report expands on that work along with setting forth an acoustic sound power measurement calibration for directional sources. This effort in the LeRC hardwall 9 x 15 foot wind tunnel is unique with respect to calibration of the adjoining tunnel chambers for sound power measurement. In addition, the hardwall tunnel characteristics which limit direct field measurements are defined.

3.0 ACOUSTIC MODELS

Analytic models are appropriate for the evaluation of the acoustic properties of a facility. The models describe the relationships between acoustic and other physical parameters.

In the case of the hardwall 9 x 15 foot wind tunnel, one model serves as a framework for the application of experimental data to the reverberant calibration. Another series of models describes the functional behavior of various candidate noise sources, which is applicable to noise source diagnosis.

3.1 Reverberant Chamber Model

A wind tunnel may be acoustically modeled as either a duct with propagating waves or as a collection of interconnected semi-reverberant rooms. The approach selected depends on both the intended purpose of the modeling exercise and on the physical characteristics of the tunnel. The mathematical acoustic model adopted has four interconnected semi-reverberant chambers including the test section. These chambers, along with the acoustically important volumes and areas, are shown in Figure 2. The tunnel is well suited for this model for the following reasons:

1. The facility had received acoustic treatment for community noise abatement. As a result, the 8 x 6 test section is isolated acoustically from the 9 x 15 test section, Figure 1.

2. The three chambers adjoining the test section are each somewhat isolated from the rest of the tunnel and lend

themselves to the measurement of sound power eminating from the test section.

3. The test section has exhibited a fairly uniform reverberant field using an omni-directional source (16).

The interrelationships of the appropriate acoustical parameters are given in various references on room acoustics (17-18). For standard atmospheric conditions, the sixty dB reverberation decay time and total absorption are related by:

$$S\alpha_t = \frac{55.2V}{c\,T_R} \qquad (1)$$

where S = area, $ft.^2 (m^2)$

$\alpha_t = \alpha_{SAE} + 4\,mV/S$ = total average absorption

α_{SAB} = Sabine absorption (in the absence of atmospheric absorption)

V = volume, $ft.^3$ (m^3)

T_R = reverberation time, 60 dB decay, sec.

m = atmospheric absorption term, 1/ft. (1/m)

c = speed of sound, ft/sec (m/sec)

The atmospheric absorption term is primarily a function of relative humidity and frequency with some variation with temperature. Available data for reverberant chambers (19) have been summarized into a single curve, Figure 3. Atmospheric absorption is also a factor in direct field sound propagation above 1000 Hz for test section to settling chamber distances. For direct field sound propagation, the excess atmospheric attenuation is usually expressed in terms of dB/1000 ft (m). Standard values for octave and one-third octave bands as a function of humidity and temperature have been published by the Society of Automotive

Engineers (20,21). Octave band data from Reference 21 are reproduced as Figure 4.

With an acoustic source in the room, sound power and sound pressure level are related by

$$SPL = PWL + 10 \log \left[\frac{Q}{4\pi r^2} + \frac{4}{S\alpha_{SAB} + 4mV} \right] + 10 \qquad (2)$$

where SPL = sound pressure level, dB re 20 $\mu N/m^2$

PWL = sound power level, dB re 10^{-12} Watt

Q = SPL along sound source geometric centerline (-) SPL of an omnidirectional source having equivalent sound power, measured at same radius

r = radius from source ft. (m)

Subtract 10 dB from the right hand side for SI units.

The hall radius is the point at which the direct field and reverberant sound pressure levels are equal. From Equations 1 and 2:

$$r_H = \left[\frac{QS\alpha_t}{16\ \pi} \right]^{1/2} = \left[\frac{55.2VQ}{16\ \pi c T_R} \right]^{1/2} \qquad (3)$$

The sound power output of propulsion inlets has, in the past, been evaluated by LeRC on a relative basis by measurement of settling chamber sound pressure levels. The SPL-PWL relationship, equation 2, provides a means to calculate the sound power in the settling chamber. However, knowledge of the fractional portion of the source sound power exiting to the settling chamber is also required.

Recognizing these factors which contribute to settling chamber levels, the previous sound power calibration method (16) has been revised to place more reliance on the chamber decays

and to include physically significant acoustic source power distribution terms.

The recommended chamber reverberant calibration is represented in equation form:

$$PWL_{source} = SPL_i + 10 \log \left[S\bar{\alpha} SAB_i + 4mV_i \right] - 10 \log P_i - 16 \quad (4)$$

where P_i = fraction of source sound power exiting to the ith chamber

$10 \log P \equiv \Pi$, power index

Add 10 dB to the right hand side for SI units.

If all the source sound power is inserted into the particular chamber, P = 1.0, and the chamber reverberant relation results.

$$PWL = SPL + 10 \log S\alpha_t - 16 \quad (5)$$

$$\text{or } PWL - SPL = 10 \log \frac{55.2V}{cT_R} - 16$$

$$= 10 \log \frac{V}{cT_R} + 1.5$$

Add 10 dB to the right hand side for SI units.

The ratio of source power to that exiting to the settling chamber, the preparation room, or the diffuser depends both on the tunnel acoustic properties and the source directivity index. The directivity index is defined as

$$DI \equiv 10 \log Q \quad (6)$$

In words, the directivity index is the ratio of sound pressure

levels from directional and omni-directional sources having the same sound power. This directivity index may be determined from directionality plots or from concomitant direct field sound pressure and sound power level measurements. For directionality plots, the DI determination results from integrating the product of intensity and area. Since accurate integration of this product is tedious, a -3 dB to -5 dB point approximation can be used. That is, the transition from high intensity to low intensity is assumed to be instantaneous and to occur between -3 dB and -5 dB on the directionality plot. For example, for loudspeaker data, the -5 dB point gives a better approximation (22). In addition, if the directionality pattern is symmetrical in the horizontal and vertical directions, the projected area is a circular segment and the directivity index is given by the equation

$$DI = 10 \log \frac{2}{1-\cos \gamma} \qquad (7)$$

where γ = the angle between the source centerline and the representative transition point.

The directivity index may also be computed from sound pressure and sound power using the following equation:

$$DI = SPL_{1.0 \text{ ft (m)}} - PWL_{source} + 1 \qquad (8)$$

where $SPL_{1.0 \text{ ft (m)}}$ = Direct field, centerline sound pressure level dB re 20 $\mu N/m^2$, at 1.0 ft (m)

Add 10 dB to the right hand side for SI units.

The relation between source directivity index and the power index is best determined experimentally. However, note that this dependence on source characteristics is required because

only one chamber measurement is used. In order to minimize inaccuracies arising from the variability of P with source characteristics, the use of preparation room and diffuser measurements, along with settling chamber levels, is recommended. In that situation, only the acoustic energy absorbed in the test section is not accounted for by chamber measurements.

3.2 Tunnel and Microphone Noise Models

Tunnel generated noise and turbulent wind induced microphone noise place amplitude limits on the measurement of source generated noise in both low velocity chambers and the higher velocity test section. The candidate noise sources contributing to test section and settling chamber measured levels are as follows:

1. Microphone self noise in the presence of wind.
2. Test section turbulent boundary layer noise.
3. Turbulence--test object vortex noise.
4. Settling chamber cooler coil vortex noise.
5. Tunnel drive fan noise propagating through the dryer bed and up the diffuser.

Noise from the 8 x 6 foot supersonic wind tunnel by way of the settling chamber, Figure 1, is not considered significant. Levels measured at the exit prior to construction of the 9 x 15 foot wind tunnel were lower than present settling chamber levels as indicated in Table I.

3.2.1 Microphone Wind Noise

Microphone self noise in the presence of wind is generally attributed to fluctuating dynamic pressure -

TABLE I

COMPARISON OF UPSTREAM SOUND PRESSURE LEVELS,
dB re 20 $\mu N/m^2$

Condition	Octave Band Center Frequency, Hz						
	125	250	500	1K	2K	4K	8K
Mach 1.9 in 8 x 6, prior to 9 x 15 construction, no ram jet (2)	60	55	56	57	51	45	37
Present settling chamber levels, q = 25 psf (16)	89 to 95	87 to 93.5	83.5 to 88	81.5 to 87	72 to 81	67 to 79	65 to 70

$$q + p(t) = 1/2\ \rho(U + u)^2 = 1/2\ \rho[U^2 + 2Uu + u^2] \quad (9)$$

where q = dynamic pressure, lb/ft^2 (N/m^2)
p(t) = fluctuating dynamic pressure lb/ft^2 (N/m^2)
ρ = density, $slugs/ft^3$ (kg/m^3)
U = mean velocity, ft/sec (m/sec)
u = fluctuating velocity, ft/sec (m/sec)

since U and q are not time variant and U > u,

$$p(t) \approx \rho U u \quad (10)$$

and

$$\overline{p^2(t)} = \rho^2 U^2 \overline{u^2} \quad (11)$$

where $\overline{p^2(t)}$ = time average variance of the pressure, $\frac{lb^2}{ft^4}\left(\frac{N^2}{m^4}\right)$

The fluctuating velocity is usually expressed in terms of a turbulence index, a fraction of the mean velocity, $\tau = u/U$.

Substituting into equation (11) yields

$$\overline{p^2(t)} = \rho^2 U^4 \overline{\tau^2} \quad (12)$$

Taking ten times the logarithm of both sides of equation 12, using the air density for standard conditions, and converting to $20\mu N/m^2$ reference

$$SPL = 40 \log U + 20 \log \tau + 75. \quad (13)$$

Add 20.5 dB to the right hand side for SI units.

In terms of dynamic pressure, q:

$$SPL = 20 \log q + 20 \log \tau + 133.8 \qquad (14)$$

Subtract 33.6 dB from the right hand side for SI units.

In review of aero-acoustic measurements, Fuchs (23) presents data showing that the U^4 dependence holds for circular jets and free stream measurements. However, the basic constant of proportionality differs by a factor of 1/2 from equation 12, as follows:

$$p(t) = 1/2\ \rho U u \qquad (15)$$

In addition, for non-homogeneous turbulent boundary layers, a form proportional to $U^2\ \tau^{0.5}$ gives a better fit. These results suggest that the constant of proportionality, equations 13 and 14, may have a sizable variability or may even be in error. However, since the experimental results do not consist of well documented concommitant turbulence and dynamic pressure data measurements, the analytically correct form, equation 12, will be used.

In order to model the response of typical microphones in the presence of turbulent flow, the following additional information is required:

1. Experimental assurance that microphone wind noise depends on U^4.
2. Data on the improvement afforded by microphone nose cones.
3. The intensity and spectral characteristics of the turbulence in the 9 x 15 foot test section.

Data from tests by B&K (24,25) and Noiseux (26) collapse nicely (to different curves) if normalized by velocity to the sixth power. However, the mid-to-high frequency spectra of both sets of data are decreasing with increasing frequency, approximately to the second power. If the higher velocity measurements are shifted down in frequency, they are then related to the lower velocity measurements by U^4.

Rasmussen (25) shows an average of 15-25 dB decrease in wind noise with a nose cone for one-half inch microphones and 10-15 dB for one-quarter inch microphones in the frequency range from 100 to 5000 Hz. For those tests, the reference data were measured with a protection grid which may induce local turbulence, especially in high frequency bands. This would tend to increase the apparent nose cone improvement. Noiseux (27) presents concomitant turbulence and wind noise data for a B&K one-half inch microphone with nose cone. The microphone exhibited levels which are approximately 16 dB lower than the fluctuating dynamic pressure levels calculated from equation 13. From these limited experiments, 15 dB is taken as the expectation for wind noise reduction with the addition of a nose cone for one-quarter inch microphones.

The turbulence intensity in the center of the 9 x 15 foot test section averages 0.75% (1). The intensity averages 1.3% as the measurement location is moved to within 10 inches of the floor or ceiling. The electrical signals from the hot wire probes used for those measurements were passed through low pass filters at the time of measurement (28). The one-third octave band spectrum of the turbulence was inferred from these measurements to essentially flat, with a level of - 56.5 dB re unity. Combining the confirmation of the U^4 dependence, the 10 dB nose cone improvement, and measured turbulence levels, the

predicted one-third octave band wind noise sound pressure level is 90 dB re $20\mu N/m^2$ for a tunnel dynamic pressure of 25 psf (1196 N/m^2). The microphone wind noise is also predicted to increase as U^4 (or q^2).

3.2.2 Turbulent Boundary Layer Noise

From unpublished BBN work acoustic power radiated from a turbulent boundary layer can be expressed as follows:

$$PWL(\omega) \approx 10 \log\left(\frac{\rho S U^7}{c^3 \omega \delta^*}\right) + 41 \quad \text{when } \frac{\omega\delta^*}{U} > 1 \tag{16}$$

$$\approx 10 \log\left(\frac{\rho S U^5 \delta^* \omega}{c^3}\right) + 41 \text{ when } \frac{\omega\delta^*}{U} < 1 \tag{17}$$

where PWL (ω) = the sound power level for one-third octave bandwidth, dB re 10^{-12} Watt

ρ = air density, lb sec^2/ft^4 ($N\ sec^2/m^4$)

S = radiative area, ft^2 (m^2)

U = free stream velocity, ft/sec (m/sec)

c = speed of sound, ft/sec (m/sec)

δ^* = boundary layer displacement thickness, ft (m)

$\omega = 2\pi f$ = radial frequency, radians/sec

Subtract 11.5 dB from the right hand side of equations 16 and 17 for SI units.

In the transitional frequency region where $\omega\delta^* \approx U$, one-third octave band levels will increase approximately as U^6. Unfortunately, the constant of proportionality in equations 16 and 17 has a variability of $\pm$ 20 dB.

For a representative tunnel flow condition of q = 25 psf, and a boundary layer displacement thickness of 0.5 inch or 13 mm (1), the transition point frequency, $f = U/\delta^* 2\pi = 561$ Hz. Taking the radiative area as the test section area (1643 ft^2 or 153 m^2), equations 16 and 17 both yield sound power estimates of 85 dB re 10^{-12} watt. The one-third octave band sound power levels diminish at a rate of 3 dB per octave on both sides of the transition point one-third octave band, centered at 561 Hz.

The diffuser would also be expected to generate turbulent boundary layer noise. However, the 1:3 reduction in velocity occurring in the diffuser effects almost a 30 dB reduction in the sound power production per unit of radiative area at the diffuser end, relative to the test section, from equations 16 and 17. The contribution of the diffuser turbulent boundary layer is estimated to be, at most, equal to that of the test section. This would add 3 dB to the estimate for the test section to arrive at a total turbulent boundary layers sound power estimate.

3.2.3 Vortex Noise

With respect to vortex noise, theoretical and experimental work has also been done to understand the basic process of noise generation by the interaction of flow with rigid surfaces. Current noise prediction techniques are summarized by Hayden (29) for the cases of:

a) flow past a single discontinuity-trailing edge,
b) rigid body in disturbed flow,
c) spoilers in confined environments.

Analyses show that the noise sources for (a) and (c) above are dipole, and the resulting sound power varies as U^6. Point dipole sources are also postulated for incoming turbulence although deviations apparently exist.

For flow past a single discontinuity trailing edge, the engineering form of the acoustic generation prediction is as follows:

$$PWL_{OA} = 10 \log \left(\delta W U^6\right) - 21 \qquad (18)$$

where PWL_{OA} = overall sound power, dB re 10^{-12} Watt
δ = boundary layer thickness, ft (m)
W = edge length, ft (m)
U = tunnel mean flow velocity, ft/sec (m/sec)

Add 41.3 dB to the right hand side for SI units.

The one-third octave band spectrum peaks at a frequency $f_p = 4 \times 10^{-2}\ U/\delta$ and at a level 10 dB lower than the overall sound power level. The spectrum decreases at 3 dB per octave above the peak frequency band.

Two trailing edges are candidate noise producers - the diffuser end, and the transition from the test section to the diffuser. The latter is postulated not so much for the clean empty test section as for when test hardware or test section wall irregularities are present, promoting local or general boundary layer separation, similar to a trailing edge situation.

For a representative test section flow condition of q = 25 psf (1196 N/m^2), the noise related parameters and predicted sound power generation are as follows:

End of Diffuser	End of Test Section
$\delta \approx 1$ ft (0.3 m)	$\delta = 0.4$ ft (0.12 m) (1)
W = 80.5 ft (24.5 m)	W = 48 ft (14.6 m)
U = 50.2 ft/sec (15.3 m/sec)	U = 147 ft/sec (44.8 m/sec)
f_p = 2 Hz	f_p = 15 Hz
PWL_{OA} = 100.1 dB	PWL_{OA} = 121.8 dB

With respect to a rigid body in disturbed flow, Hayden (29) comments that "there still exists no coherent, experimentally verified theory which enables one to predict accurately sound production from an arbitrarily shaped body in an arbitrary inflow." This absence of a general prediction methodology is balanced by the ease of application of the spoiler noise model. Hayden (29) and Beranek (30) summarize work by Yudin (31) and Gordon (32) on the noise generated by an obstruction in a duct or pipe. The model relates sound power production to the pressure drop across the spoiler spanning a pipe. If the pressure drop is assumed to be equal to the product of the dynamic pressure and coefficient of drag of the spoiler, the following engineering equation results:

$$PWL_{OA} = 30 - \log qC_d + 20 \log D_p - 76.1 \qquad (19)$$

where PWL_{OA} = overall sound power dB re 10^{-12} Watt

q = dynamic pressure, $16/ft^2$ (N/m^2)

D_p = diameter of pipe on test section, ft (m)

C_d = Coefficient of drag

Subtract 37.4 from the right hand side for SI units.

The width of the spoiler is not a factor in Equation 19 because the formulation assumes the sound power level is dependent on the peak frequency squared, which in turn is inversely dependent on spoiler width.

The one-third octave band spectra peaks at 10 dB below the overall and at a frequency of $f_p = 0.2\ U/d$, where d is the diameter of the spoiler. This frequency must be below the pipe cutoff frequency for Equation 19 to be applicable. The cutoff frequency is defined as $f_c = 0.5\ c/D_p$. The one-third octave band spectra decreases at 3 dB/octave above and below the peak spectral level.

For a 1.5 foot diameter pipe spanning the average test section dimension, and for representative tunnel flow conditions, q = 25 psf in the test section, Equation 19 predicts an overall sound power of 98.5 dB re 10^{-12} Watt. The predicted spectrum peaks at a frequency of 19.6 Hz.

3.2.4 Settling Chamber Cooler Coil Vortex Noise

Upon completion of the return leg of the 8 x 6 foot supersonic wind tunnel circuit in 1957, a serious noise problem was identified and corrected (33). The bank of cooler coils, Figure 1, exhibited discrete frequency vortex shedding which matched one or more "organ pipe resonances" of the heat exchanger boundaries, along with structural resonances. This narrow band phenomenon was eliminated by installation of three vertical baffles in each of seven foot wide sections. In addition, V-shaped plates were installed in place of flat plates between adjacent sections. With completion of the cooler modifications, the noise level was reported to have

been reduced 60 dB in the range from 110 to 170 Hz. No broadband noise measurements are reported for any mid-to-high frequency bands.

Fortunately, a reasonably accurate (±5 dB) method exists for estimating the overall sound power generated by flow obstructions, such as air conditioning diffusers. Beranek (34) presents an empirical method, attributable to Humbert (35), as follows:

$$PWL_{OA} = 10 \log S + 30 \log \varepsilon + 60 \log U - 31.3 \qquad (20)$$

where S = area, ft^2 (m^2)
ε = pressure drop divided by dynamic pressure, dimensionless
U = velocity, ft/sec (m/sec)

Add 41.3 dB to the right hand side for SI units.

The estimated one-third octave band spectrum is haystack in shape, peaking at 10 dB below the overall level at a frequency $f_p = 457\ U/U_{ref}$, where U_{ref} = 10 ft/sec (3 m/sec). The spectral level decreases approximately 3 dB per octave above and below the peak frequency.

The dimensions of the cooler coils are 32 by 47 feet (14.3 m by 9.7 m). The pressure drop across the cooler coil bank was measured prior to installation of the 9 x 15 foot test section (36). At maximum flow conditions, the pressure drop was 5.7 inches of water. This corresponds to approximately 17 dynamic pressure heads.

The values of the parameters of equation 20, for a test section dynamic pressure of 25 psf (1196 N/m^2) are as follows:

$S = 1504\ ft^2\ (140\ m^2)$
$\epsilon = 17$
$U = 13.2$ ft/sec (4 m/sec)
$PWL_{OA} = 104.4$ dB re 10^{-12} Watt
$f_p = 603$ Hz

Considering that one-half of the acoustic energy propagates upstream, the power transmitted to the settling chamber in the one-third octave band centered at 603 Hz would be 91.4 dB re 10^{-12} Watt.

3.2.5 Tunnel Drive Fan Noise Propagating Through the Dryer Bed

Fan generated noise is attributed by various authors (37,38) to combinations of mechanisms including:

a) Steady blade forces
b) Interference noise (from upstream obstructions)
c) Vortex shedding
d) Inlet turbulence

The first two mechanisms produce sinusoidal tones at the blade passage frequency and multiples thereof. The compressor fan for the facility turns at an average speed of 810 rpm. The drive fan has 52 blades, yielding a blade passage frequency of 702 Hz. The acoustic transmission properties of the dryer bed are not known, making the noise source level estimation impossible. However, identification of contributions from

these noise sources should be relatively easy because of their sinusoidal nature.

Fan vortex shedding and inlet turbulence exhibit the same U^6 parametric dependence as turbulent boundary layer and vertex noise. However, the velocity through the 9 x 15 foot low speed test section is controlled with the flow control doors with the compressor speed and flow held approximately constant. Therefore, any broadband noise from the tunnel drive fan would not be dependent, in either amplitude or frequency, on the low speed test section flow velocity.

4.0 EXPERIMENTAL RESULTS AND DISCUSSION

The experimental evaluation of the hardwall acoustic measurement characteristics of the 9 x 15 foot low speed wind tunnel took place over a period of time from 29 November 1973 to 17 July 1974. The resulting data and discussion of their significance are organized as follows:

- Chamber Reverberant Decay Measurement
- Sound Power Measurement Calibration
- Directionality Measurement Demonstration
- Tunnel and Microphone Wind-On Noise

4.1 Chamber Reverberant Decay Measurements

The graphic display and measurement of the decay of impulsive or steady state acoustic signals permits identification of dominant reflecting surfaces as well as calculation of the average absorption. Impulsive decays were recorded on 29 November 1973, 24 February 1974, and 27 February 1974. The relative humidity was not measured in the tunnel, but Cleveland Weather Bureau data, shown in Table II, indicate an average of 60% for those days. Based on a limited number of subsequent measurements, the relative humidity in the settling chamber is estimated to be significantly lower than the ambient relative humidity, especially on cold days.

The equipment used for all decay measurement is shown in Figure 5a. The recordings were played back through an octave band filter onto a grphic level recorder, and the reverberation times were calculated. With the use of an impulsive noise source, a graphic level recorder tends to over-react

TABLE II

Relative Humidity, Cleveland, Ohio, Airport
on Static Acoustic Test Days, %

	Date	Type Test	Time of Day		
			10 a.m.	3 p.m.	9 p.m.
Hardwall	29 Nov. 1973	Pistol Decays, ILG	64	54	75
	24 Feb. 1974	Pistol Decays	60	68	78
	27 Feb. 1974	Pistol Decays	45	46	51
	3 April 1974	ILG	43	87	78
	11 July 1974	Shotgun Mic	66	57(38)*	49
	12 July 1974	Shotgun Mic	53	54	40
	15 July 1974	Horn, Reverb. Cal.	64	60	66
	16 July 1974	Horn, Reverb. Cal.	61	46	47
	17 July 1974	Horn, Sword, Direct.	50	35	53

*Measured In Test Section

to the instantaneous increase in signal. This obscures the initial part of the subsequent decay. To overcome this difficulty, the magnetic tape was played in reverse.

Typical settling chamber octave band decays are presented in Figure 6. The reverberant decays are well behaved with a single slope. This indicates the predominance of a single class of room modes, probably floor to ceiling and wall to wall.

Decays for the diffuser section and preparation room are presented in Figures 7 and 8, respectively. As with the settling chamber, the curves are well behaved with little or no ambiguity about the appropriate reverberation time to use to characterize the acoustic properties.

The test section decay curves, Figure 9, all have a double slope characteristic. The initial slope is identified with the reverberant decay of the test section itself, the energy is exiting to the other three chambers. The subsequent slope, which starts 15 to 20 dB from the initial test section level, is associated with the decay of the settling chamber with some input from the diffuser and preparation room.

The reverberation times for all the pistol shot recordings were calculated and averaged. The average reverberation times were used to calculate the absorption, hall radius, and sound power-sound pressure difference, for the settling chamber, preparation room, and diffuser section, Table III.

For the test section, the initial part of the decay was considered an inaccurate descriptor of the average absorption

TABLE III

Acoustic Properties of Wind Tunnel Chambers
Determined from Decay Measurements and
Calibrated Sound Power Source, Low Relative Humidity (25%)

Chamber	Property	Octave Band Center Frequency, Hz					
		250	500	1K	2K	4K	8K
Settling Chamber	Reverb. Time Sec.	3.6	3.5	3.0	2.5	1.65	0.95
13,000 ft^2 ($1208m^2$)	$S\alpha_t$, ft^2	1360	1400	1630	1960	2970	5160
100,000 ft^3 ($2832m^3$)	α_t	0.10	0.11	0.13	0.15	0.23	0.40
	Hall Radius, ft.	5.2	5.3	5.7	6.2	7.7	10.1
	PWL (-) SPL, dB	15.3	15.5	16.1	16.9	18.7	21.3
Diffuser Section	Reverb. Time, Sec.	5.0	4.9	4.1	3.3	1.9	1.0
20,000 ft^2 ($1860m^3$)	$S\alpha_t$, ft^2	1370	1400	1670	2100	3600	6900
140,000 ft^3	α_t	0.07	0.07	0.09	0.11	0.19	0.35
($3965m^3$)	Hall Radius, ft.	5.2	5.3	5.7	6.4	10.6	11.7
	PWL (-) SPL, dB	15.4	15.5	16.2	17.2	19.6	22.3
Preparation Room	Reverb. Time, Sec.	2.6	2.7	2.4	2.0	1.4	0.68
23,000 ft^2 ($2137m^2$)	$S\alpha_t$, ft^2	1885	1815	2040	2450	3500	7200
100,000 ft^3	α_t	0.08	0.08	0.09	0.11	0.15	0.31
($2832m^3$)	Hall Radius, ft.	6.1	6.0	6.4	7	8.3	12
	PWL (-) SPL, dB	16.8	16.6	17.1	17.9	19.4	22.6
Test Section	Reverb. Time, Sec.	0.8/4.0	1.1/3.4	0.8/2.8	1.2/2.6	0.8/1.6	0.7
1643 ft^2 ($153m^2$)	$S\alpha_t$, ft^2 (T_{60})	236	172	236	158	236	270
3861 ft^3 ($109m^3$)	PWL (-) SPL (ILG)	9.5	9	9	9.2	10.5	10.7
	$S\alpha_t$, ft^2, (ILG)	355	316	330	445	457	470
	α_t	0.22	0.19	0.2	0.27	0.28	0.29
	Hall Radius, ft	2.7	2.5	2.6	3.0	3.0	3.0

because of the short decays and limited number of reflections. This inaccuracy was confirmed by observing that the test section effective absorbing area, $S\alpha_t$, calculated from the pistol decays was consistently less than the area opening to the adjoining chambers (337 ft^2). To overcome this measurement problem and resulting inaccuracy, an ILG centrifugal blower, calibrated, omnidirectional, acoustic source (39) was placed in the test section and octave band sound pressure levels were measured at various locations in the test section. A reasonably uniform acoustic field was observed at radii beyond five feet, and the test section reverberant properties were calculated from these data, Table III.

4.2 Sound Power Measurement Calibration

4.2.1 Omni Directional Source

On two occasions, 29 November 1973, and 3 April 1974, settling chamber sound pressure levels were measured while the ILG source was in the test section. These data had been used to calibrate the settling chamber microphones for source sound power in the previous report (16). With use of decays for the settling chamber calibration, these data have now been used to determine π, the fractional portion of the source sound power exiting to the settling chamber, Table IV. The calculated values of π differ by 0.2 to 4.8 dB for the two sets of data. These differences are attributable to one or both of the following:

1. source sound power output variability,
2. relative humidity uncertainty.

TABLE IV

Estimation of Sound Power Output of ILG Omnidirectional Source In Wind Tunnel Test Section Using Settling Chamber Sound Pressure Level Measurements

Test	Relative Humidity Estimate	Property	Octave Band Center Frequency					
			250	500	1K	2K	4K	8K
29 Nov. 1973 Test 1, 2	25%	SPL_{sc}	60	60	61.7	60.2	53.5	44
		$\Delta, PWL_{sc}-SPL_{sc}$	15.3	15.5	16.1	16.9	18.7	21.3
		$PWL_{sc}=SPL_{sc}+\Delta$	75.3	75.5	77.8	77.1	72.2	65.3
		PWL_{ILG}	80.5	81	81.7	82	79	75.5
		$\Pi, PWL_{ILG}-PWL_{sc}$	-5.2	-5.5	-4.9	-4.9	-6.8	-10.2
3 April 1974 Test II, Test Section Station 0,0	70%	SPL_{sc}	57.5	58	62	61	57.5	52
		$\Delta, PWL_{sc}-SPL_{sc}$	15.3	15.5	15.7	16.0	17.2	18.2 *
		$PWL_{sc}=SPL_{sc}+\Delta$	72.8	73.5	78.2	77.0	74.7	70.2
		PWL_{ILG}	80.5	81	81.7	82	79	75.5
		$\Pi, PWL_{ILG}-PWL_{sc}$	-7.7	-7.5	-3.5	-5.0	-4.3	-5.3
Average		$\Pi_{ave}, PWL_{ILG}-PWL_{sc}$	-6.5	-6.5	-4.2	-5	-5.5	-7.7
Ratio, connecting area to total test section absorption, Table III		$10 \log(9x15)/S\alpha_t$	-4.2	-3.7	-3.9	-5.2	-5.3	-5.4

*Table III values corrected for relative humidity, equation 4 and Figure 3.

The average value of Π is approximately -6 dB with some frequency dependence. This says that one-fourth of an omnidirectional source's acoustic energy goes to the settling chamber.

The bottom line of Table IV lists the ratio of total test section absorption to the area of the 9 x 15 foot opening into the settling chamber, expressed in dB. If the test section were truly reverberant and the settling chamber levels negligible, these values would correspond to Π. These values are different from the average Π values by -0.2 to 3.9 dB. This is indicative of the sound power estimation accuracy which can be achieved with an omnidirectional source in the middle of the test section using only settling chamber measurements.

In addition to this measurement variability, the acoustic power distribution also depends on the source location in the test section. This has been demonstrated by moving the ILG source within the test section, Figure 10, and by observing the effect of angle of attack (position) of a 5.5 inch fan inlet, Figure 11.

In order to overcome the dependence of sound power estimates on source position, and to an even greater extent the dependence on directionality, the ILG-induced acoustic levels in the diffuser and preparation room were utilized along with the settling chamber levels. The sound pressure levels measured with a hand held sound level meter are listed in Table V. These octave band levels were converted to sound power estimates using the PWL-SPL values, Table III, plus a humidity correction. The humidity was approximately 25% for the

TABLE V

SOUND PRESSURE LEVELS WITH ILG OMNIDIRECTIONAL SOURCES IN WIND TUNNEL TEST SECTION, HAND HELD SOUND LEVEL METER
3 APRIL 1974, RELATIVE HUMIDITY ESTIMATE 70%

TEST NO.	SOURCE LOCATION	MICROPHONE SC	PR	DS	OCTAVE BAND CENTER FREQUENCY 250	500	1K	2K	4K	8K
II	Test Section, Station 0, 0	X			57.5	58	62	61	57.5	52
			X		62	59.5	58	57.5	54.5	49
				X	57.5	58	58	57	52	46
III	Test Section Station 7, 0	X			58	59.5	61	61.5	59	53
			X		60	58.5	58	56.5	54	48.3
				X	57	57.5	58	56.5	52	45
IV	Test Section, Station 0, -3.5	X			57.5	58.5	61	60.5	59	52.5
			X		60	59	58	57.5	54.5	50
				X	57.5	58	59	57.5	52	43
V	Test Section, Station -15, 0	X			56	56.5	59	59	56.5	49
			X		58.5	56	56.5	56	53.5	47
				X	59.5	61	60.5	59.5	55.5	49
VIII	Test Section, Station -0, 0	X			58	59.5	60	59	57	50.5
			X		61	59.5	59	57.5	54.5	50
				X	57.5	57.5	59	60	55.5	48

chamber calibrations and approximately 70% for the ILG measurements. The $S\alpha_t$ values, Table III, equation 4 and the humidity absorption, Figure 3, were used to calculate humidity corrections, Table VI.

TABLE VI

HUMIDITY CORRECTION, $10 \log \left[\frac{S\alpha_t \ (25\%)}{S\alpha_t \ (70\%)}\right]$

Chamber	Frequency Hz			
	1000	2000	4000	8000
Settling Chamber	0.4	0.9	1.5	3.1
Preparation Room	0.4	1.0	2.2	3.2
Diffuser Leg	0.5	1.2	2.1	3.3

The corrected chamber calibrations were applied to the measured sound pressure levels in all three chambers to arrive at sound power estimates, Table VII. The sound power estimates for the individual chambers were summed and compared with the source sound power, Table VII. The summed results are independent of source position. In addition, the difference in source and measured sound power agrees well with the ratio of total test section absorption to open area (expressed in dB), Table VII. This indicates that all of the omni-directional source sound power is accounted for; it is either absorbed in the test section or is divided between the adjoining chambers. Thus, the sound power estimation accuracy for an omni-directional source can be improved to ± 1 dB if all three chamber measurements are used.

4.2.2 Sound Power Measurement Calibration Directional Source

As mentioned in the preceding section, early tests by LeRC with a 5.5 inch fan-inlet noise source showed variation in settling

TABLE VII

SOUND POWER OUTPUT OF ILG OMNIDIRECTIONAL SOURCE IN WIND TUNNEL USING MEASUREMENTS IN THREE CHAMBERS
PWL* = SPL + Δ (TABLE III) + RELATIVE HUMIDITY CORRECTION, TABLE VI

TEST NO.	SOURCE LOCATION	MICROPHONE SC PR DS TOTAL	OCTAVE BAND CENTER FREQUENCY 250	500	1K	2K	4K	8K
II	Test Section, Station 0, 0	X	72.8	73.5	77.7	77.0	74.7	70.2
		X	78.8	76.1	74.7	74.4	71.7	68.6
		X	72.9	73.5	73.7	73.0	69.5	64.8
		X	80.5	79.2	80.4	79.8	77.2	72.8
III	Test Section, Station 7, 0	X	73.3	75.0	76.7	77.5	76.2	71.2
		X	76.8	75.1	74.7	73.4	71.2	68.1
		X	72.4	73.0	73.7	72.5	69.5	63.8
		X	79.2	79.3	79.5	79.7	78.0	73.3
IV	Test Section, Station 0, -3.5	X	72.8	74.0	76.7	76.5	76.2	70.7
		X	76.8	75.6	74.7	74.4	71.7	69.6
		X	72.9	73.5	74.7	73.5	69.5	61.8
		X	79.3	78.6	80.5	79.7	78.2	73.7
V	Test Section, Station -15, 0	X	71.3	72.0	74.7	75.0	73.7	67.2
		X	75.3	72.6	73.2	72.9	70.7	66.6
		X	74.9	76.5	76.2	75.5	73.1	67.8
		X	78.8	78.7	79.5	79.2	77.3	71.9
VIII	Test Section, Station -0, 0	X	73.3	73.0	76.1	75.0	74.2	68.7
		X	77.8	76.1	76.1	74.4	71.7	69.6
		X	72.9	73.0	74.7	76.0	72.9	66.8
		X	80.0	79.1	80.1	79.8	77.8	73.1
	PWL Average	X	79.6	79.0	80.0	79.6	77.7	73.0
	ILG SOUND POWER AVERAGE CALIB.	X	80.5	81.0	81.7	82.0	79.0	75.5
	$PWL_{ILG} - PWL_{EST}$	X	0.9	2.0	1.7	2.4	1.3	2.5
REF, 10 log ($S\alpha_t/337$)			1.1	0.7	0.9	2.2	2.3	2.4

*PWL, dB re 10^{-12} Watt; SPL dB re 20 μ N/m^2

chamber sound pressure level with angle of attack, Figure 11. The measurement variation was attributed to source directionality as well as location in the test section. In order to understand source acoustic power distribution and improve measurement accuracy, a sound power measurement calibration was performed in July 1974, with a highly directional source of known characteristics (40). The source and rotational drive are shown in Figure 12. In addition to the four settling chamber microphones, preparation room and diffuser leg microphones were used, Figure 5c. The microphone signals were averaged on line with time division multiplexers, passed thru log converters, and plotted as a function of source-to-boom angle ψ of 360° while positioned at angles of attack, α = 0, 30 and 90°. The horn was driven with octave band noise centered at 500, 1000 and 2000 Hz, then with one-third octave band noise centered at 6300, 8000 and 10,000 Hz. The averaged chamber sound pressures were plotted on-line as a function of ψ, Figure 13.

The curves for each chamber were replotted and averaged using the source angle in the tunnel ($\alpha + \psi$) as the common absissa Figure 14. The average responses so obtained for the individual chambers were converted to sound power estimates using the chamber calibrations, Table III, plotted together for each octave band, and summed. These resulting summation plots had an inordinate contribution from the preparation room microphone. The summed sound power estimate rose 3 dB when the source was directed towards the side walls. The preparation room contributions were then reduced by 3 dB. This was justified by considering that the preparation room microphones were directly under the test section and were measuring near field as well as reverberant noise.

The results of the calibration with the directional source so obtained are presented in Figures 15 through 17. The calculated summations of sound power vary only ±1 dB with source angle even though the variation within individual chambers is as great at ±10 dB. The indicated sound power levels are compared with the calibrated source levels, Table VIII.

TABLE VIII

ESTIMATION OF SOUND POWER OUTPUT OF HORN DIRECTIONAL SOURCE IN WIND TUNNEL USING MEASUREMENTS IN THREE CHAMBERS

Data Source	Band Center Frequency, Hz						
	500	1K	2K	4K	6.3K	8K	10K
Indicated Level	112	112	111	107	105	103	100
Calibrated Source Level (40)	(112.5)	112	111	104	100.5	97.5	93.5
Difference, Indicated (-) Cal	-0.5	0	0	3	4.5	5.5	6.5

The differences between indicated and calibration levels are attributed to the direct field radiation of the horn source dominating the settling chamber microphone reverberant field. The direct field and reverberant field contributions for three different sources are calculated in Table IX. As would be expected, the more directional the source, the higher the direct field contribution relative to the reverberant.

The same trends are expected for diffuser and preparation room measurements, because the distance from source to microphone are similar. This is confirmed by observing that the sums of estimated sound power were invariant with angle, Figures 15, 16 and 17.

TABLE IX

ESTIMATION OF REVERBERANT AND DIRECT FIELD CONTRIBUTION TO MEASURED SETTLING CHAMBER SOUND PRESSURE LEVELS FOR THREE DIFFERENT SOURCES

SOURCE	FIELD	QUANTITY	BAND CENTER FREQUENCY, H_z 250	500	1000	2000	4000	6300	8000	10,000
ILG	Rev	PWL_{ts}	80.5	81.0	81.7	82.0	79.0	-	75.5	-
		Π (Table IV)	-6.5	-6.5	-4.0	-5.0	-5.5	-	-7.5	-
		$PWL_{sc}=PWL_{ts}+\Pi$	74.0	74.5	77.7	77.0	73.5	-	68.5	-
		$\Delta^*, PWL_{sc}-SPL_{sc}$	15.3	15.5	16.0	16.8	18.4	-	21.0	-
		$SPL_{sc}=PWL_{sc}-\Delta$	58.7	59.0	61.7	60.2	55.1	-	47.5	-
	Dir	SPL_{10}	58.2	61.5	63.7	63.3	56.0	-	50.0	-
		$\Delta_r = 20 \log 7 + A^*$	17.0	17.0	17.0	17.3	18.0	-	19.4	-
		$SPL_{70}=SPL_{10}-\Delta_r$	41.2	44.5	46.7	46.0	38.0	-	30.6	-
		$DI=SPL_{10}-PWL+21$	-1.3	1.5	3	2.3	-2	-	-4.5	-
LE5-2 Speaker, 0.25 Amp	Rev	PWL_{ts}	-	96.2	94.7	96.3	94.7	-	93.7	-
		Π (est)	-	-3.0	-3.0	-3.0	-2.0	-	-2.0	-
		$PWL_{sc}=PWL_{ts}+\Pi$	-	93.2	91.7	93.3	92.7	-	91.7	-
		$\Delta, PWL_{sc}-SPL_{sc}$	-	15.5	16.0	16.8	18.4	-	21.0	-
		$SPL_{sc}=PWL_{sc}-\Delta$	-	77.7	75.7	76.5	73.3	-	70.7	-
	Dir	PWL	-	96.2	94.7	95.7	94.7	-	93.7	-
		10 log Q = DI	-	5.5	7.0	7.0	13.0	-	14.0	-
		$SPL_{1.0}=PWL+DI-1$	-	101.7	100.7	101.7	106.7	-	106.7	-
		$\Delta_r=20 \log 70+A$	-	37.0	37.0	37.3	38.0	-	39.4	-
		$SPL_{70}=SPL_1-\Delta_r$	-	64.7	63.7	64.4	68.7	-	67.3	-
Horn 0.25 Amp	Rev	PWL_{ts}	-	112.5	112.0	111.0	104.0	100.5	97.5	93.5
		Π(Fig 15,16,17)	-	-2.0	-1.0	-0.5	-0.5	-0	-0	-0
		$PWL_{sc}=PWL_{ts}+\Pi$	-	110.5	111.0	110.5	104.5	100.5	97.5	93.5
		$\Delta, PWL_{sc}-SPL_{sc}$	-	15.5	16.0	16.8	18.4	20.0	21.0	22.1
		$SPL_{sc}=PWL_{sc}-\Delta$	-	95.0	94.0	93.7	96.1	80.5	76.5	71.4
	Dir	PWL	-	112.5	112.0	111.0	104.0	100.5	97.5	93.5
		10 log Q = DI	-	12	19.0	18.5	18.0	22.0	23.5	26.5
		$SPL_{1.0}=PWL+DI-1$	-	123.5	130.0	128.5	121.0	121.5	120.0	119.0
		$\Delta_r=20 \log 70+A$	-	37.0	37.0	37.0	37.3	38.7	39.4	40.2
		$SPL_{70}=SPL_{1.0}-\Delta_r$	-	86.5	93.0	92.0	93.7	82.8	80.6	79.8

*All atmospheric absorption terms calculated for conditions of relative humidity, 30%, temperature 68° F; A = atmospheric absorption,70 ft. from Fig.4

The implication is that reverberant sound power measurement is dependent on source directivity, even if all three chamber microphones are used. Fortunately, typical inlets are not expected to have directionality indices (DI) in excess of 20 dB like the horn source. The LE5-2 speaker has DI's ranging from 6.5 to 14, which may be more typical. The speaker has a worst case settling chamber sound pressure contribution of reverberant = 70.7 dB versus direct = 67.3 dB. This would raise the measured levels measured by the settling chamber microphones by 1.6 dB, compared with the 6.5 dB worst case error with the horn source.

4.2.3 Hardwall Reverberant Calibration Summary

The measurement of sound power in the hardwall configuration depends on three factors:

a. The PWL-SPL calibration from the settling chamber, (and preparation room plus diffuser if used)

b. The fractional part of the source energy exiting to the settling chamber (or absorbed in test section if all three chamber measurements used).

c. The contribution of the source direct field to the microphone signals in the receiving chambers.

Approximations for these three factors are presented as Figures 18, 19 and 20 respectively. Since the three chambers are reasonably close in response, Figure 18 may be used as the PWL-SPL calibration for all three.

The use of these figures is best explained by example. Suppose the following data were taken in the 4000 Hz octave band when

the measured relative humidity was 50%.

Chamber	SPL
Settling Chamber	84
Preparation Room	81
Diffuser Leg	81

From Figure 18, Δ = 18 dB.

From experience, the source directionality index is assumed to be 10 dB, with the main lobe pointing towards the settling chamber. From Figure 19, Π = -3dB, and from Figure 20 $SPL_{rev} - SPL_{dir}$ = 10 dB.

Using only the settling chamber reading

$$PWL = SPL + \Delta - \Pi$$

$$= 84 + 18 + 3 = 105 \text{ dB}$$

Correcting for the direct field contribution (10 dB below the reverberant field), the final source sound power estimate is 104.6 dB re 10^{-12} watt.

Using all three chamber readings

$$PWL_{sc} = 84 + 18 = 102$$

$$PWL_{pr} = 81 + 18 = 99$$

$$PW_{ds} = 81 + 18 = 99$$

Total 105 dB

Again, correcting for the direct field contribution to the measured sound pressure levels, the source sound power estimate is 104.6 dB re 10^{-12} watt.

4.3 Direct Field Calibration

As previously reported (16), the direct field measurement characteristics of omni, and directional sources have been evaluated by two methods. The decrease in sound pressure level with distance from a 5.5 inch fan-inlet noise source was measured by LeRC for both the hard wall (present configuration) and soft wall cases. The information of interest were the near field characteristics of the nonideal source and the extent of the direct acoustic field.

The second method utilized the ILG sound power source to define the properties of the test section reverberant field (Table III).

Both methods led to an evaluation of the radius at which the reverberant and direct fields are equal. This radius is nominally 3.0 feet from all frequencies. Some consistent variations occur with position in the test section, but precise analysis is frustrated by the nonstationarity of the fan as a noise source.

The ability to describe directionality patterns of highly directional sources has subsequently been evaluated by rotating the microphone boom around the horn for 180 combinations of horn orientation, microphone radii, and frequency. The testing was performed on 17 July 1974. The horn and microphone boom with omnidirectional microphones are shown in Figure 21. The omnidirectional microphones are mounted on weathervaning "swords"

to keep the microphone pointing into the flow, minimizing microphone wind noise.

The test conditions and the measured centerline sound pressure levels are listed in Tables X and XI. These tables show that the centerline sound pressure level of a highly directional source can be measured accurately at radii from 2 to 10 feet. More specifically, the data indicate the following:

1. The reproducability of the results for a given frequency band and orientation in the tunnel, expressed as one standard deviation, ranges from 0.6 to 1.7 dB.

2. Angling the source towards the wall (Table XI) raised the measured source centerline levels from the measurements made with the source pointing downstream (Table X) in five of six bands.

3. The accuracy in measurement of the one-foot centerline sound pressure levels, relative to the calibrated free field levels, range from -1.5 dB to 3.4 dB.

4. The decreasing amount of test data for large microphone radii (5 and 10 feet) as the source is positioned and angled towards the wall (Table XI) emphasizes the geometrical constraints in the 9 x 15 foot test section.

5. The data measured at the three foot microphone position for $\alpha = 30°$, $\psi = -90°$, in frequency bands 1000, 2000, and 4000 Hz, average 10 dB lower than comparable data. It was assumed that an attenuator switch position was improperly

Table X. Hardwall Directionality Test Condition Summary With Measured Horn Centerline Sound Pressure Levels, Source Pointing Down Tunnel Centerline

Angle of attack α	Horn angle re inlet ψ	Boom Length ft.	Mic Radius from Horn Face, r, ft.	20 log d, d= r + 4	Input Signal Band Center Frequency Hz											
					1000		2000		4000		6300		8000		10,000	
					Mic SPL+ at radius		Mic SPL at radius		Mic SPL at radius		Mic SPL at radius		Mic SPL at radius		Mic SPL at radius	
					r	1.0'	r	1.0'	r	1.0	r	1.0'	r	1.0'	r	1.0'
0°	0°	4	2	15.5	113	128.5	112	127.5	106.0	121.5	106.5	122	107	122.5	103.2	118.7
		10	2	15.5	114.3	129.8	112.5	128	106	121.5	107	122.5	106	121.5	102	117.5
		6	2.5	16.3	114.5	130.8	113	129.3	106	122.3	107	123.3	106	122.3	102	118.3
		4	3	16.9	111.7	128.6	109.5	126.4	105.0	121.9	105.2	122.1	105.2	122.1	100.7	117.6
		6	3.5	17.5	112.0	129.5	112	129.5	106.0	123.5	105.0	122.5	103.5	121	99.5	117
		4	4	18.1	110.5	128.6	108	126.1	103.3	121.4	104.0	122.1	104	122.1	99.5	117.6
		10	5	19.1	112	131.1	111	130.1	105	124.1	104.5	123.6	102.7	121.8	99	118.1
		6	6	20	109.5	129.5	110	130	104	124	102.5	122.5	102.2	122.2	98.5	118.5
		10	10	22.9	107.5	130.4	107.3	130.2	101	123.9	99	121.9	99.2	122.4	98	120.9
30°	-30°	4	2	15.5	112.2	127.7	112	127.5	105.8	121.3	106.5	122	106.6	122.1	103.3	118.8
		10	2	15.5	114	129.5	112.6	128.1	106	121.5	108	123.5	106.8	122.3	102.2	117.7
		6	2.5	16.3	108	124.3	112	128.3	101	117.3	105.5	121.8	105.5	121.8	100.5	116.8
		4	3	16.9	111	127.9	111	127.9	105.7	122.5	105.8	122.7	106	122.9	102	118.9
		6	3.5	17.5	111.7	129.2	111.6	129.1	105.8	123.3	103	120.5	104	121.5	98.6	116.1
		4	4	18.1	109.7	127.8	109.5	127.6	104.3	122.4	104	122.1	104.9	123	101.8	119.9
		10	5	19.1	111.8	130.9	111.6	130.7	105.1	124.2	103.5	122.6	103.8	122.9	98.3	117.4
		6	6	20	108.6	128.6	109	129	104	124	102	122	102	122	98	118
		10	10	22.9	107.8	130.7	108	130.9	101.5	124.4	98.8	121.7	100.3	123.2	96.5	119.4
Average value (0°/0° and 30°/-30°)					---	129.1	---	128.7	---	122.5	---	122.3	---	122.2	---	118.2
Measurement standard deviation, dB					---	1.6	---	1.4	---	1.7	---	0.7	---	0.6	---	1.2
Free Field, Table IX and Ref. (40)					---	130	---	128.5	---	121	---	121.5	---	120	---	119
Difference, Free Field (-) Average					---	0.9	---	0.2	---	1.5	---	0.8	---	2.2	---	-0.8

+SPL, dB re 20 μ N/m², Horn current 0.25 ampere

Table XI. Hardwall Directionality Test Condition Summary With Measured Horn Centerline Sound Pressure Levels, Source Angled Towards Wall

Angle of attack α	Horn angle re inlet ψ	Boom Length ft.	Mic Radius from Horn Face r,ft.	20 log d, d = r + 4	Input Signal Band Center Frequency Hz											
					1000		2000		4000		6300		8000		10,000	
					Mic SPL at Radius		Mic SPL at Radius		Mic SPL at Radius		Mic SPL at Radius		Mic SPL at Radius		Mic SPL at Radius	
					r	1.0'	r	1.0'	r	1.0'	r	1.0'	r	1.0'	r	1.0'
0°	-60°	4	2	15.5	112.7	128.2	113	128.5	107	122.5	107	122.5	108.5	124	105	120.5
		4	3	16.9	112	128.9	112	128.9	107	123.9	106.7	123.6	107.5	124.4	105.3	122.2
		4	44	18.1	111.2	128.3	111	129.1	106	124.1	105.7	123.8	106.5	124.6	103	121.1
30°	-90°	4	2	15.5	113.4	128.9	112.6	128.1	107.1	122.6	107.3	122.8	108.0	123.5	104.0	119.5
		4	3	16.9	102.2	119*1	102.0	118*9	97.9	114*8	105.5	122.4	106.3	123.2	104.9	121.8
		6	3.5	17.5	110	127.5	112.0	129.5	107.0	124.5	104.2	121.7	105.4	122.9	103.6	121.1
		4	4	18.1	100.8	118*9	100.9	119*	97.9	116*	104.8	122.9	105.9	124	102.4	120.5
		6	6	20	107.9	127.9	111.2	131.2	106.4	126.4	103.5	123.5	104.5	124.5	101.5	121.5
Average value (0°/-60°,30°/-90°)					---	128.5	---	129.1	---	124.4	---	122.9	---	123.9	---	121
Measurement standard deviation, dB						0.6		0.9		1.4		0.7		±0.6		±0.9
Free Field, Table IX and Ref. 40					---	130	---	128.5	---	121	---	121.5	---	120	---	119
Difference, Free Field (-) Average					---	-1.5	---	0.6	---	3.4	---	1.4	---	3:9	---	2.0

*Levels increased by 10 dB for averaging

documented. The levels were arbitrarily increased by 10 dB for averaging.

Typical directionality plots obtained on-line are presented in Figure 22. Typical horn directivity curves were replotted relative to the source centerline levels and compared with anechoic conditions in Figures 23 through 26. These figures show the characteristic result that the main lobe of the directionality pattern is well defined to the 3 dB point where it begins to broaden out. This characteristic does not change significantly with radius from the source. However, the skirt of the directionality pattern is raised by acoustic reflections for the six foot radius measurements (Figures 25 and 26) relative to the three foot radius measurements (Figures 23 and 24). Therefore, the hall radius which is 3.0 feet for hardwall test section appears to be a limitation on the direct field measurement of highly directional sources as well as omni-directional sources.

4.4 Tunnel and Microphone Wind-On Noise

With the tunnel running, both the settling chamber and test section microphones evidence levels in excess of the electrical noise floor. Typical settling chamber measurements are presented as Figure 27 for test section dynamic pressures (q) ranging from 9.5 to 45 psf (455 to 2153 N/m^2). Normalizing these data by the third power of the dynamic pressure yields a good fit, Figure 28. In addition to the normalized sound pressure levels, Figure 28 also shows the prediction of grille noise attributed to the cooler coil bank. This prediction was derived from the sound power generation model, Section 3.2.4 of this report, and the

settling chamber calibration, Table III. The low frequency cooler coil predicted levels are significantly lower than the measured levels. Above 2000 Hz, the predicted levels approach the measured levels, suggesting a significant contribution.

Figure 29 shows normalized sound pressure levels for the preparation room. These levels are similar to those measured in the settling chamber. This is the same result as observed with an omnidirectional source in the test section, Table V.

Test section microphone, wind-on, noise measurements for dynamic pressures of 20 to 60 psf (957 to 2871 N/m^2) are shown in Figure 30. These data were normalized by 30 log q/q_{ref}, and are presented in Figure 31. Also presented in Figure 31 are predictions of microphone wind noise, turbulent boundary layer noise, and vortex noise from inlet support and trailing edges. The sound pressure level predictions are derived from the sound power level predictions, Sections 3.2.1, 3.2.2, and 3.3.3, respectively, along with the test section calibration, Table III. Only the noise predicted for the transition of the test section to the diffuser, which is admittedly inappropriate, agrees with the measured data over all frequency bands. In spite of inappropriate application of the noise generation model, the favorable comparison of model and measured results indicates that significant noise generation may be associated with flow entering into the diffuser. The microphone turbulence generated predicted levels intersect the measured levels in the high frequency bands, indicating a contribution to the test section microphone measured levels, at least for $q \leq 25$ psf.

With respect to microphone wind noise, the shape of the predicted spectra is different from the measured spectra, Figure 31. In

addition, the measured spectrum is different, in shape, from other microphone, turbulence generated, noise measurements. Figure 32. Finally, the measurements made in the test section vary as U^6, not U^4. All these factors suggest that the test section microphone is sensing acoustic noise, not pseudo-noise from turbulence.

Figure 33 compares the normalized settling chamber measurements with levels which could be attributed to test section sources. The agreement again suggests that the measured test section levels are indeed acoustic.

5.0 CONCLUSIONS AND RECOMMENDATIONS

The results of this study indicate that accurate source sound power estimations can be made in the hardwall configuration using settling chamber sound pressure level measurements along with relative humidity levels and approximations of source directivity. The measurement standard deviation ranges from 0.2 to 3.9 dB.

The accuracy of source sound power estimations can be improved if preparation room and diffuser leg sound pressure level measurements are used along with settling chamber sound pressure level measurements. In addition, approximation of source directivity would be required only to avoid errors due to direct field levels exceeding reverberant field levels, not for sound power distribution. With these steps the measurement standard deviation may be reduced to $\pm$ 1.0 dB.

Accurate direct field measurements in the test section are limited to a radius of 3 feet by the reverberant field, with the one exception of a highly directional source pointing directly upstream. The measurement reproducibility ranges from 0.6 to 1.7 dB (one standard deviation). The source measurement accuracy ranges from - 1.5 to 3.4 dB. This may be due in part to source strength variation.

The dominant source of wind-on microphone noise cannot be precisely identified from analytic models and available data. However, the results suggest the following conclusions:

1. Sound pressure levels measured by test section microphones are due to true acoustic levels, not turbulence induced pseudo-noise.

2. The most likely area of significant noise generation is the transition from the test section to the diffuser.

If reduction of wind-on noise is required, measurements should be made to support or contradict these conclusions. Removing the nose cone from a test section microphone and measuring wind-on noise would be the most instructive. Surveys down the diffuser would also be of benefit.

The conduct of these tests has served to emphasize various procedural errors, equipment problems, and pitfalls. The following recommendations are intended to help avoid subsequent problems.

1. Measure relative humidity in the settling chamber and relate to weather bureau readings. Utilize for sound power estimation from existing settling chamber sound pressure data.

2. Utilize a calibration, electro dynamic omni-directional source for subsequent evaluation and calibrations.

3. On-line presentation of levels is feasible and should be encouraged.

4. Maintaining end-to-end calibration traceability is essential.

5. The driven shield connection between cathode follower and sword should be checked routinely (the sensitivity should not be changed by moving the microphone from cathode follower to sword).

6. The test section should be lined with acoustical absorptive material in order to measure directivity (already done).

7. When using a microphone in the preparation room for source sound power estimation, place the microphone in the center of the work area, not near the test section slots.

6.0 SYMBOL DEFINITION

The symbols used throughout this report are principally defined with English units because the wind tunnel dimensions and dynamic pressure are described in English units. However, nondimensional and engineering relations are expressed in both English and SI units for reference as follows:

Symbol	Definition	Units
A	Atmospheric absorption at 70 feet, dB	-
c	Speed of sound	ft/sec (m/sec)
C_d	Coefficient of drag	-
d	Spoiler diameter	ft(m)
DI	Directivity index, 10 log Q	-
D_p	Pipe diameter	ft (m)
f	Frequency	Hz
f_c	Cutoff frequency	Hz
f_p	Peak frequency	Hz
k	Constant of proportionality, expressed in dB	-
m	Atmospheric absorption	1/ft (1/m)
p(t)	Fluctuating dynamic pressure	lb/ft^2 (N/m^2)
p(t)	Time average rms pressure	lb/ft^2 (N/m^2)
P_i	Fraction of source sound power to that exiting to the ith chamber	-
PWL	Sound power level, dB re 10^{-12} Watt	-

Symbol	Definition	Units
PWL_{OA}	Overall sound power level, dB re 10^{-12} Watt	-
$PWL(\omega)$	One-third octave band sound power level, dB re 10^{-12} Watt	-
q	Dynamic pressure	lb/ft^2 (N/m^2)
Q	Directivity	-
r	Radius	ft (m)
r_H	Hall radius	ft (m)
S	Area	ft^2 (m^2)
SPL	Sound pressure level, dB re 20 $\mu N/m^2$	-
T_R	Reverberation time (60 dB)	seconds
u	Fluctuating velocity	ft/sec (m/sec)
U	Mean velocity	ft/sec (m/sec)
V	Volume	ft^3 (m^3)
W	Edge length	ft (m)

Symbol	Definition	Units
α	Angle of attack	degrees
α	Acoustic absorption coefficient	-
α_t	Average total absorption	-
α_{SAB}	Sabine absorption (in the absence of atmospheric absorption)	-
β	Angle of microphone boom relative to inlet centerline	degrees
γ	Angle between source centerline and representative transition point	degrees
δ	Boundary layer thickness	ft (m)
δ^*	Boundary layer displacement thickness	ft (m)
Δ	$PWL_i - SPL_i$ dB	-
Δ_r	Attenuation due to spherical spreading, 20 log r	-
ϵ	Normalized pressure drop	-
Π	Power index, 10 log P	-
ρ	Density	slugs/ft^3(kg/m^3)
τ	Turbulence index, u/U	-
ψ	Angle of source relative to inlet centerline	degrees
ω	Radial frequency, $2\pi f$	radians/sec

REFERENCES

1. Yuska, J.A., Diedrich, J.H., Clough, N., "Lewis 9 x 15 Foot V/STOL Wind Tunnel," NASA TM X-2305, July 1971.

2. Beranek, Leo L., Labate, Samuel, and Ingard, Uno: Acoustical Treatment for the NACA 8-by 6-Foot Supersonic Propulsion Wind Tunnel. NACA TN 3378, 1955.

3. Rentz, P.E., Scharton, T.D., Wilby, J., "Shotgun and Cannon Directional Microphone Calibrations and Wind Tunnel Acoustic Measurements," BBN Technical Memorandum 19410-4, 18 July 1975.

4. Bies, D.A., "Investigation of the Feasibility of Making Model Acoustic Measurements in the NASA Ames 40 x 80 Foot Wind Tunnel," BBN Report 1870 (Contract NAS2-5742), April 1970

5. Bies, D.A., "Investigation of the Feasibility of Making Model Acoustic Measurements in the NASA Ames 40 x 80 Foot Wind Tunnel," BBN Report 2088 (Contract NAS2-6206), 1971.

6. Arndt, R.E.A., Boxwell, D.A., "A Preliminary Analysis of the Feasibility of Rotor Noise Measurements in the AMRDL-Ames 7 x 10 foot Wind Tunnel," NASA Working Paper, October 1971.

7. Arndt, R.E.A., Boxwell, D.A., "A State-of-the-Art Report on Aeroacoustical Testing in Conventional Wind Tunnels," Paper at 84th Meeting Acous. Soc. Amer., Miami Beach, Florida, November 1971.

8. Vér, I.L., Malme, C.I., Meyer, E.B., "Acoustical Evaluation of the NASA Langley Full-Scale Wind Tunnel," BBN Report 2100, (NAS1-9559), January 1971.

9. Vér, I.L., "Acoustical Modeling of the Test Section of the NASA Langley Research Center's Full-Scale Wind Tunnel, Bolt Beranek and Newman Report 2280, Contract NAS1-9559, November 1971.

10. Vér, I.L., "Acoustical Evaluation of the NASA Langley V/STOL Wind Tunnel," BBN Report 2288 (Contract NAS1-9559), December 1971.

11. Holbeche, T.A., Williams, J., "Acoustic Considerations for Noise Experiments at Model Scale in Subsonic Wind Tunnels," Royal Aircraft Establishment Rech. Rep. 72155, September 1972.

12. Oetting, R.B., "Preliminary Noise Measurements in the Open-Jet of the VKI Low Speed Wind Tunnel, L-1," Von Karman Institute for Fluid Dynamics Tech., Note 89, May 1973.

13. Vér, I.L., Franken, Peter A., "Conceptual Design Study of the Noise Control Treatment for the NASA Full-Scale Subsonic Wind Tunnel," BBN Report 2368, 15 June 1972.

14. Wilby, J.F., Scharton, T.D., "Evaluation of the NASA Ames #1 7 x 10 Foot Wind Tunnel as an Acoustic Test Facility," BBN Report 2936, 30 June 1975.

15. Hayden, R.E., Murray, B.S., Galaitsis, A.G., "Preliminary Investigation of Acoustic Requirements for NLR 8 x 6 m Low Speed Wind Tunnel," BBN Report 3087, June 1975.

16. Piersol, A.G., Rentz, P.E., "Utilization and Enhancement of the NASA Lewis 9 x 15 Foot V/STOL Wind Tunnel for Inlet Noise Research," BBN Report 2743, 19 May 1974.

17. Morse, P.M., Vibration and Sound, McGraw Hill Book Company, Inc., New York, 1948, page 387.

18. Beranek, L.L., Noise and Vibration Control, McGraw Hill Book Company, New York, 1971, page 228.

19. IBID, page 242.

20. Aerospace Recommended Practice, ARP 866, "Standard Values of Atmospheric Absorption as a Function of Temperature and Humidity," Revised October 1973, Society of Automotive Engineers, 485 Lexington Ave., New York, N. Y.

21. Beranek, L.L., Noise and Vibration Control, McGraw Hill Book Company, New York, 1971, page 170.

22. Beranek, L.L., Acoustics, McGraw Hill Book Company, New York, 1954, page 114.

23. Fuchs, H.V., "Note on Aero-acoustic Measurements in Open-Jet Wind Tunnels," Institut Fuer Turbulenzforschung, Berlin, Report IB357-74/4 (1974).

24. Bruel and Kjaer Production Data Brochure 13-003, "Condenser Microphone Cartridges."

25. Rasmussen, G., "Windscreening of Microphones," Bruel and Kjaer, unpublished technical report, 9 pages.

26. Noiseux, D.U., Noiseux, N.B., Kadman, Y., "Development, Fabrication and Calibration of a Porous Surface Microphone in an Aerofoil," BBN Report 3022 (NASA CR 137652), March 1975.

27. Noiseux, D.U., "Study of Porous Surface Microphones for Acoustic Measurements in Wind Tunnels," BBN Report 2539, April 1973.

28. NASA Lewis letter, Reference Contract NAS 3-19410, from J. H. Dietrich to P. E. Rentz, dated December 10, 1974.

29. Hayden, R.E., "Noise from Interaction of Flow with Rigid Surfaces: A Review of Current Status of Prediction Techniques," NASA CR-2126, April 1973.

30. Beranek, L.L., Noise and Vibration Control, McGraw Hill Book Company, New York, 1971, page 518.

31. Yudin, E. Y., "The Acoustic Power of the Noise Created by Airduct Elements," *Sov. Phys.-Acoust.*, vol. 1, pp 383-398, 1955.

32. Gordon, C., "Spoiler-generated flow noise," Part I, "The Experiment," and Part II, "Results," *J. Acoust. Soc. Am.*, vol. 43, pp. 1041-1048, 1968, and vol. 45, pp. 214-223, 1969.

33. Godman, R.R., and Stein, S., "Elimination of Noise in the Heat Exchanger of a Supersonic Wind Tunnel," NASA Lewis Flight Propulsion Laboratory internal memorandum, 1957.

34. Beranek, L.L., Noise and Vibration Control, McGraw Hill Book Company, New York, 1971, page 522.

35. Hubert, M., "Untersuchungen uber Geräusche durchstromter Gitter," doctoral dissertation, Berlin Tech. Univ., 1960.

36. Unpublished NASA Lewis report, transmitted via communication from D. Deitrick, 5/28/76.

37. Daly, B.B., "Noise Level in Fans," *Journal of the Institute of Heating and Ventilating Engineers*, pp. 39-51, May, 1958.

38. Sharland, I.J., "Sources of Noise in Axial Flow Fans," *J. Sound and Vibration*, Vol. 1, No. 3, pp. 302-322, 1964.

39. Beranek, L.L., Noise and Vibration Control, McGraw Hill Book Company, New York, 1971, page 144.

40. BBN Technical Memorandum No. 19410-3, "Directional Acoustical Source Characteristics," Peter E. Rentz and John F. Wilby, July 1975.

41. Noiseux, D. U., "Study of Porous Surface Microphones for Acoustic Measurements in Wind Tunnels," BBN Report 2539, Submitted to: NASA Ames Research Center, April 1973.

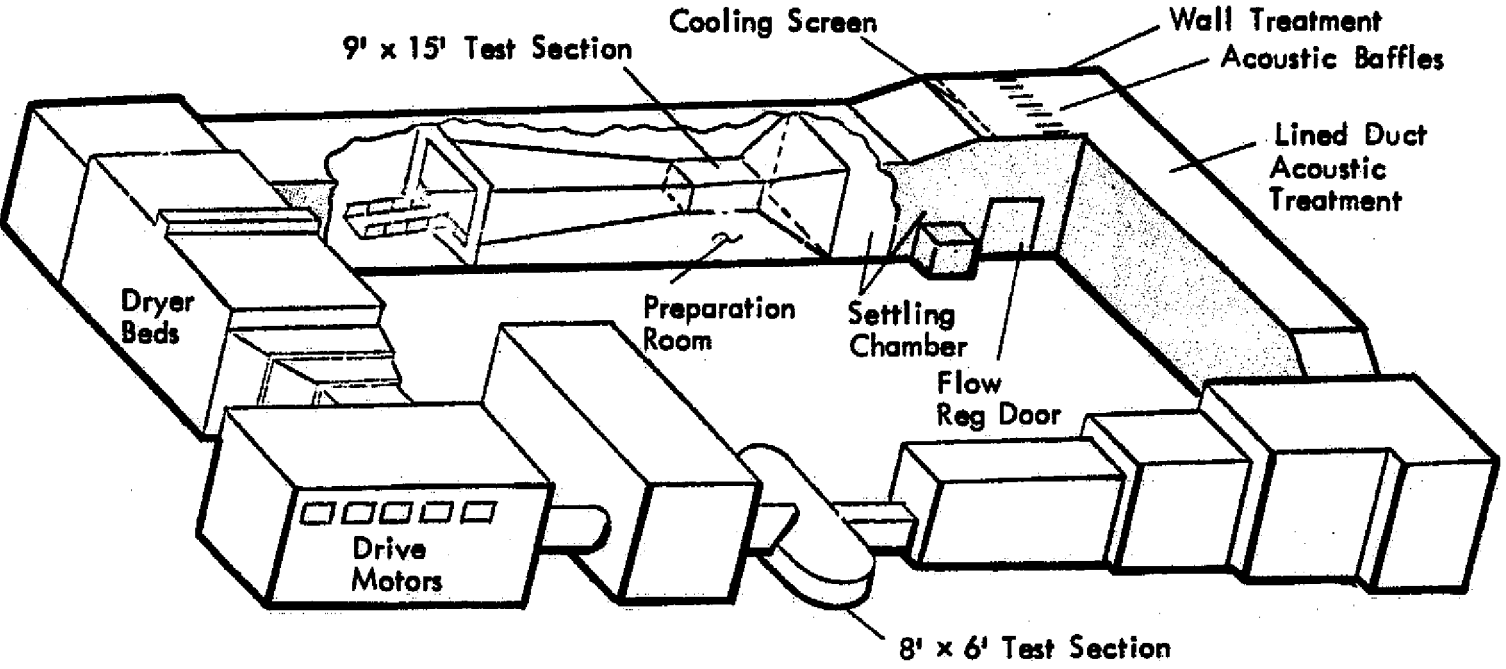

FIGURE 1. NASA LEWIS 9 x 15 FOOT LOW SPEED TEST SECTION IN RETURN LEG OF 8 x 6 FOOT SUPERSONIC WIND TUNNEL

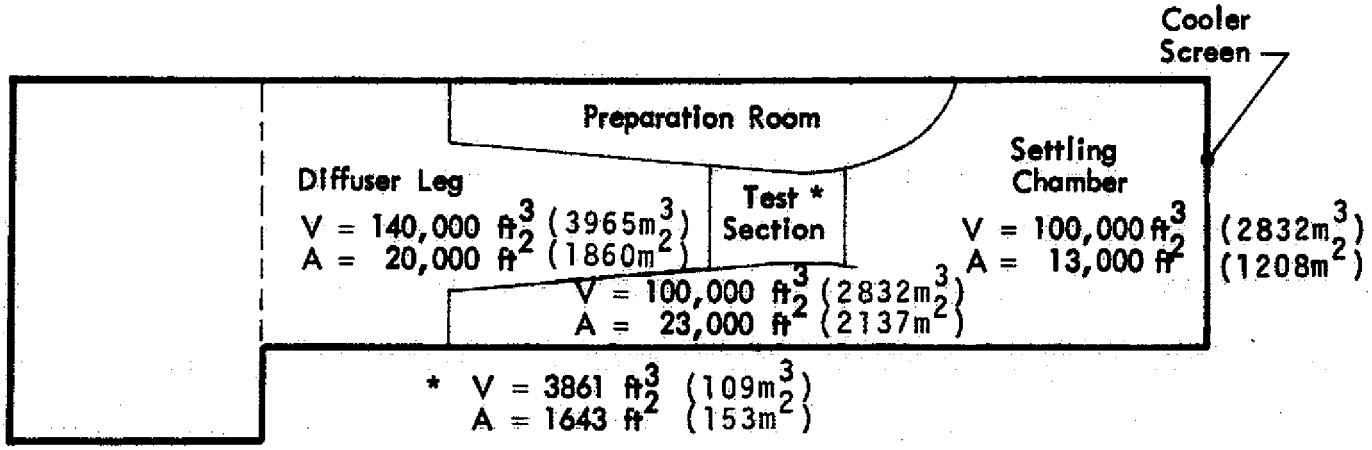

FIGURE 2. FOUR CHAMBER ACOUSTIC MODEL OF LeRC 9 x 15 FOOT LOW SPEED WIND TUNNEL

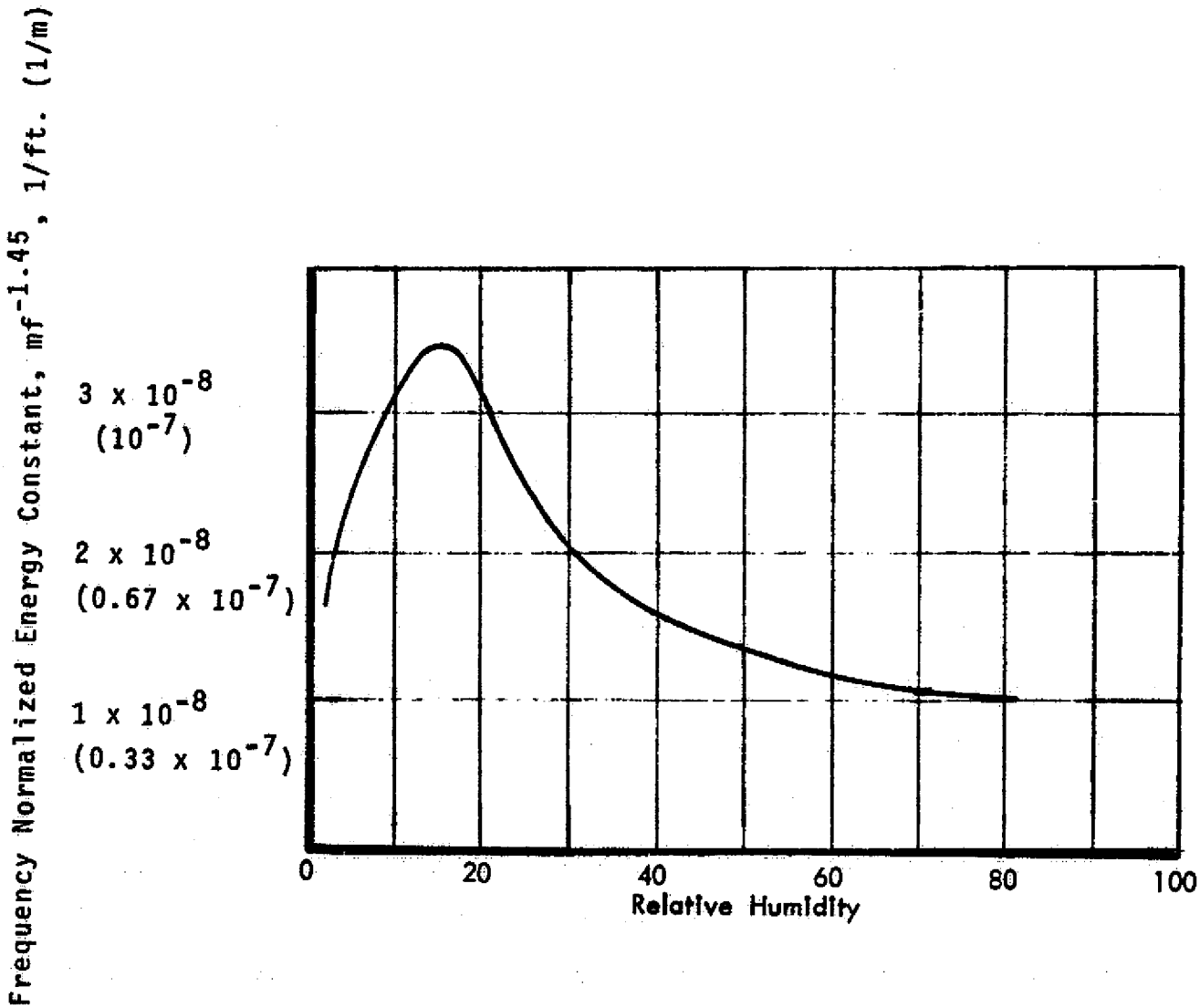

FIGURE 3. ENERGY ATTENUATION CONSTANT FOR AIR IN A REVERBERANT CHAMBER, DERIVED FROM REFERENCE 19

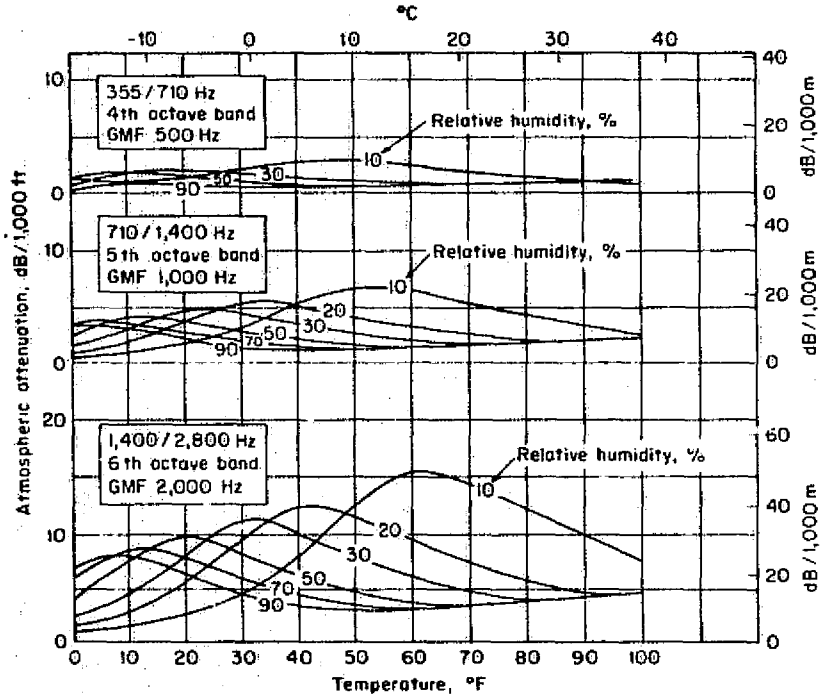

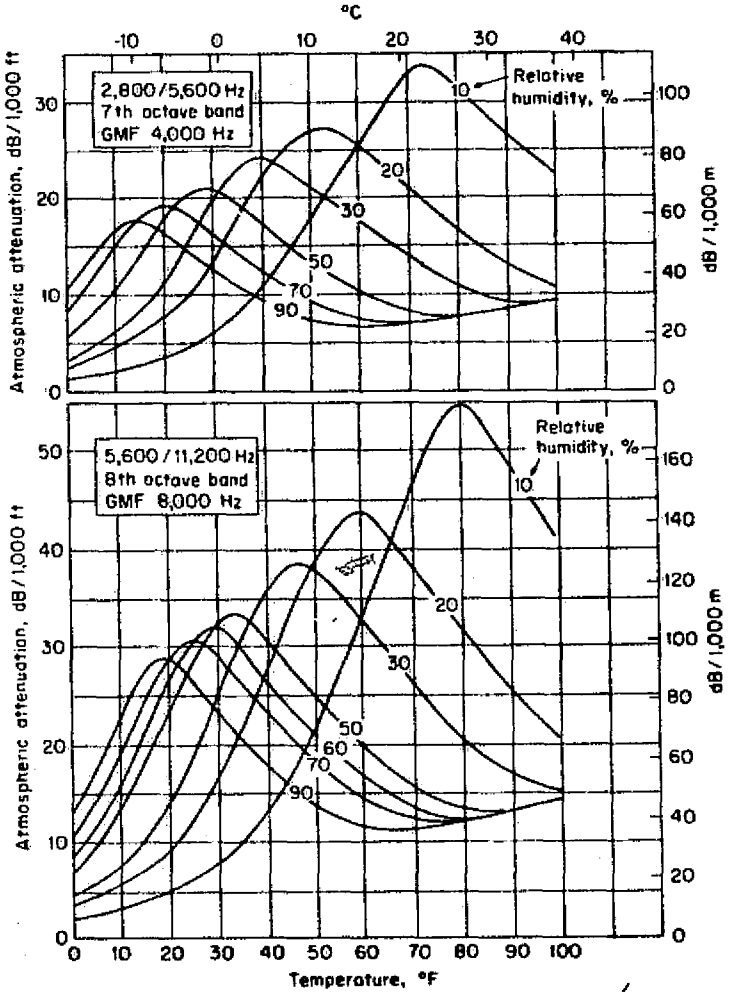

FIGURE 4. ATMOSPHERIC ATTENUATION FOR AIRCRAFT-TO-GROUND PROPAGATION IN dB/1000 FT (OR dB/1000 m) FOR OCTAVE BANDS CENTERED AT 500, 1000, 2000, 4000 AND 8000 Hz (21)

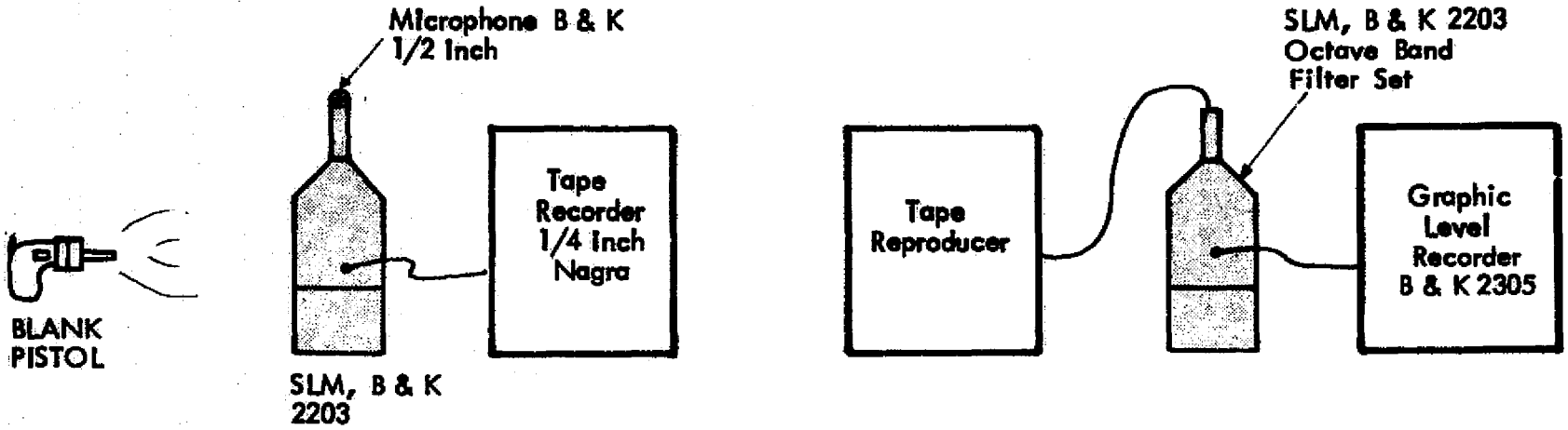

(a) IMPULSE DECAY RATE MEASUREMENT

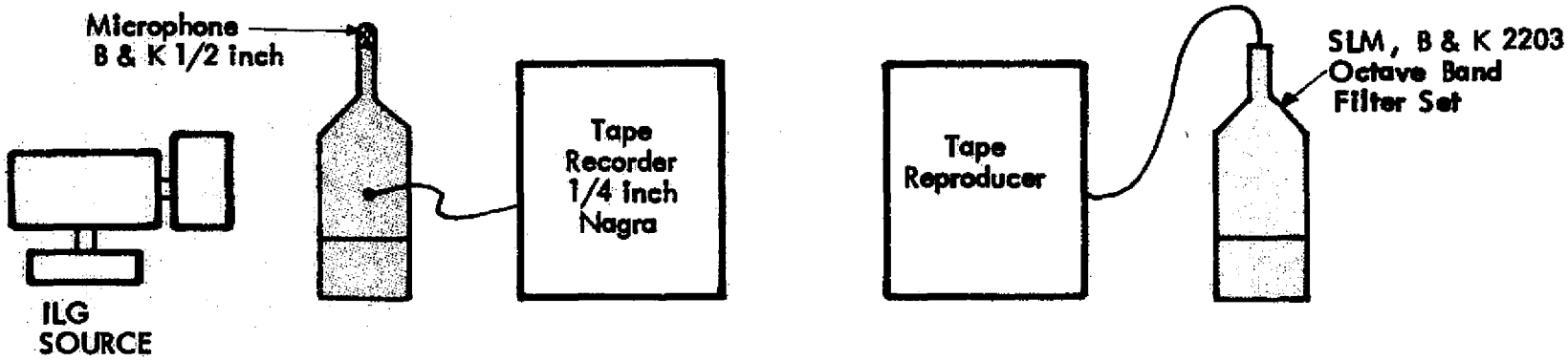

(b) SOUND PRESSURE MEASUREMENT, CALIBRATED SOUND POWER SOURCE

FIGURE 5. TEST APPARATUS AND INSTRUMENTATION BLOCK DIAGRAM

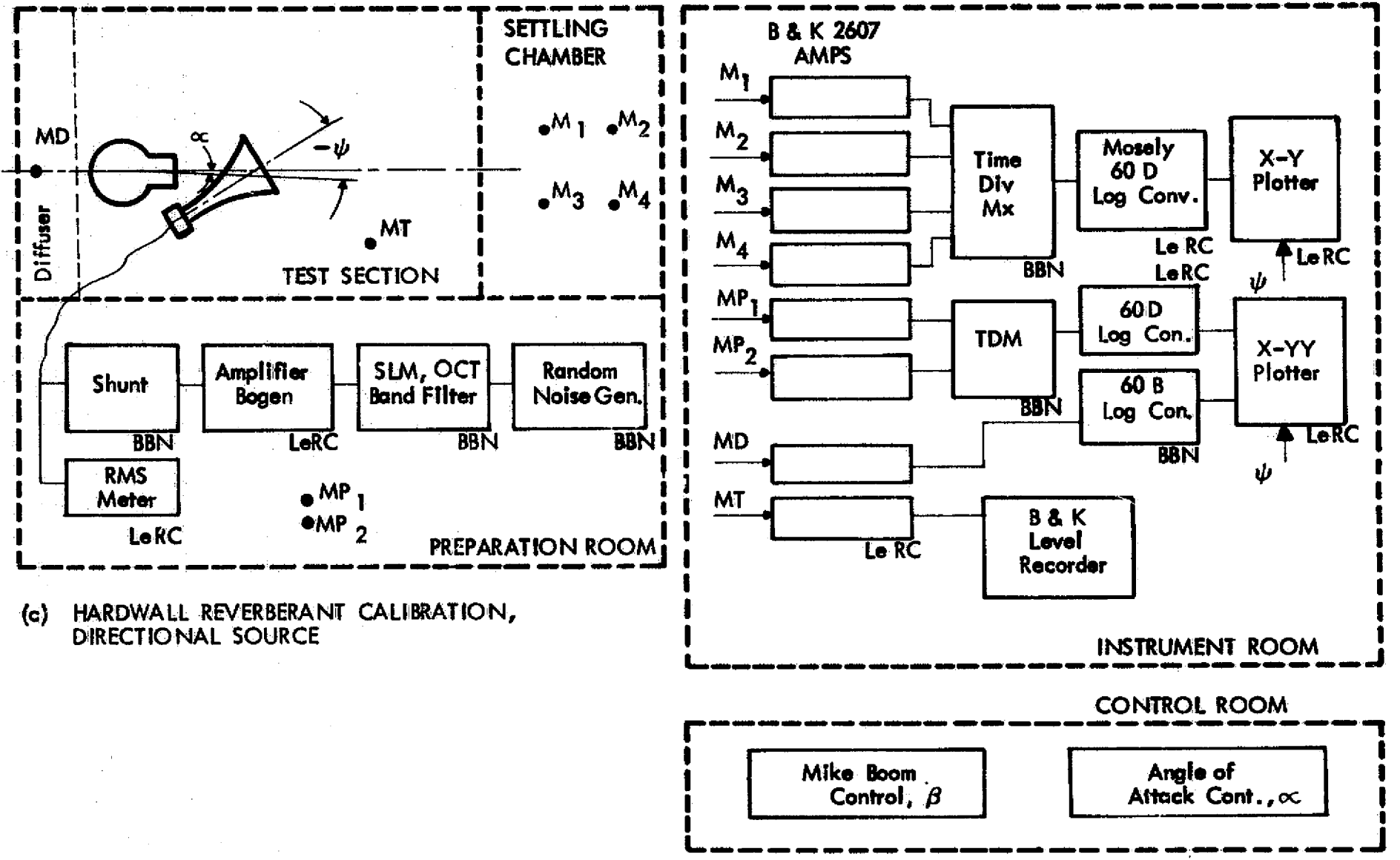

(c) HARDWALL REVERBERANT CALIBRATION, DIRECTIONAL SOURCE

FIGURE 5. (Cont)

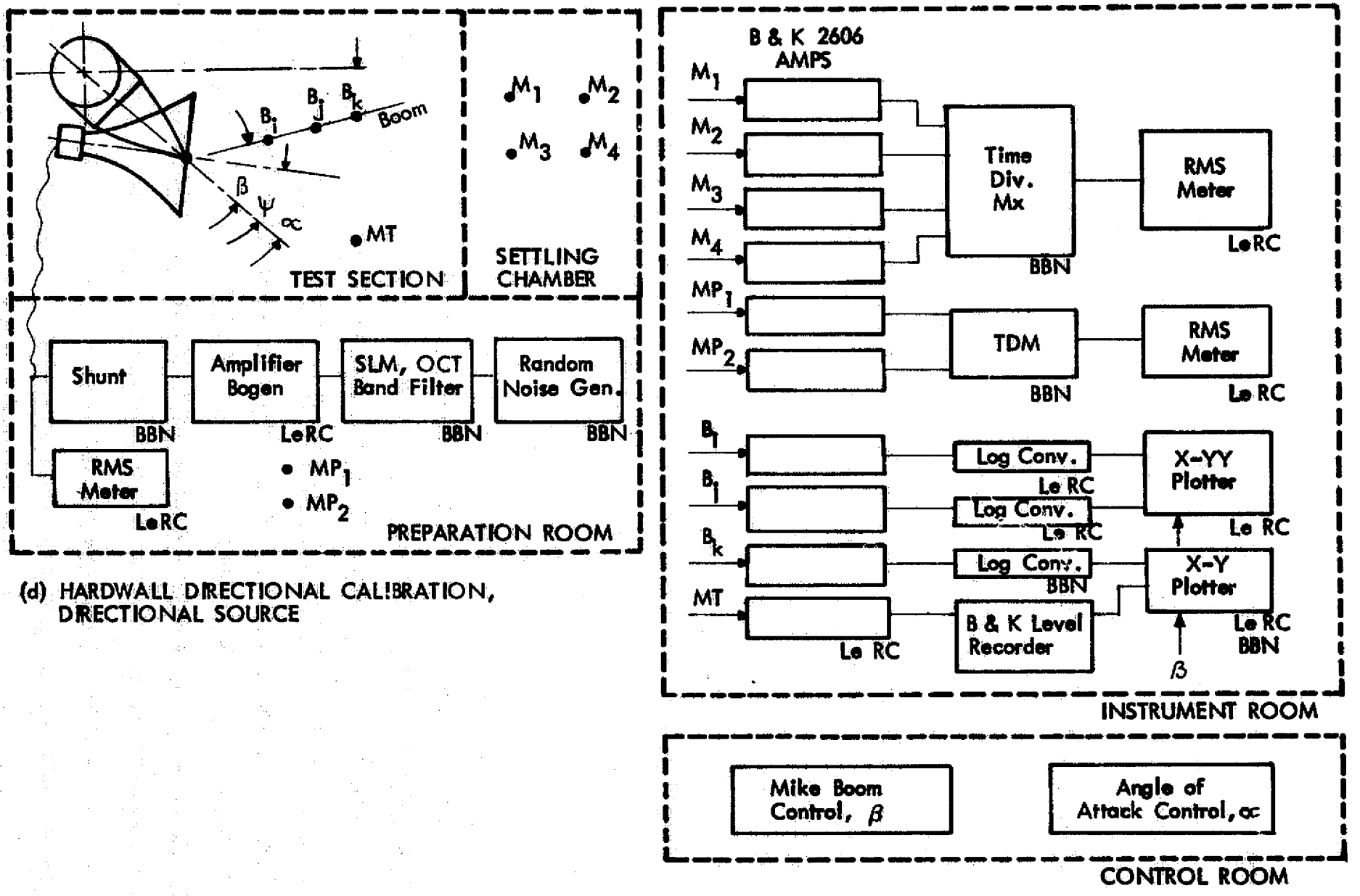

(d) HARDWALL DIRECTIONAL CALIBRATION, DIRECTIONAL SOURCE

FIGURE 5. (Cont)

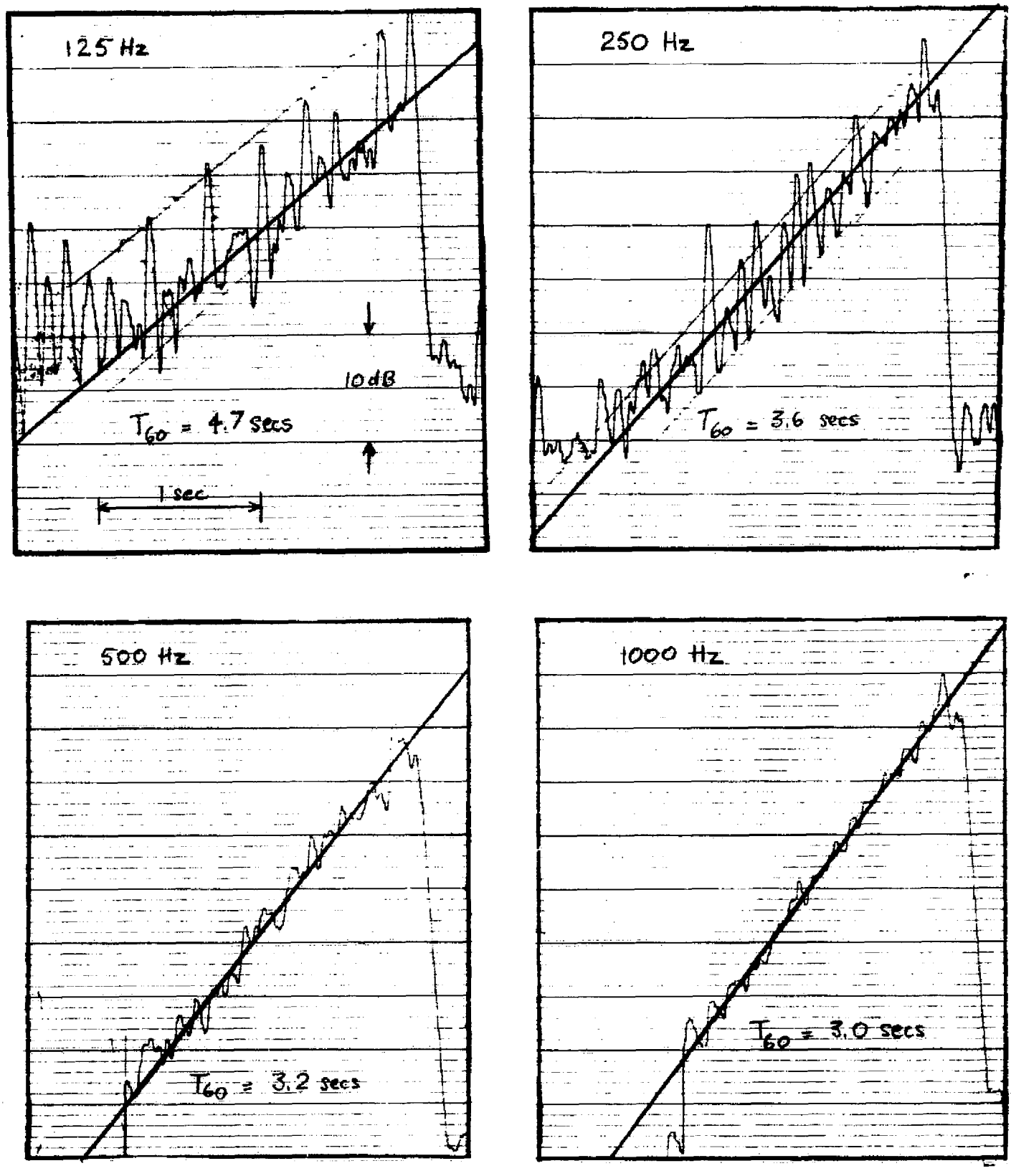

FIGURE 6. SETTLING CHAMBER OCTAVE BAND REVERBERANT DECAYS, 24 FEB 1974, TEST 2 (Tape Played Backwards)

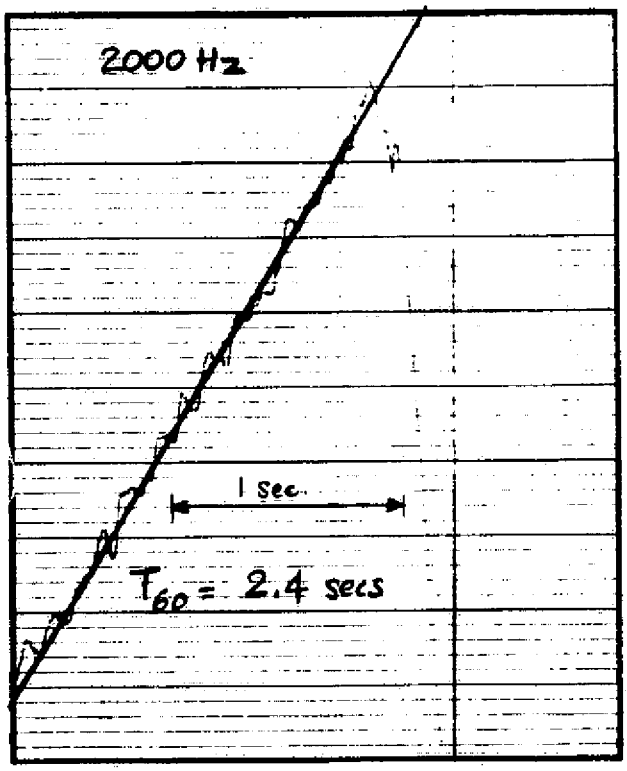

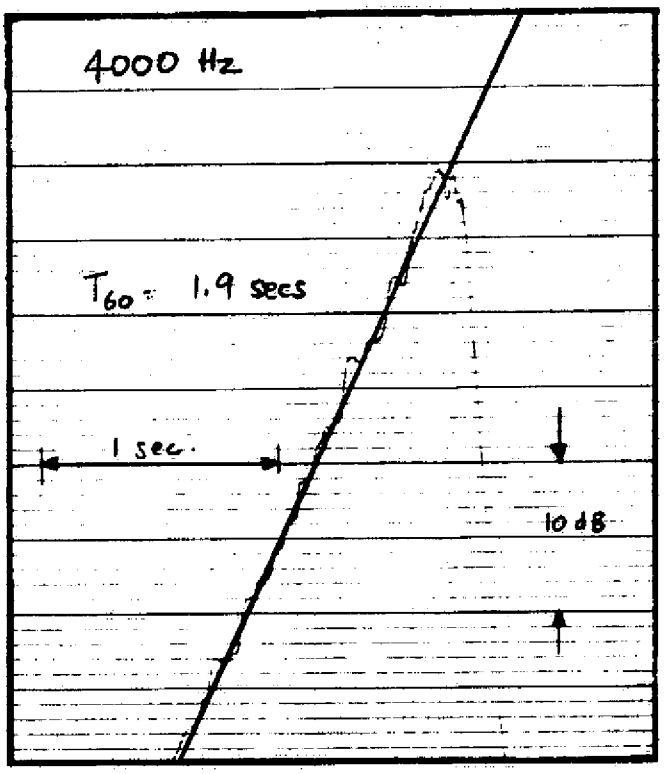

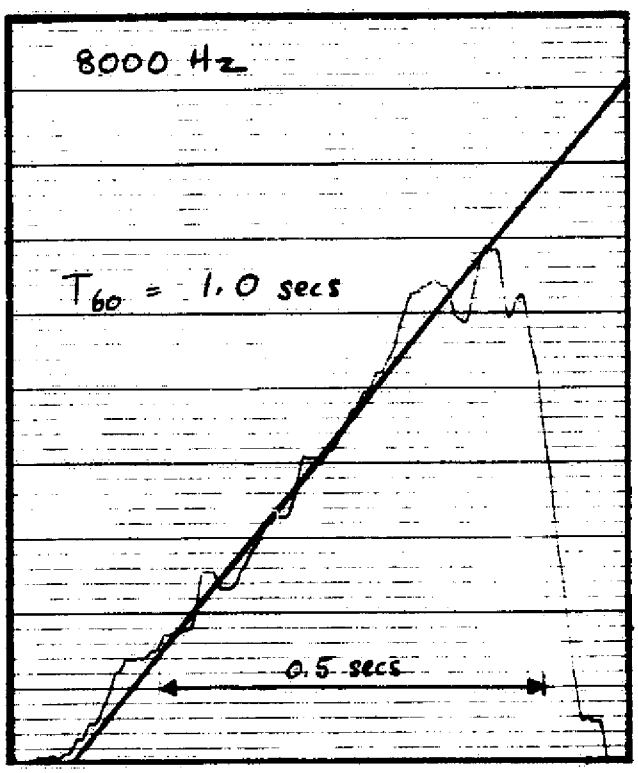

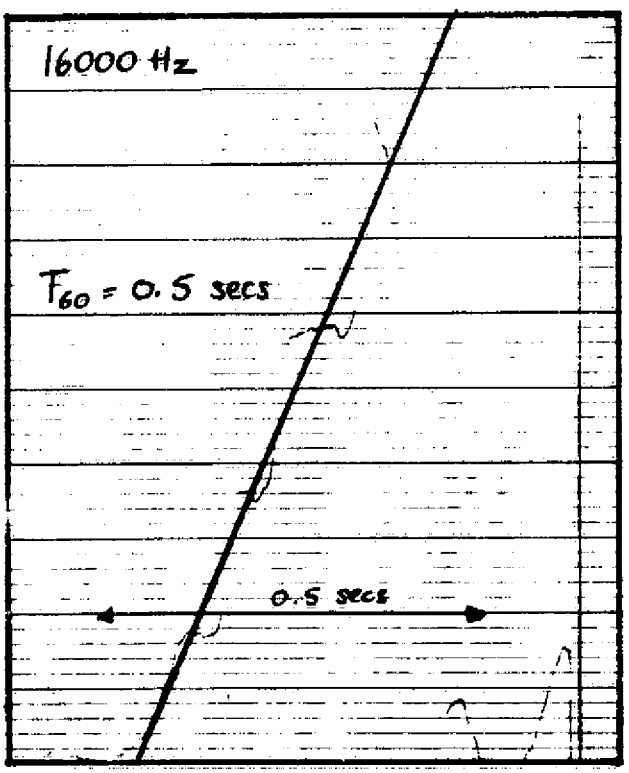

FIGURE 6. (Cont)

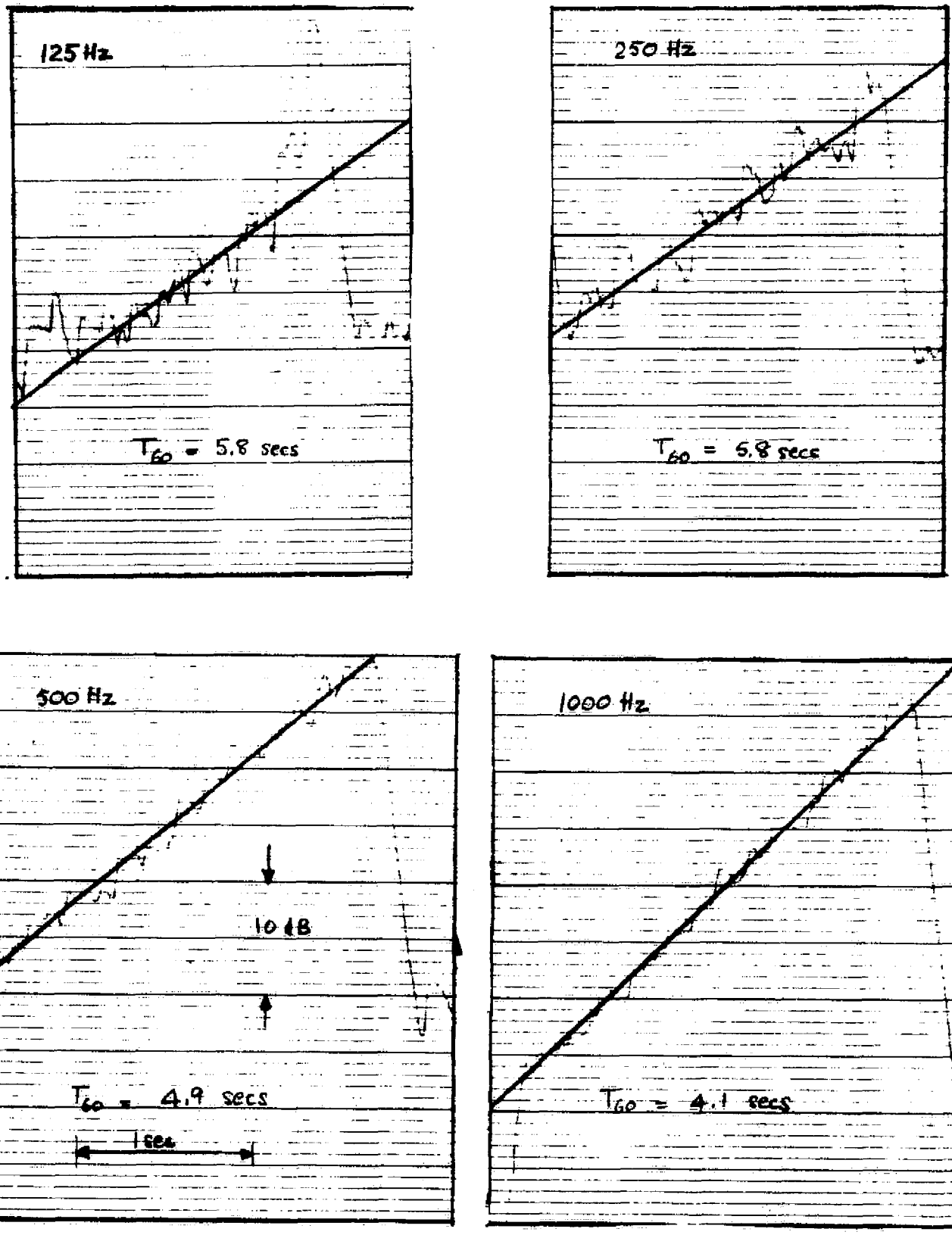

FIGURE 7. DIFFUSER LEG OCTAVE BAND REVERBERANT DECAYS, 29 NOV 1973, TEST 2 (Tape Played Backwards)

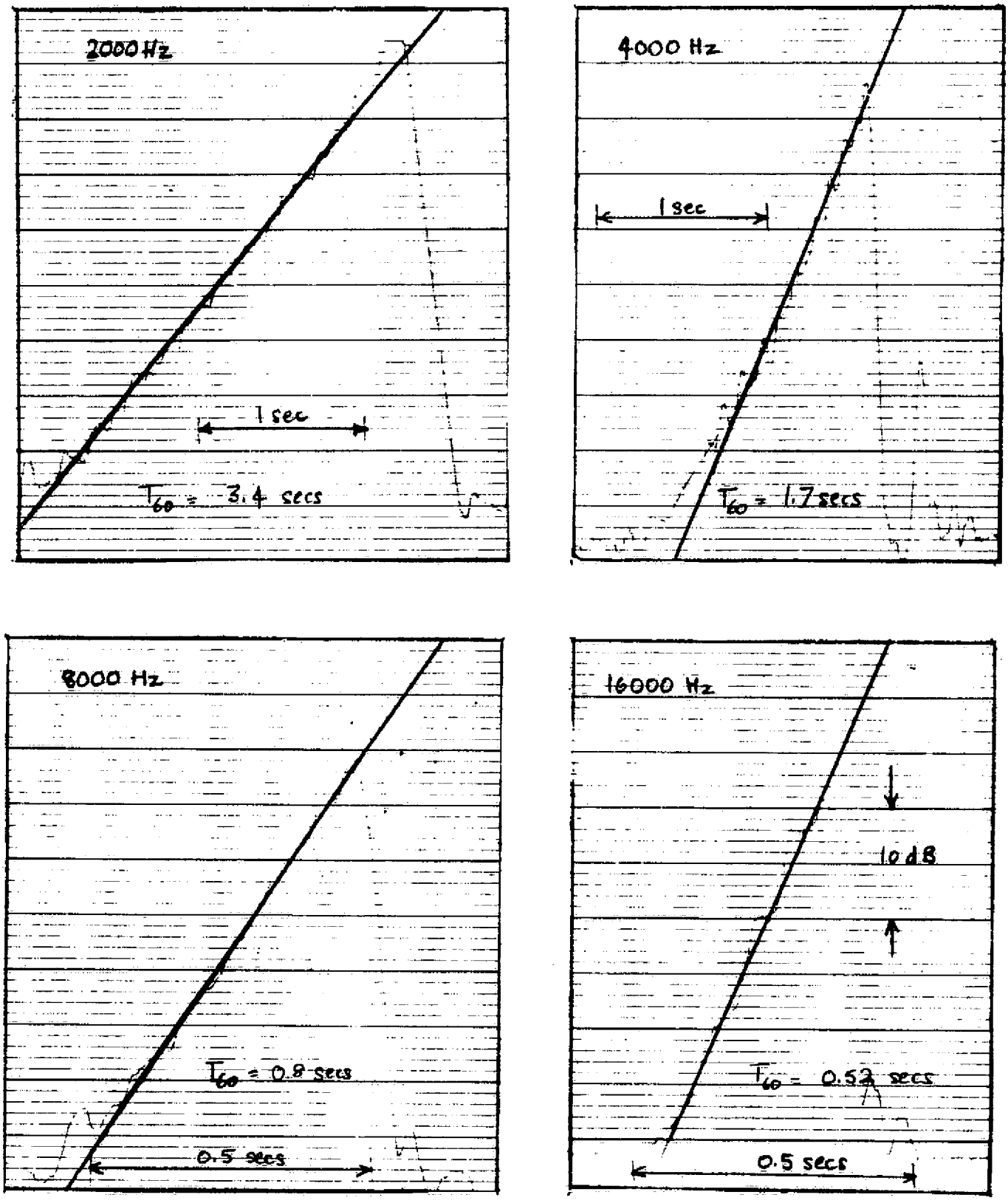

FIGURE 7. (Cont)

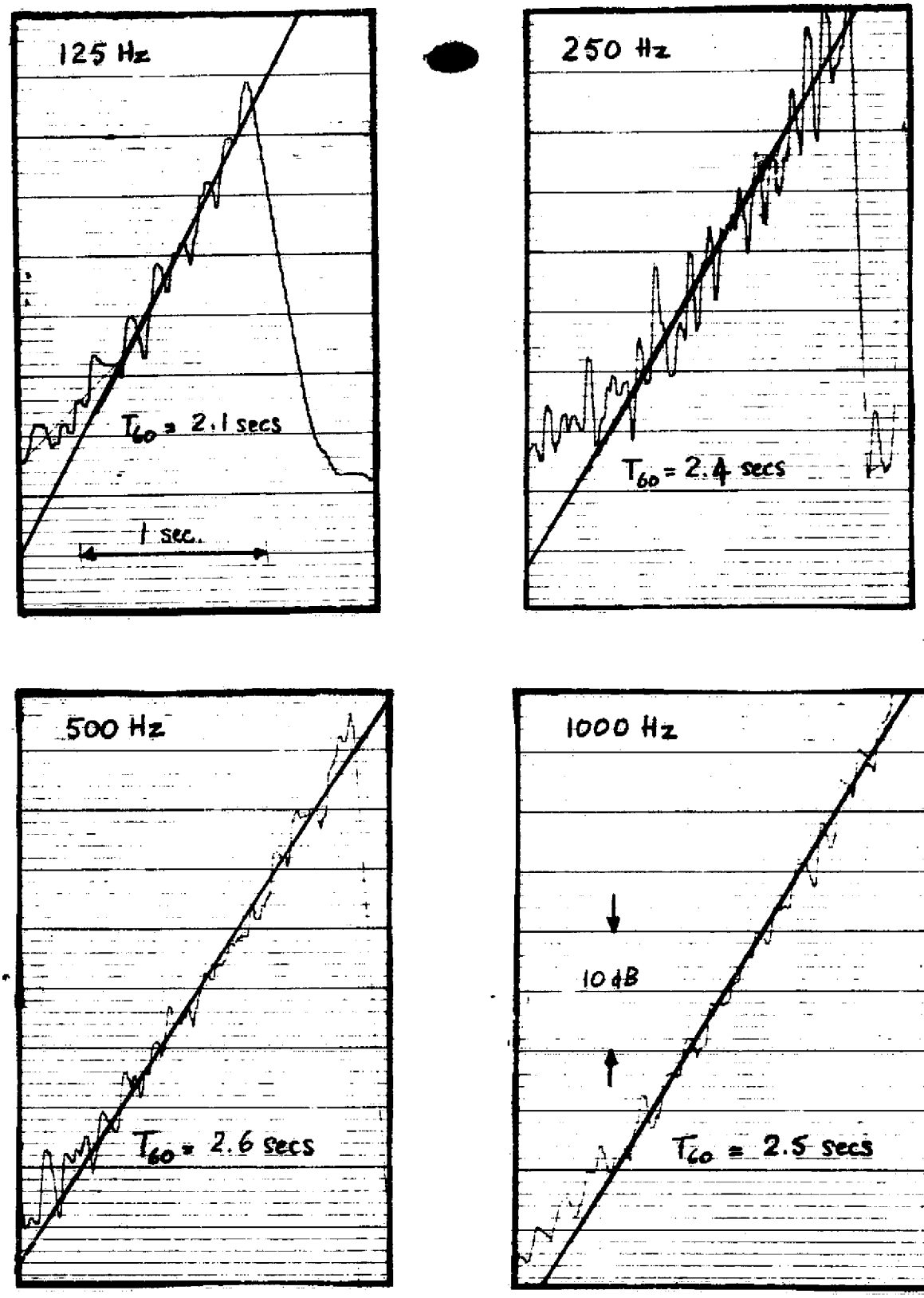

FIGURE 8. PREPARATION ROOM OCTAVE BAND REVERBERANT DECAYS, 24 FEB 1974, TEST 1 (Tape Played Backwards)

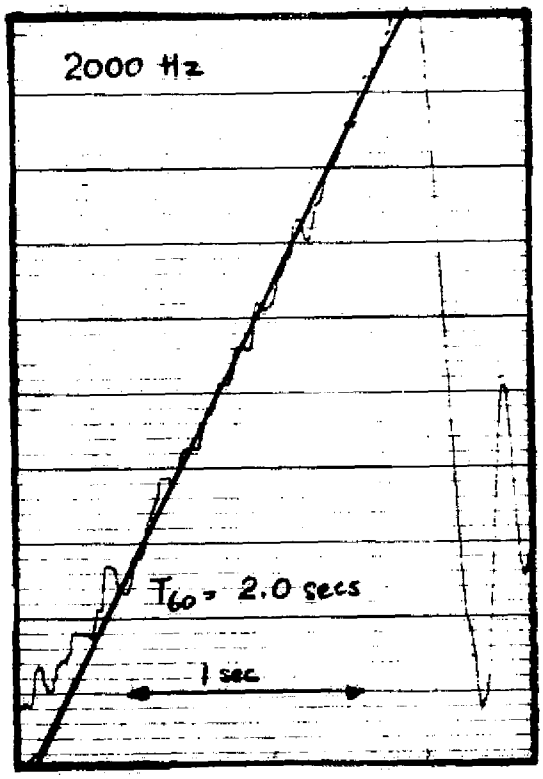

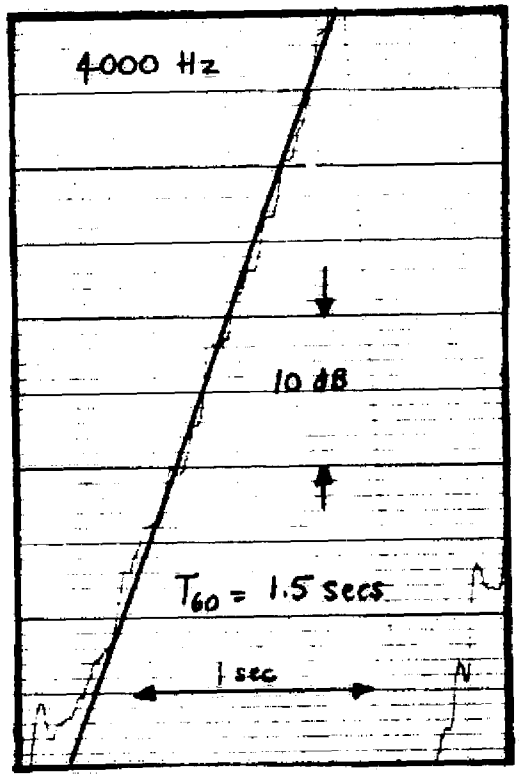

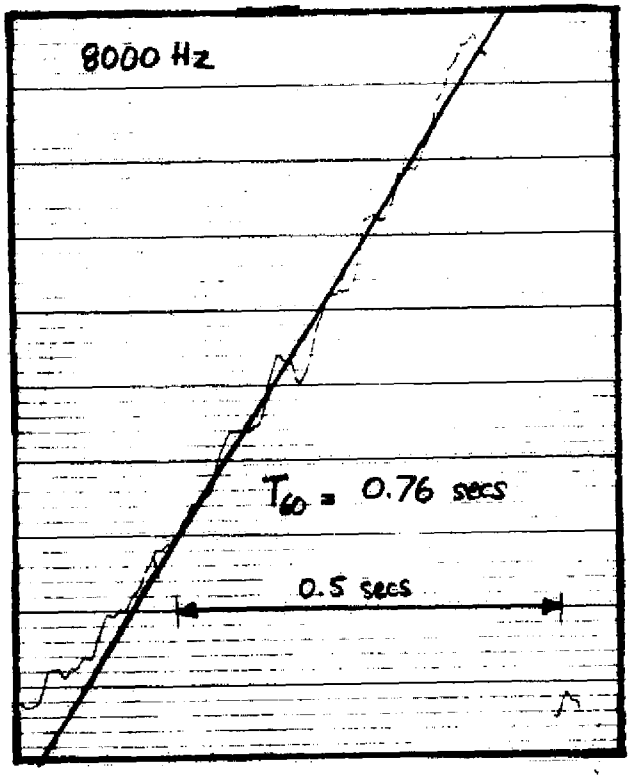

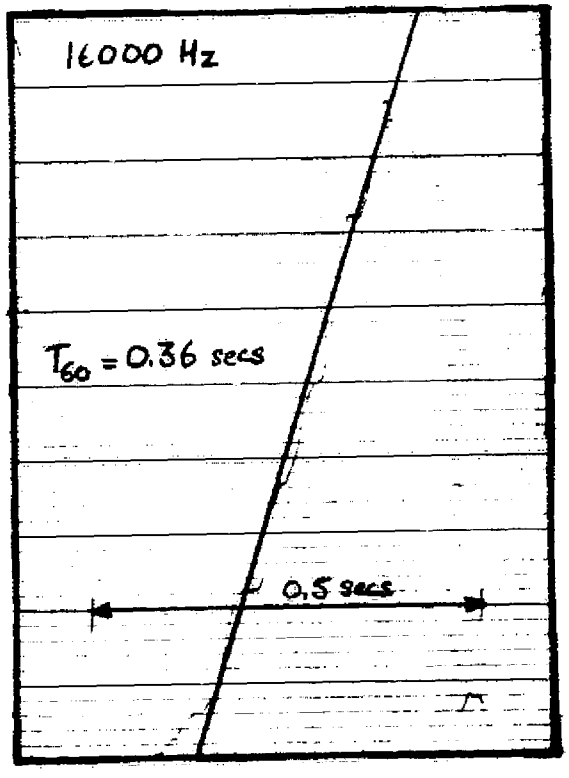

FIGURE 8. (Cont)

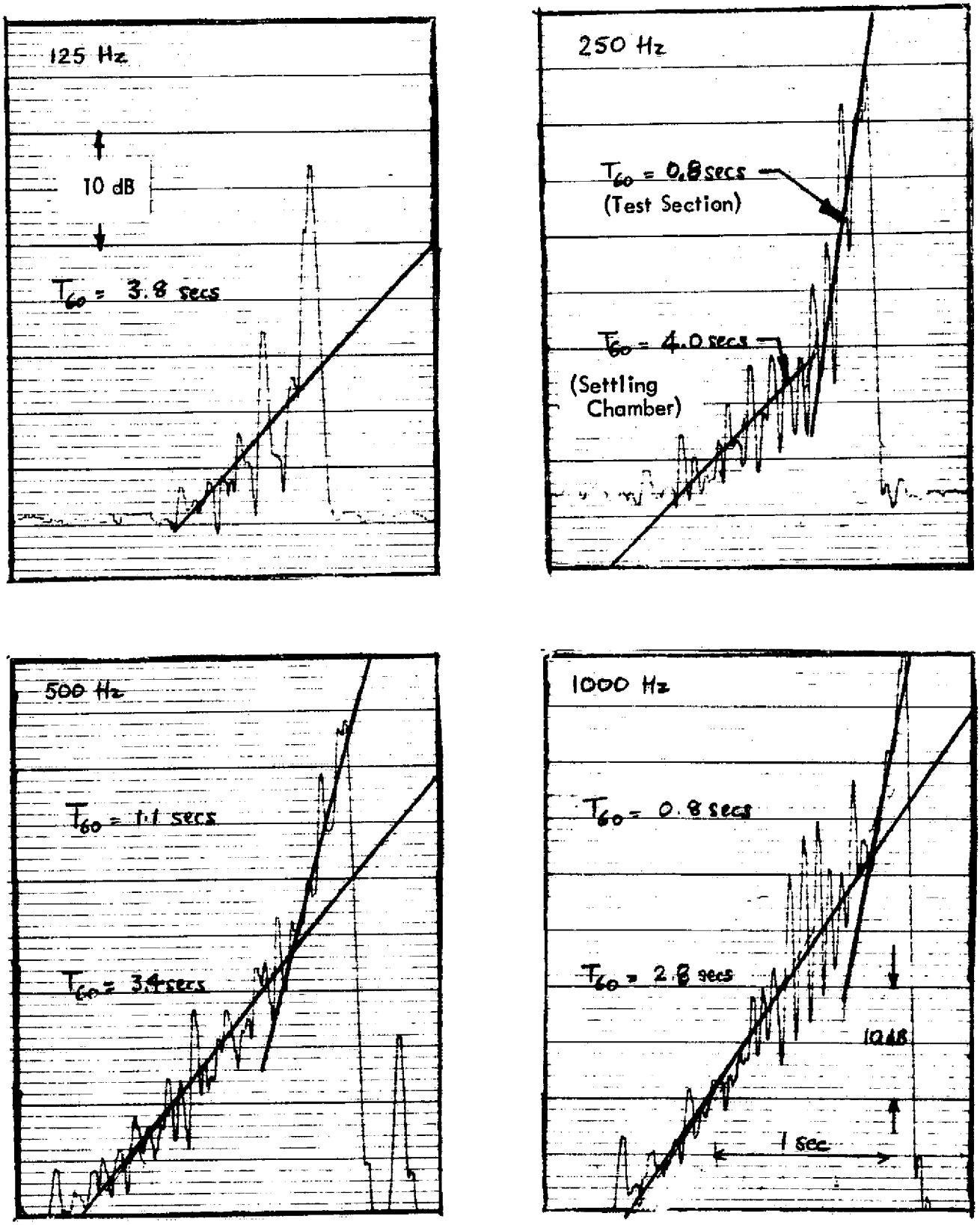

FIGURE 9. TEST SECTION OCTAVE BAND REVERBERANT DECAYS, 27 FEB 1974, TEST 2 (Tape Played Backwards)

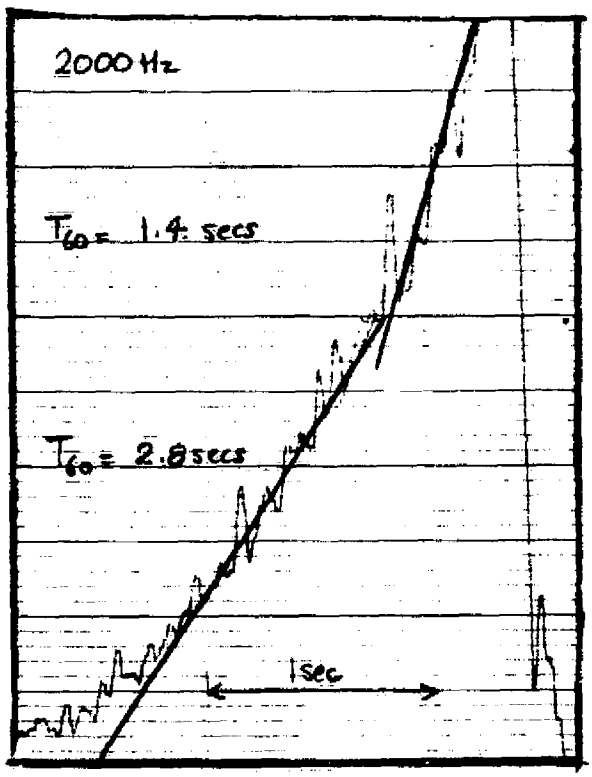

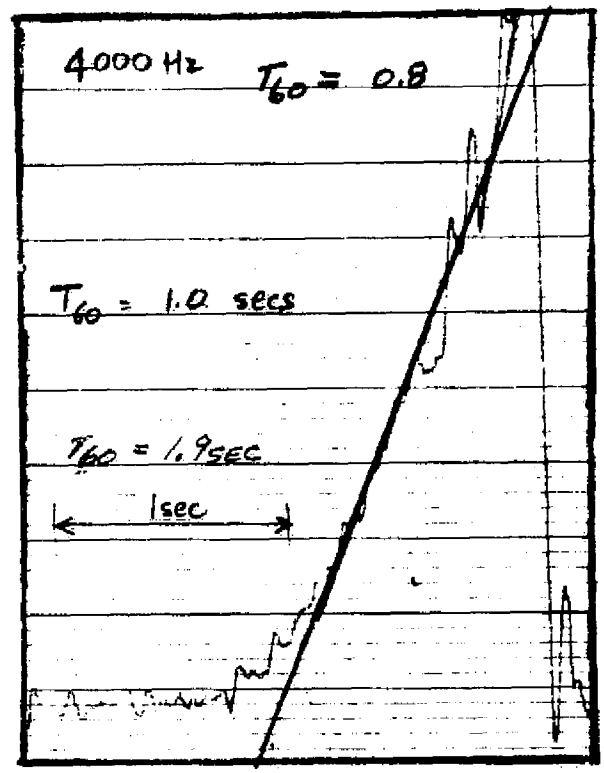

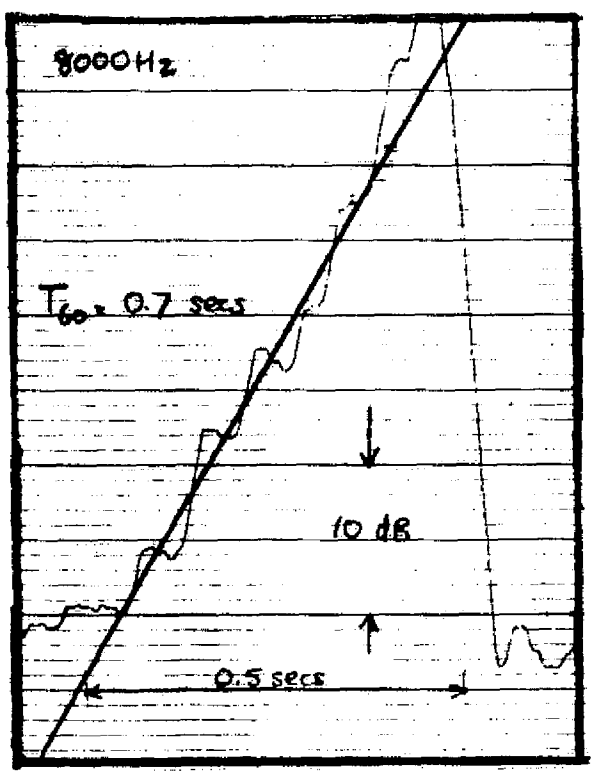

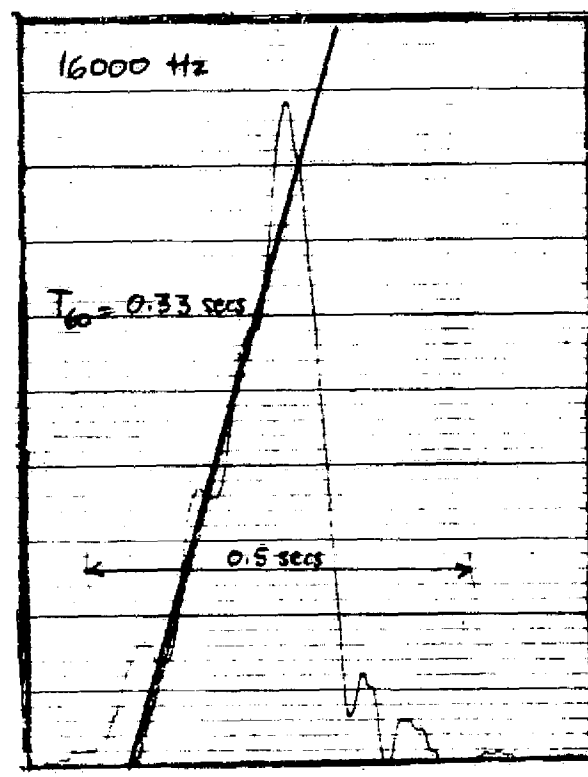

FIGURE 9. (Cont)

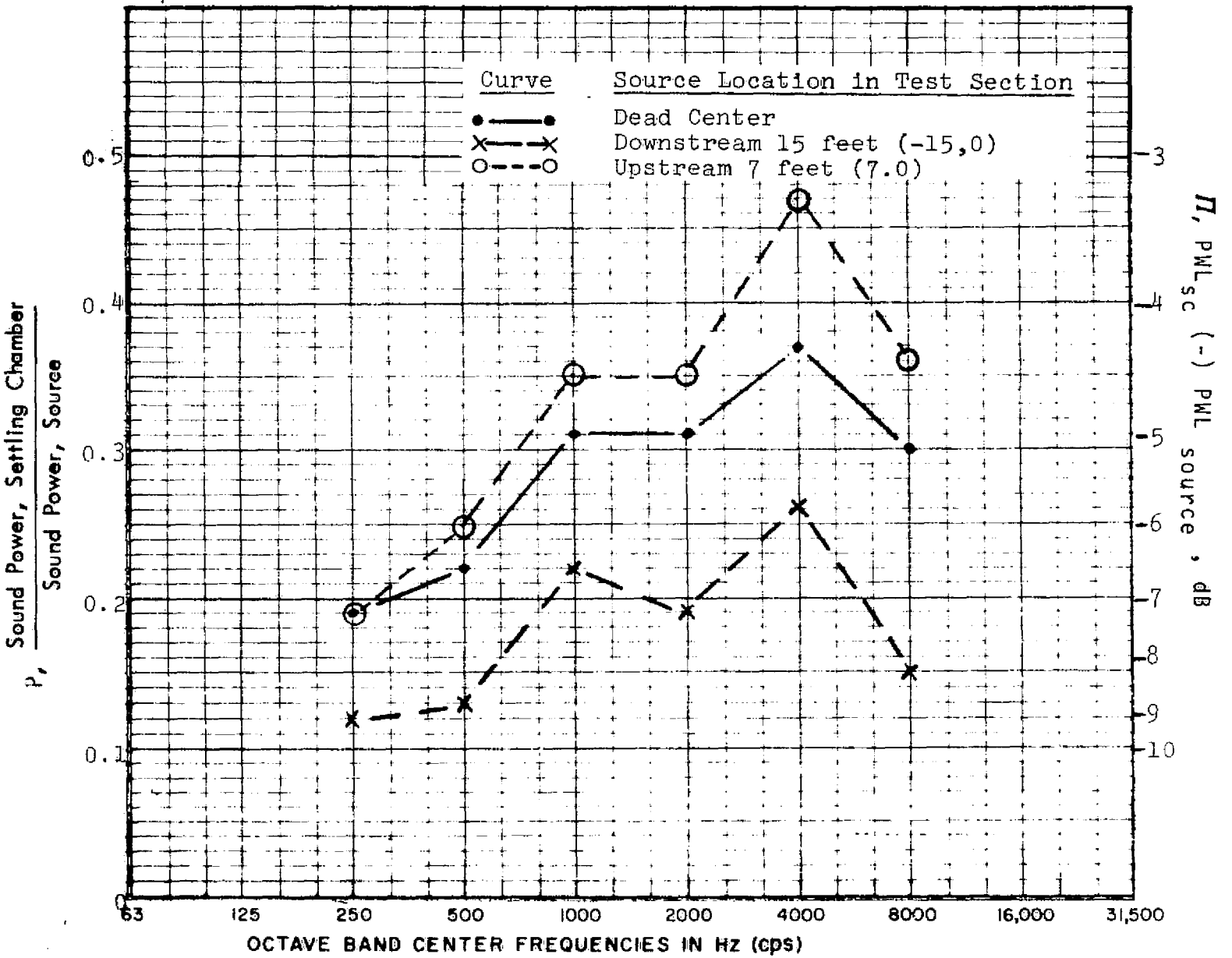

FIGURE 10. SOURCE SOUND POWER TRANSMITTED TO SETTLING CHAMBER FOR DIFFERENT ILG OMNI-DIRECTIONAL SOURCE LOCATIONS

NASA
C-74-2365

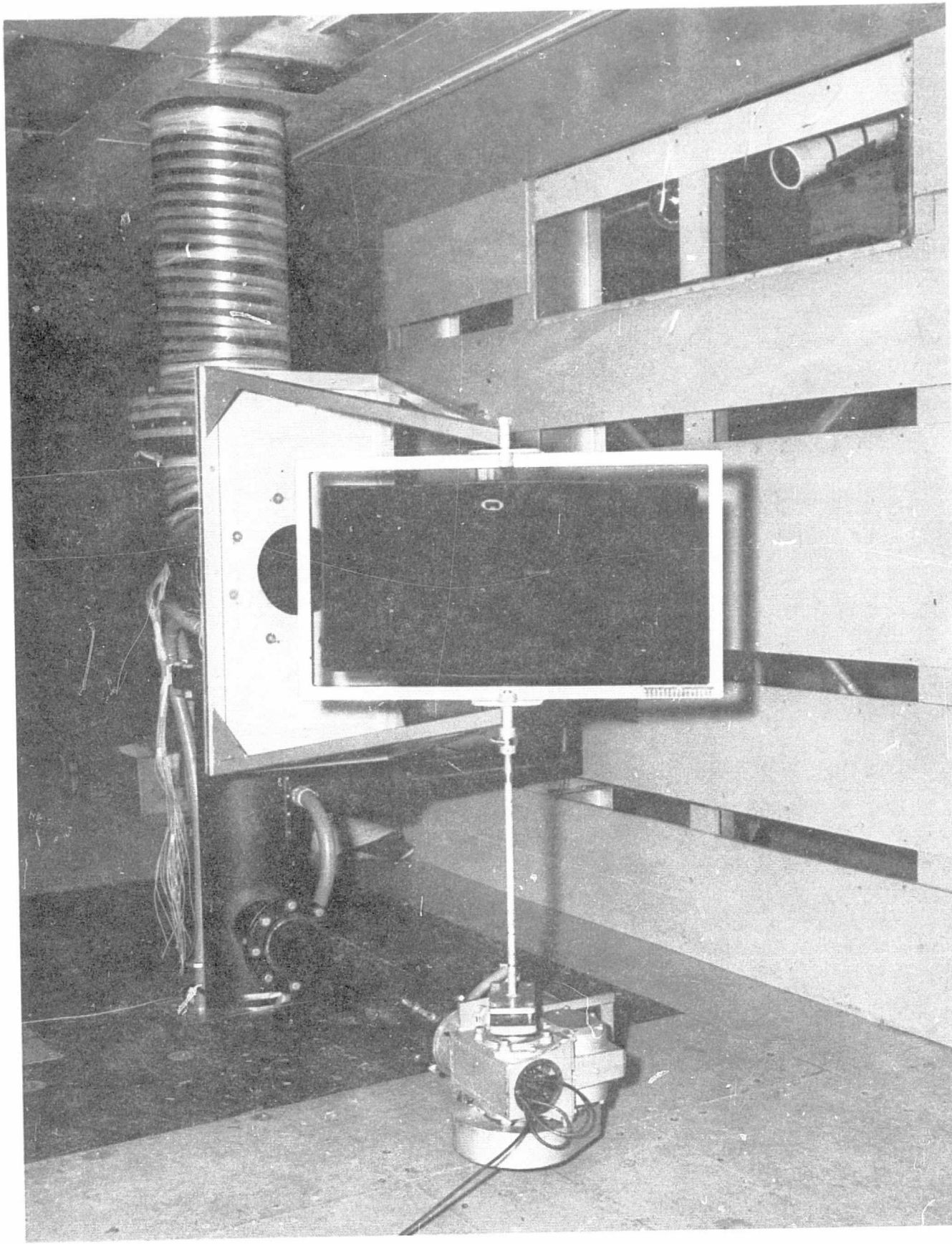

ORIGINAL PAGE IS
OF POOR QUALITY

FIGURE 12. ROTATING DIRECTIONAL SOURCE, REVERBERANT HARDWALL SOUND POWER CALIBRATION

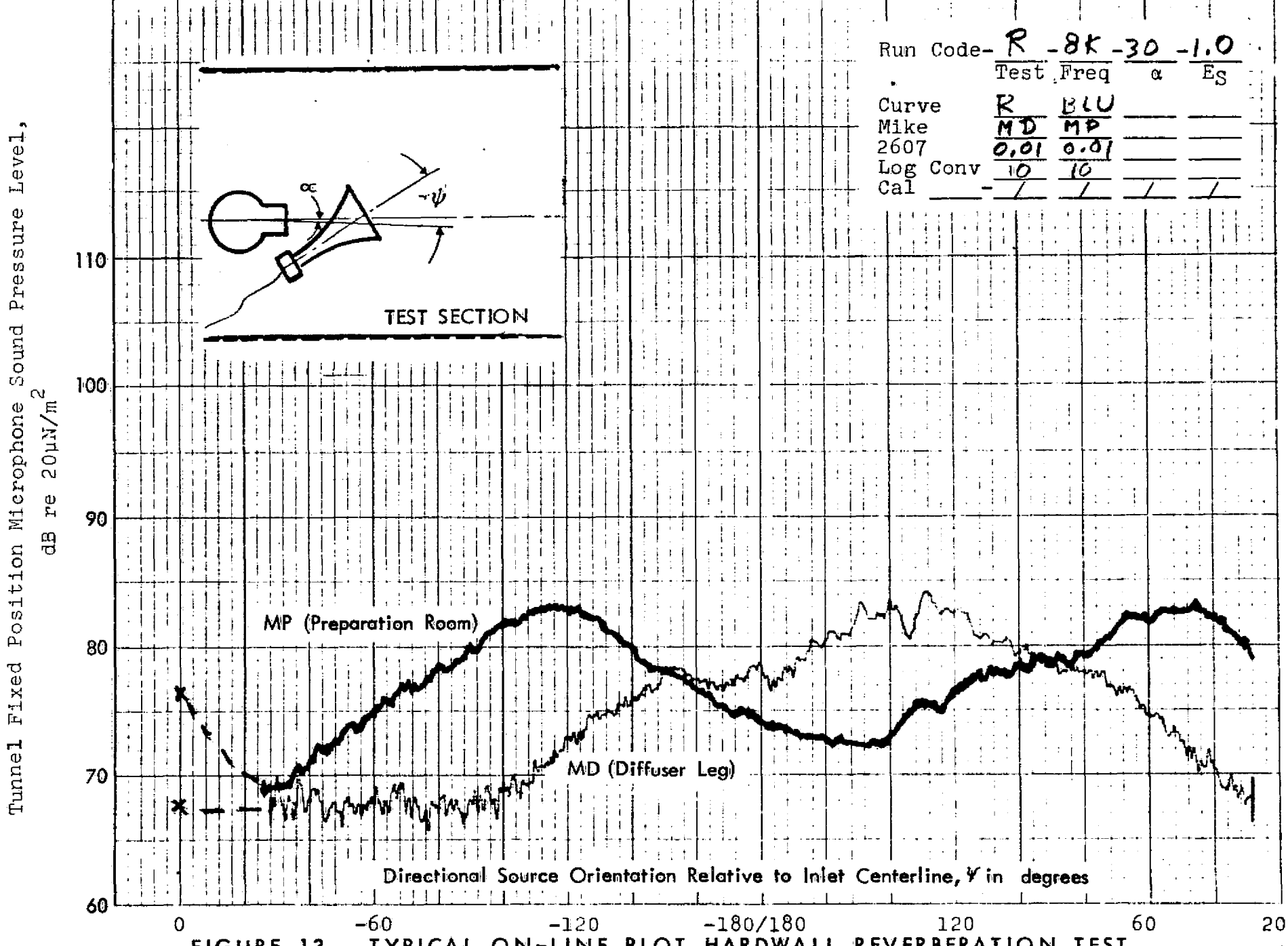

FIGURE 13. TYPICAL ON-LINE PLOT HARDWALL REVERBERATION TEST, DIRECTIONAL SOURCE, PREPARATION ROOM AND DIFFUSER LEG MICROPHONES

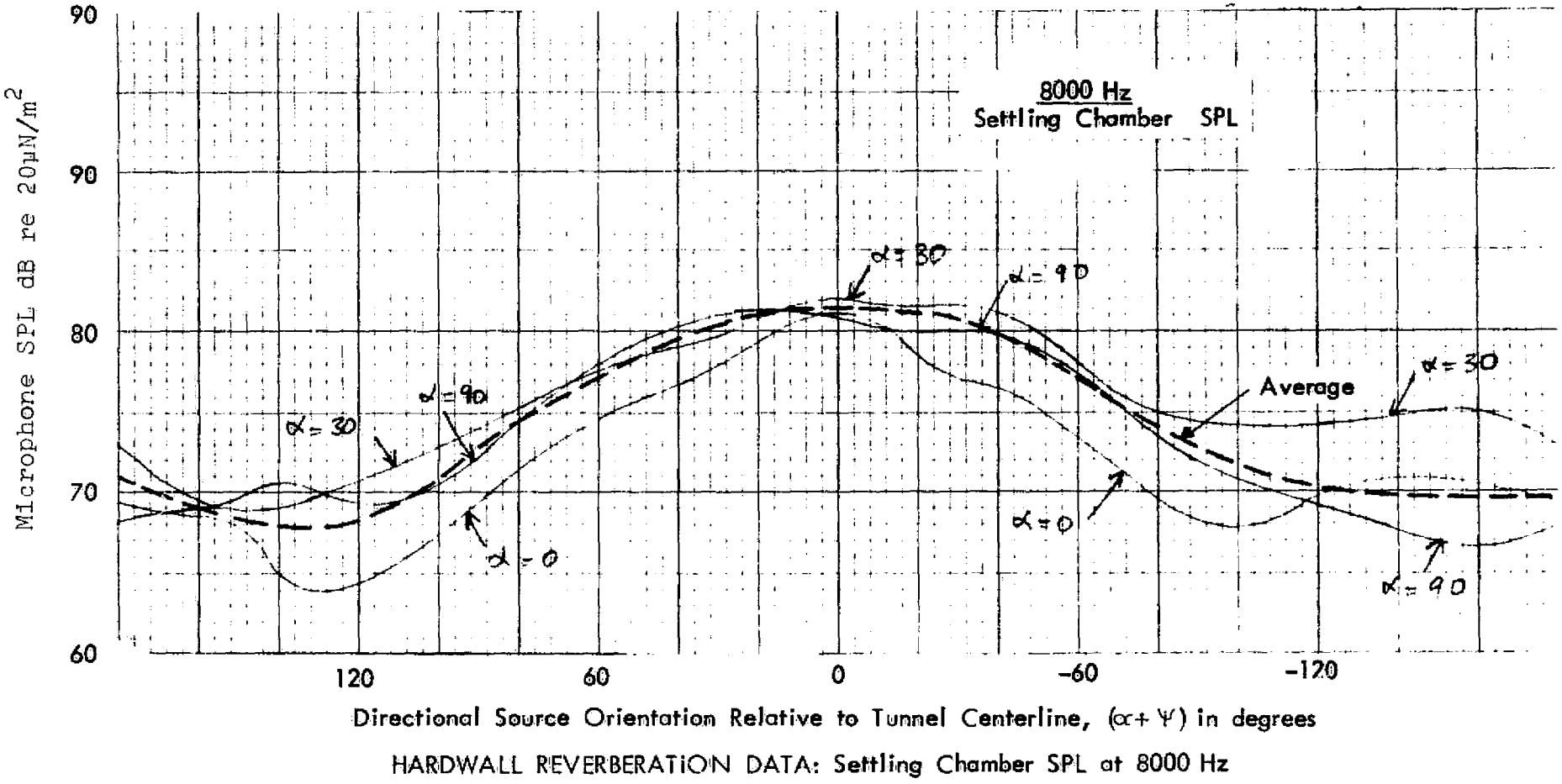

FIGURE 14. TYPICAL REPLOT OF ON-LINE DATA, HARDWALL REVERBERATION WITH DIRECTIONAL SOURCE

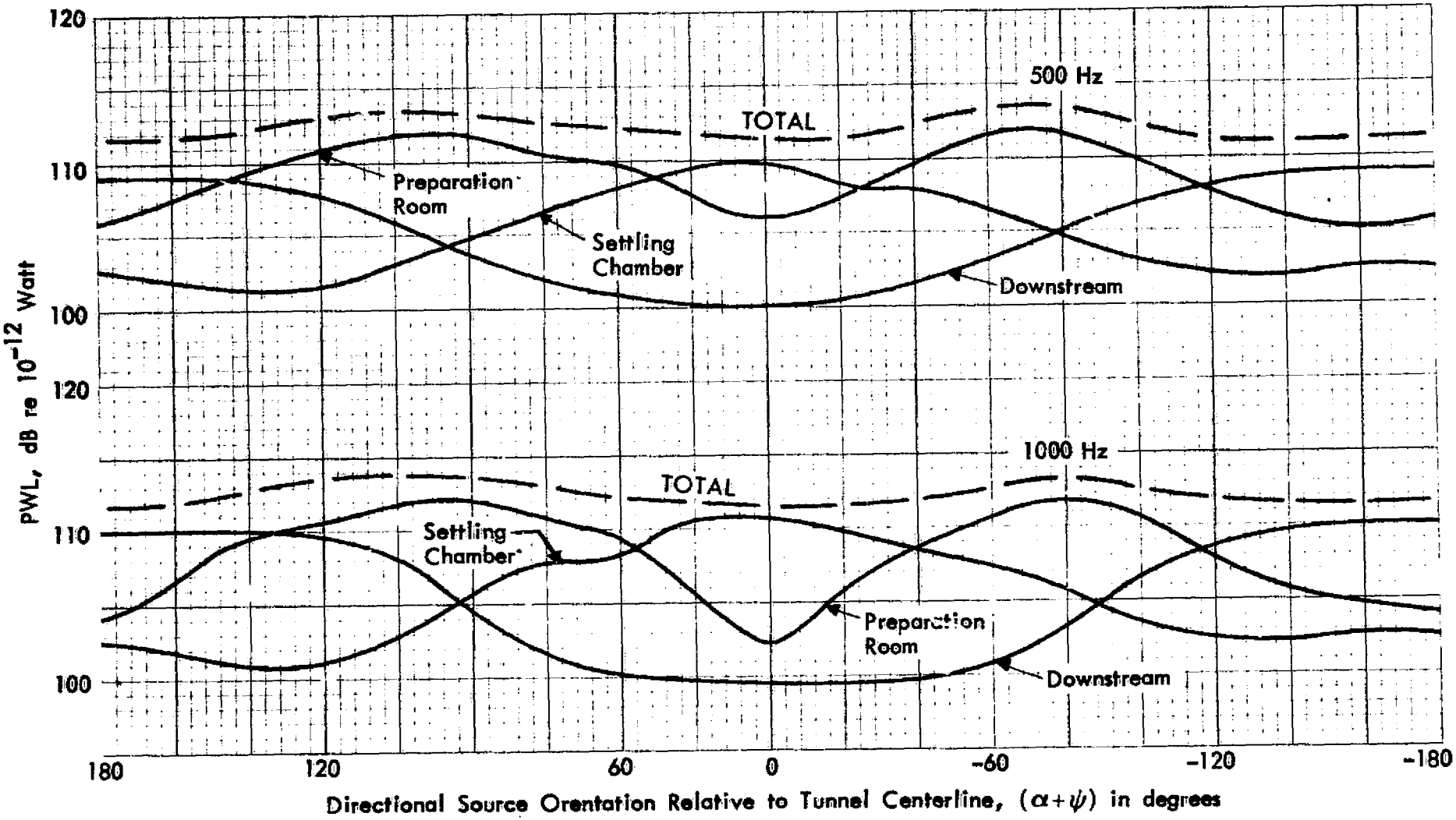

FIGURE 15. INDIVIDUAL CHAMBER AND TOTAL MEASURED SOUND POWER AS A FUNCTION OF DIRECTIONAL SOURCE ANGLE, 500 AND 1000 Hz

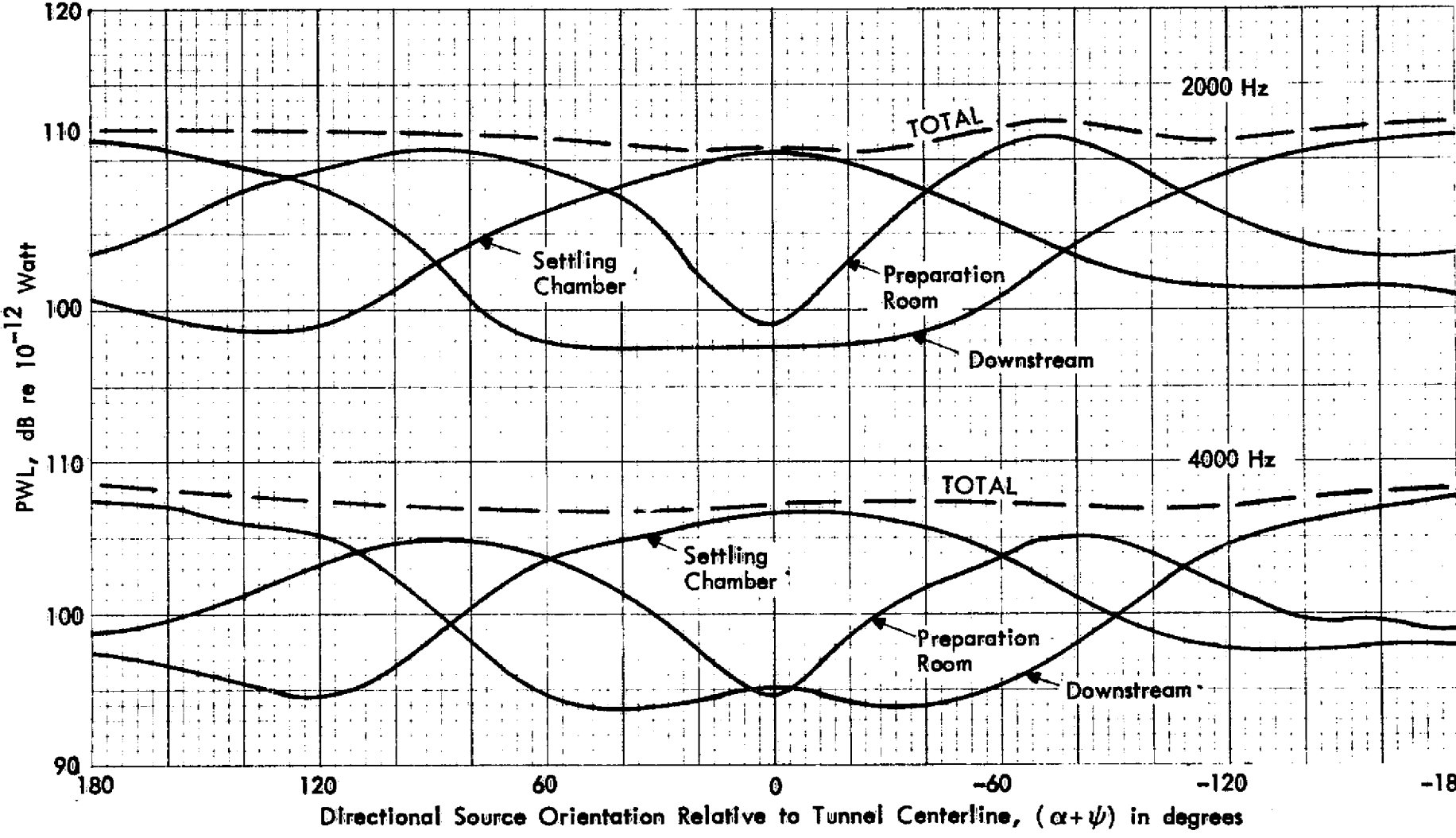

FIGURE 16. INDIVIDUAL CHAMBER AND TOTAL MEASURED SOUND POWER AS A FUNCTION OF DIRECTIONAL SOURCE ANGLE, 2000 and 4000 Hz

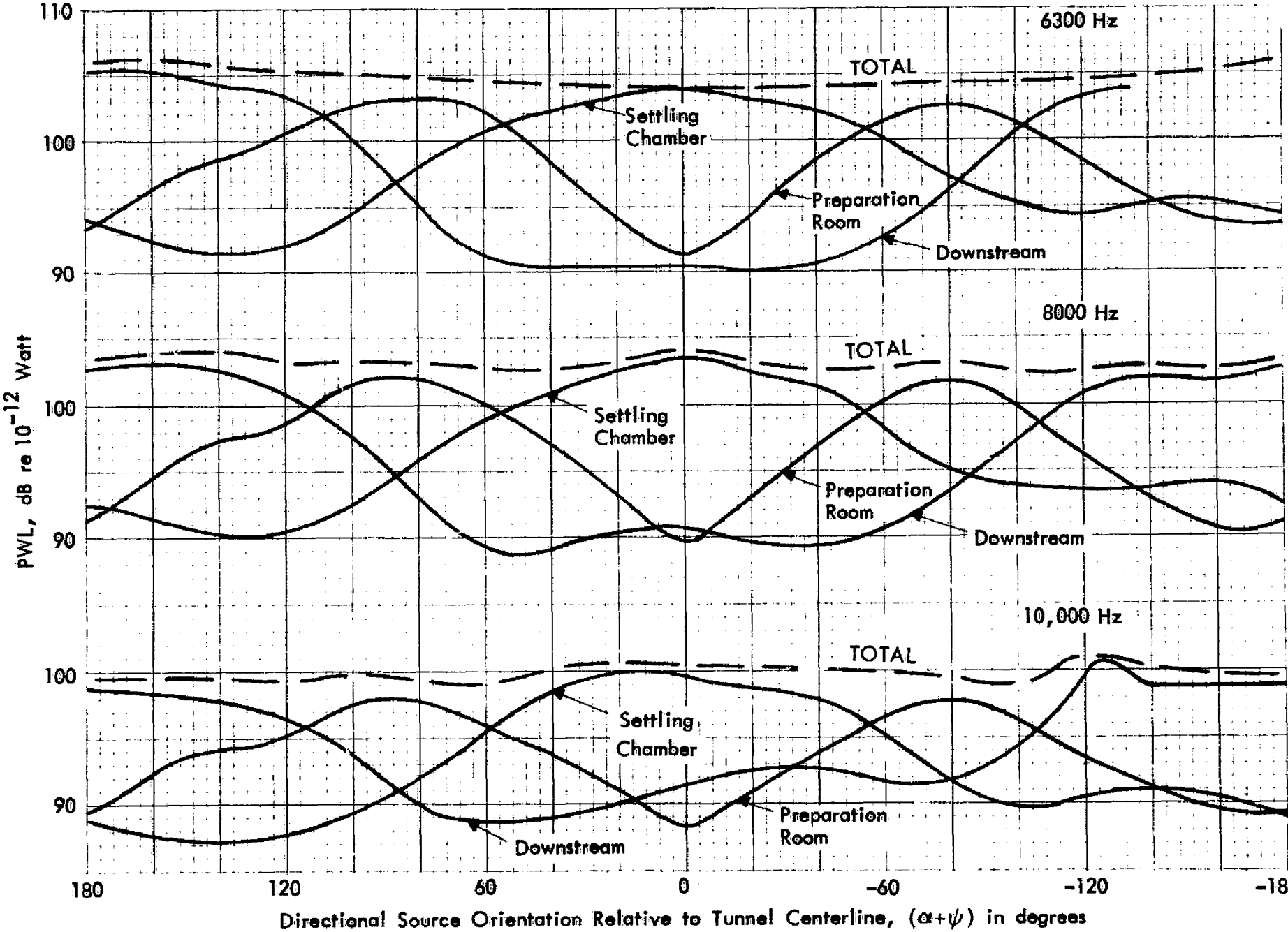

FIGURE 17. INDIVIDUAL CHAMBER AND TOTAL MEASURED SOUND POWER AS A FUNCTION OF DIRECTIONAL SOURCE ANGLE, 6300, 8000 and 10,000 Hz

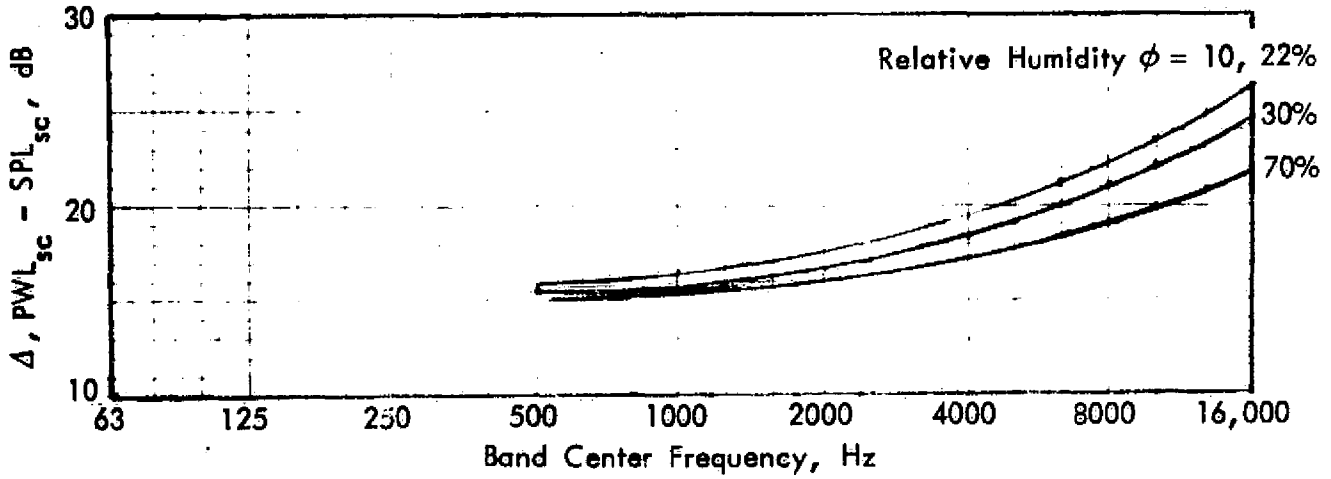

FIGURE 18. SETTLING CHAMBER SOUND POWER CALIBRATION, ALSO USABLE FOR PREPARATION ROOM AND DIFFUSER SECTION

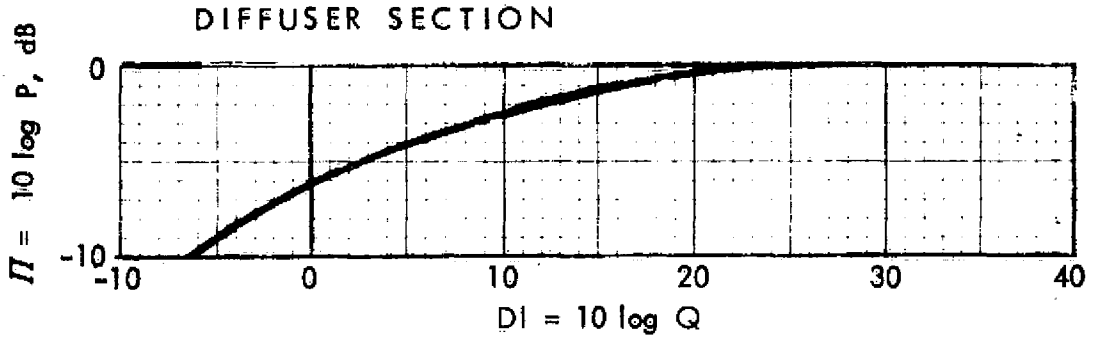

FIGURE 19. APPROXIMATION FOR SOURCE SOUND POWER EXITING TO SETTLING CHAMBER AS A FUNCTION OF SOURCE DIRECTIVITY INDEX, APPLICABLE FOR $(\alpha + \psi) = \pm 60^{\circ}$

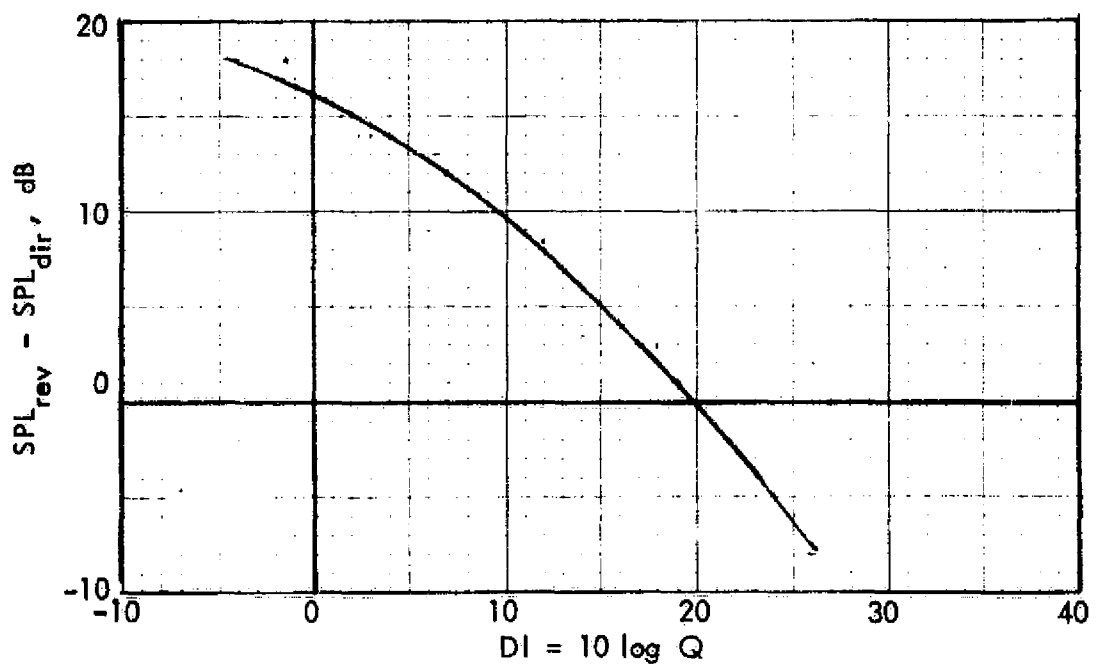

FIGURE 20. APPROXIMATION FOR DIFFERENCE IN SETTLING CHAMBER REVERBERANT AND DIRECT FIELD AS A FUNCTION OF SOURCE DIRECTIVITY INDEX

NASA
C-74-2388

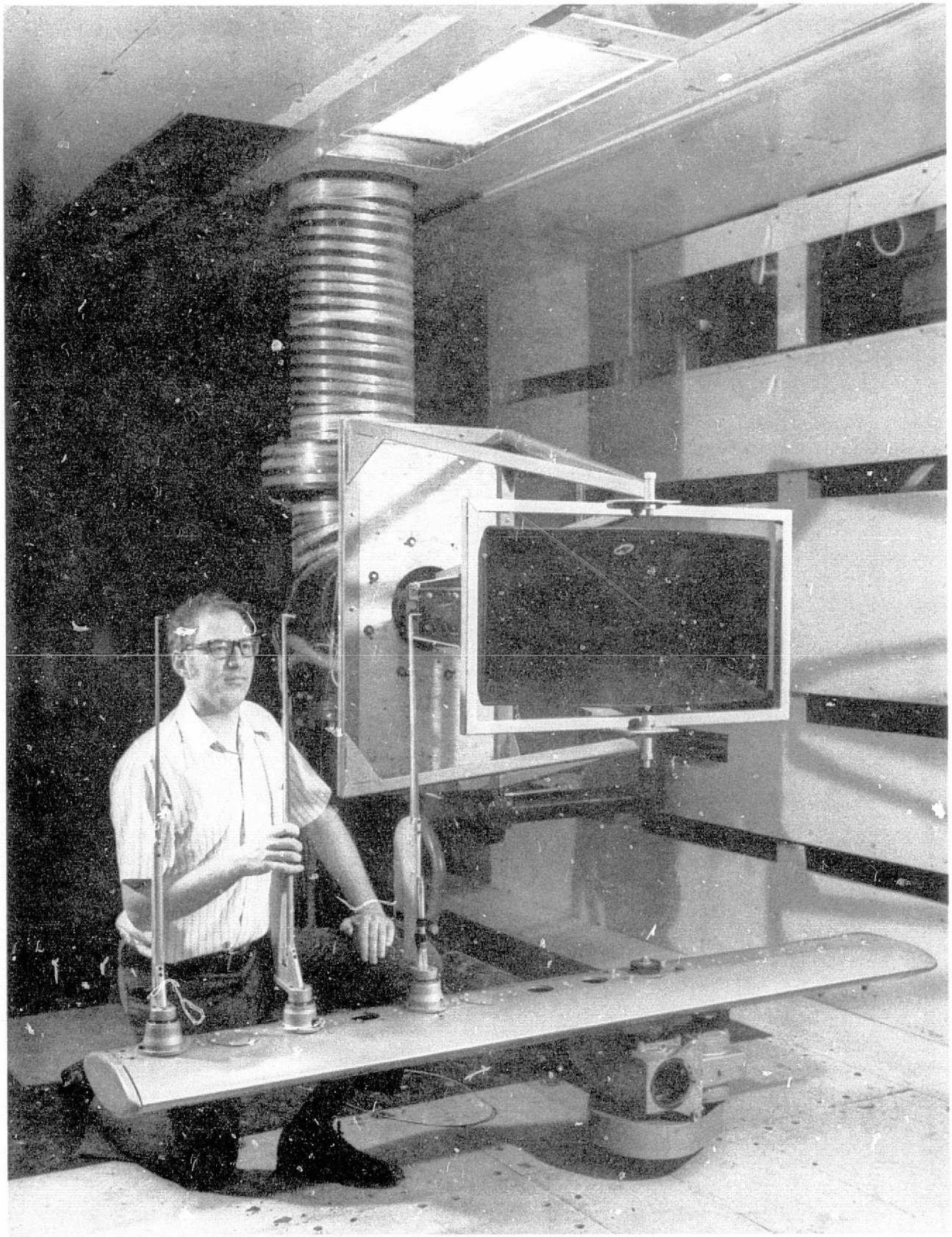

FIGURE 21. DIRECTIONAL SOURCE AND MICROPHONE BOOM WITH MICROPHONES AT 2, 3, AND 4 FOOT POSITIONS

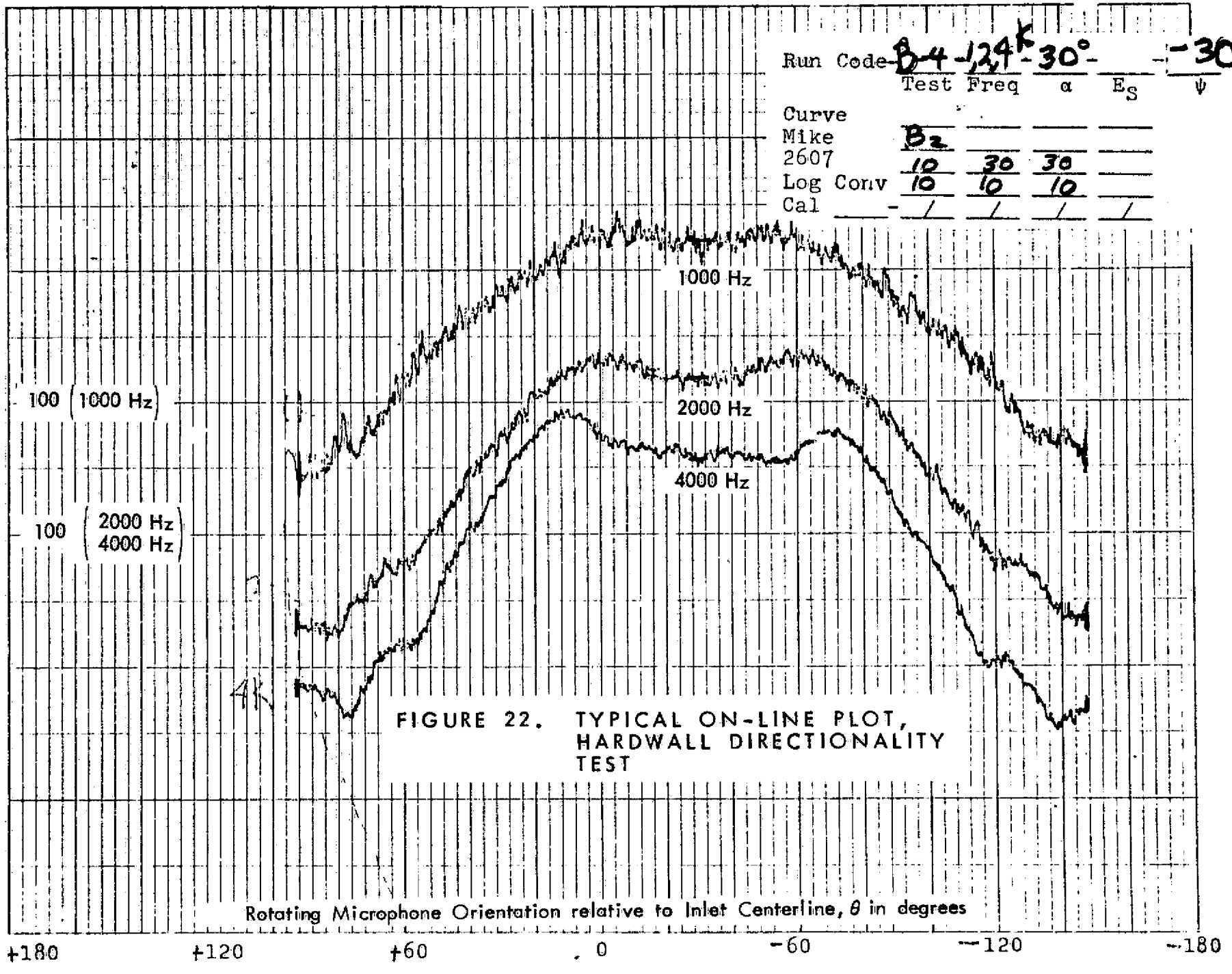

FIGURE 22. TYPICAL ON-LINE PLOT, HARDWALL DIRECTIONALITY TEST

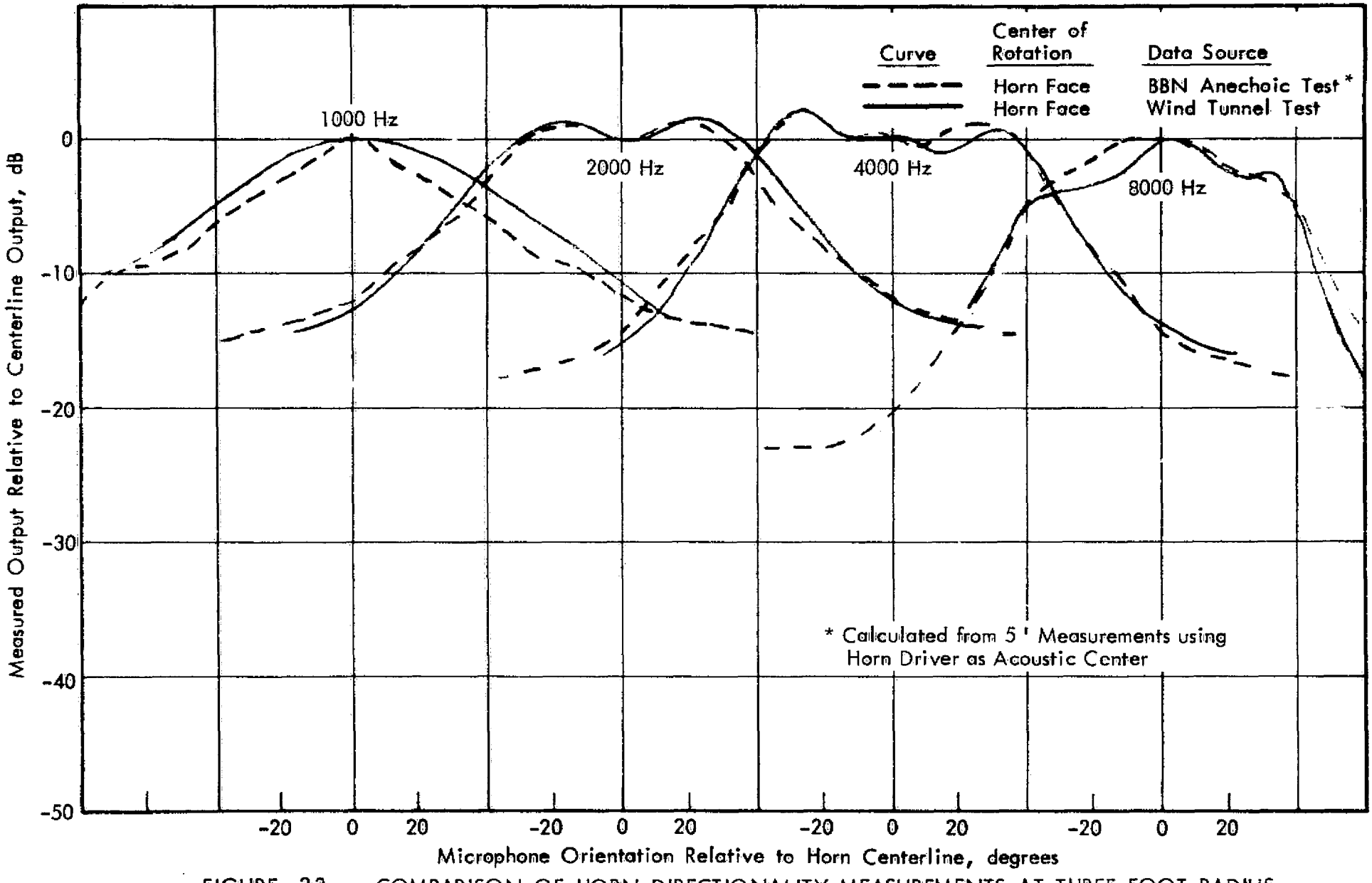

FIGURE 23. COMPARISON OF HORN DIRECTIONALITY MEASUREMENTS AT THREE FOOT RADIUS IN HARDWALL TEST SECTION, ALONG TUNNEL CENTERLINE ($\alpha = \psi = 0$), AND IN ANECHOIC CHAMBER.

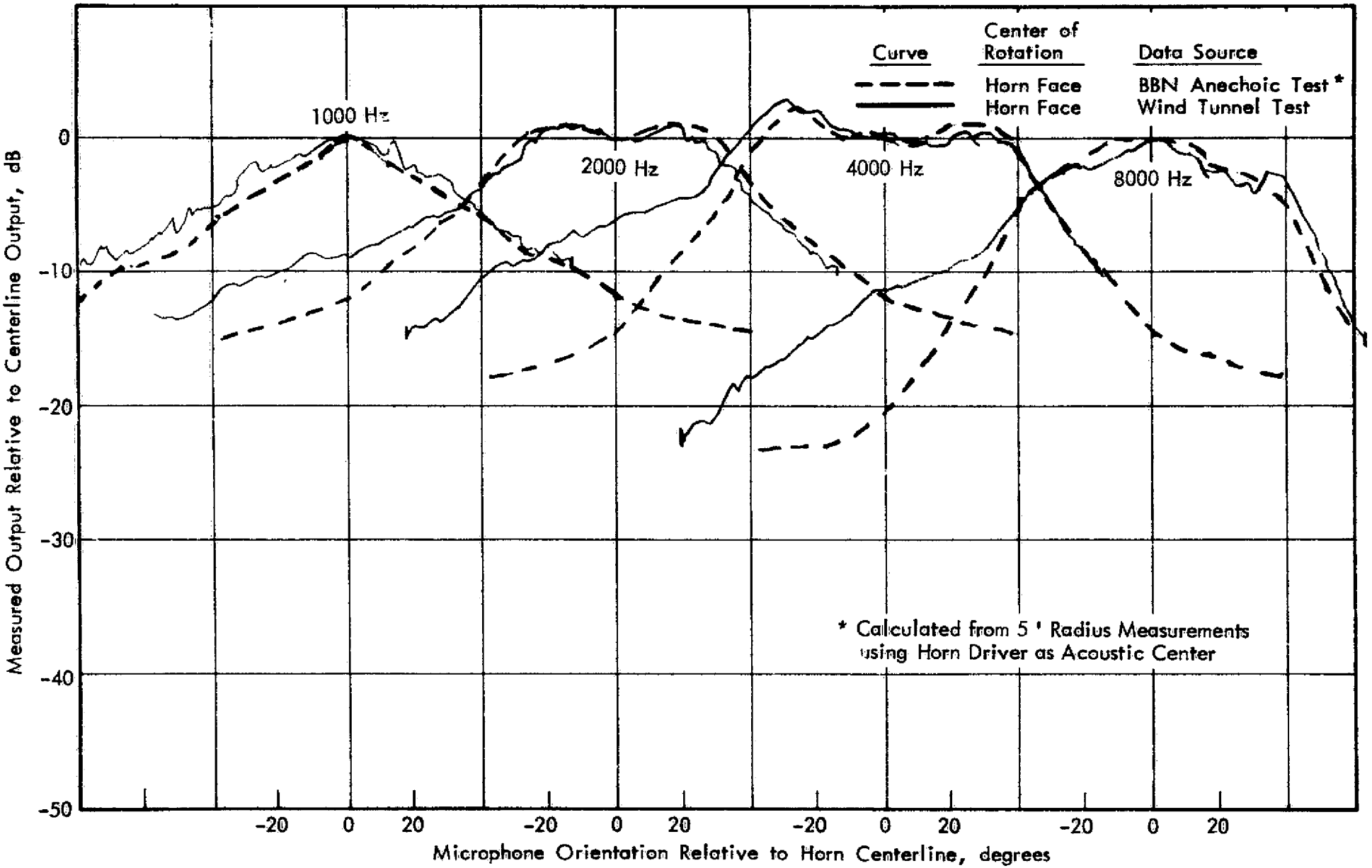

FIGURE 24. COMPARISON OF HORN DIRECTIONALITY MEASUREMENTS AT THREE FOOT RADIUS IN HARDWALL TEST SECTION, ANGLED TOWARDS WALL ($\alpha = 30^{\circ}$, $\psi = -90^{\circ}$), AND IN ANECHOIC CHAMBER.

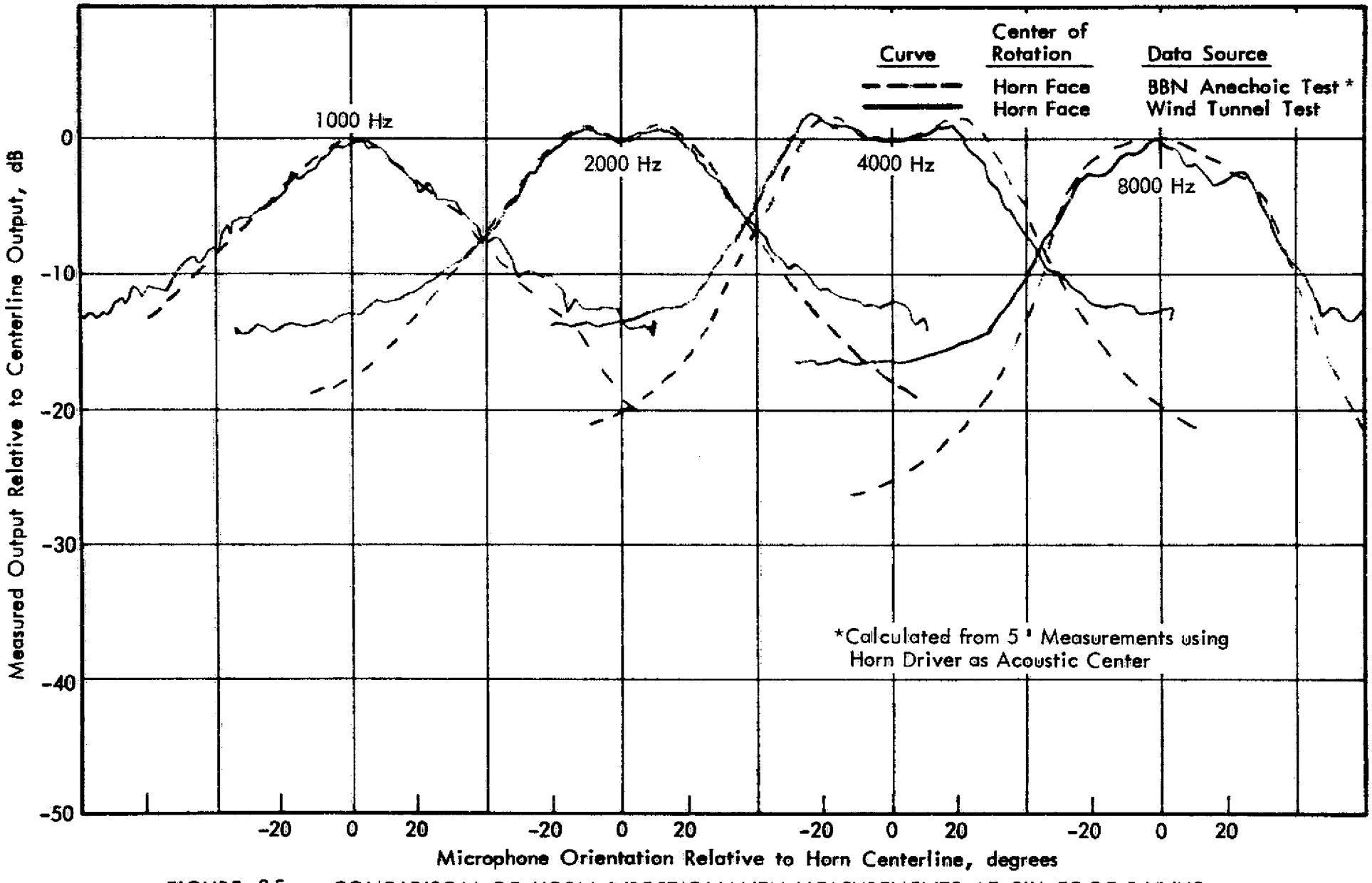

FIGURE 25. COMPARISON OF HORN DIRECTIONALITY MEASUREMENTS AT SIX FOOT RADIUS IN HARDWALL TEST SECTION, ALONG TUNNEL CENTERLINE ($\alpha = 30^{\circ}$, $\psi = -30^{\circ}$), AND IN ANECHOIC CHAMBER.

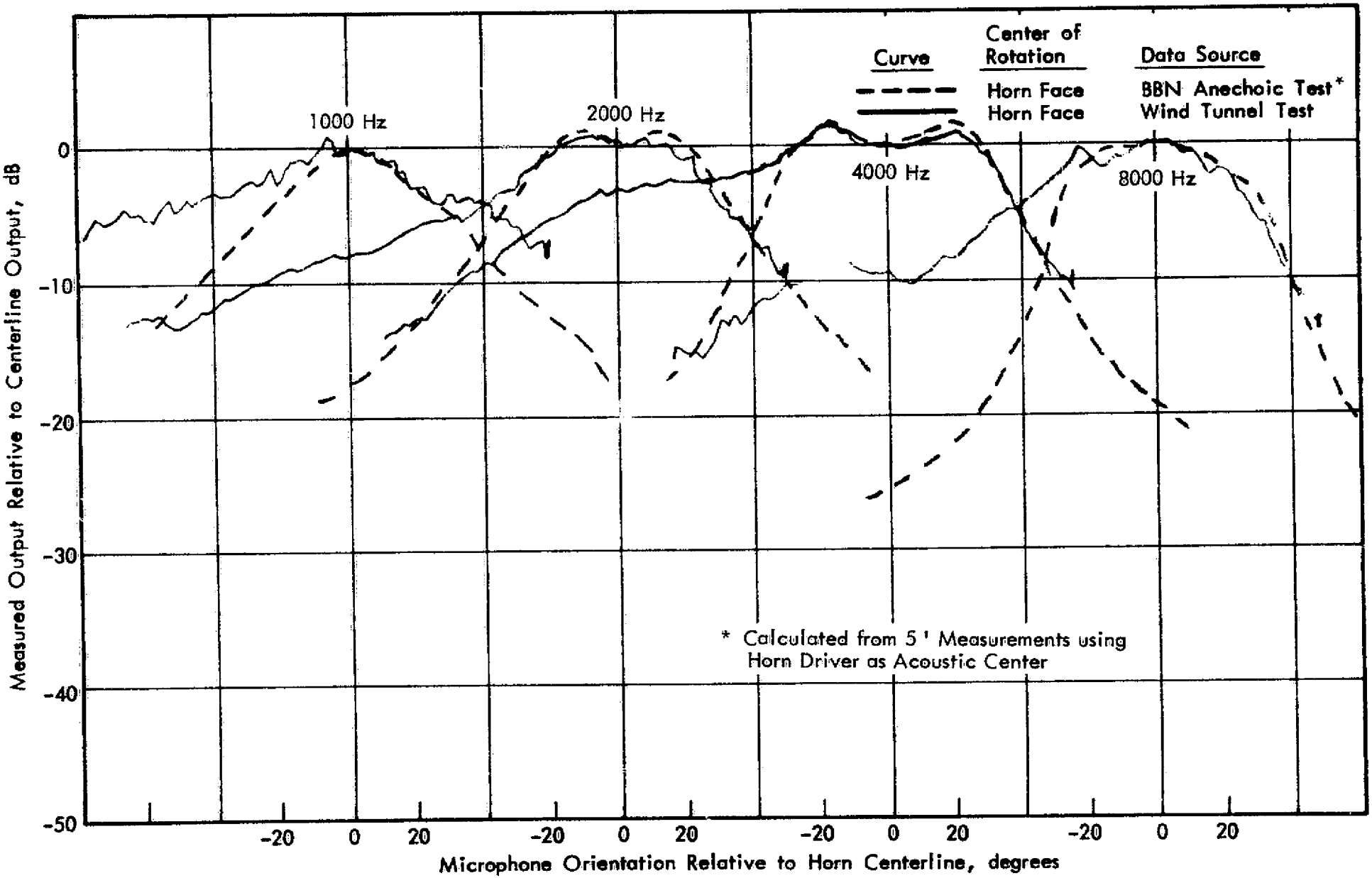

FIGURE 26. COMPARISON OF HORN DIRECTIONALITY MEASUREMENTS AT SIX FOOT RADIUS IN HARDWALL TEST SECTION, ANGLED TOWARDS WALL ($\alpha = 30^{\circ}$, $\psi = -90^{\circ}$), AND IN ANECHOIC CHAMBER.

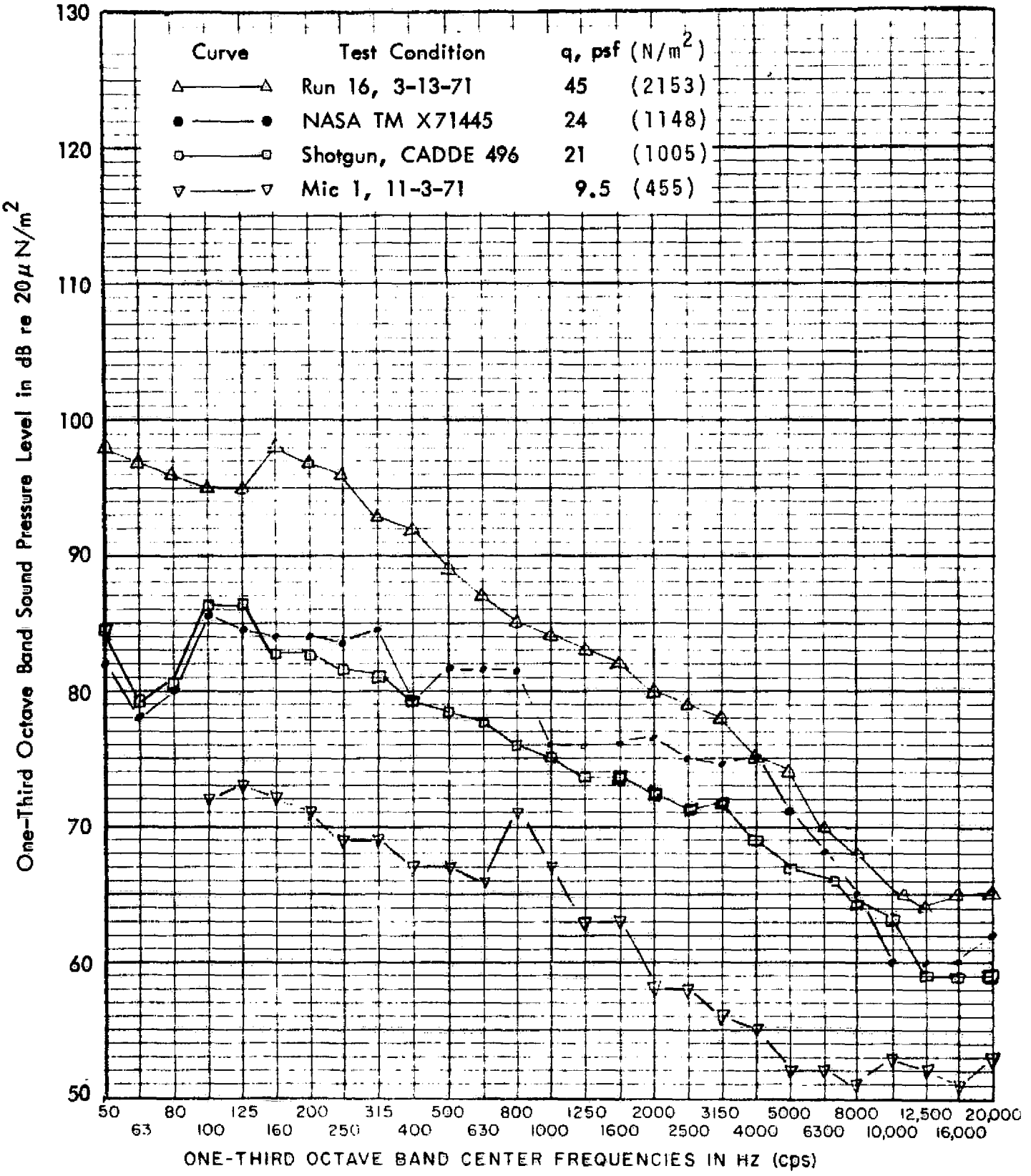

FIGURE 27. SETTLING CHAMBER, WIND-ON, MEASURED ONE-THIRD OCTAVE BAND SOUND PRESSURE LEVELS

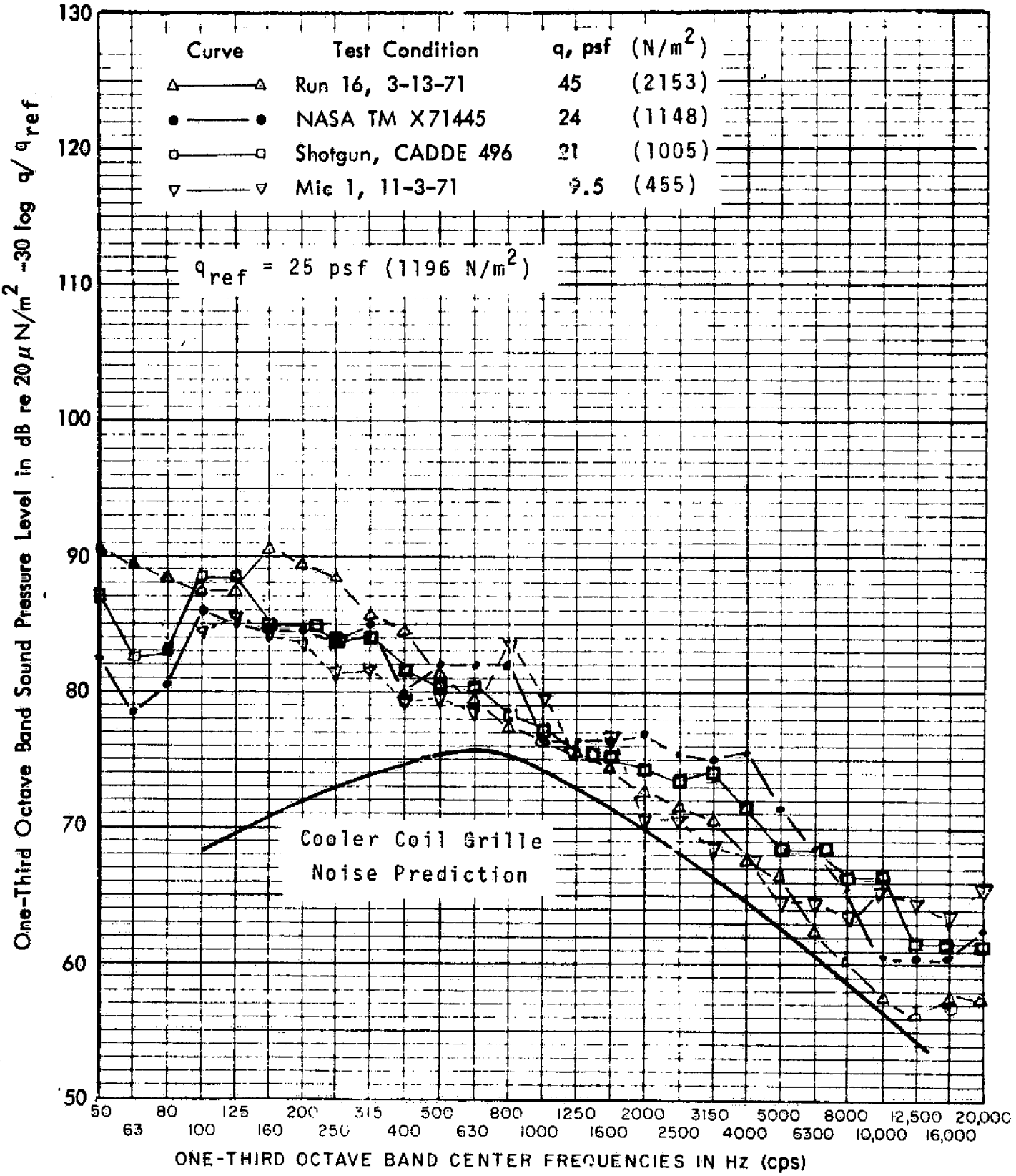

FIGURE 28. NORMALIZED SETTLING CHAMBER, WIND-ON, MEASURED ONE-THIRD OCTAVE BAND SOUND PRESSURE LEVELS

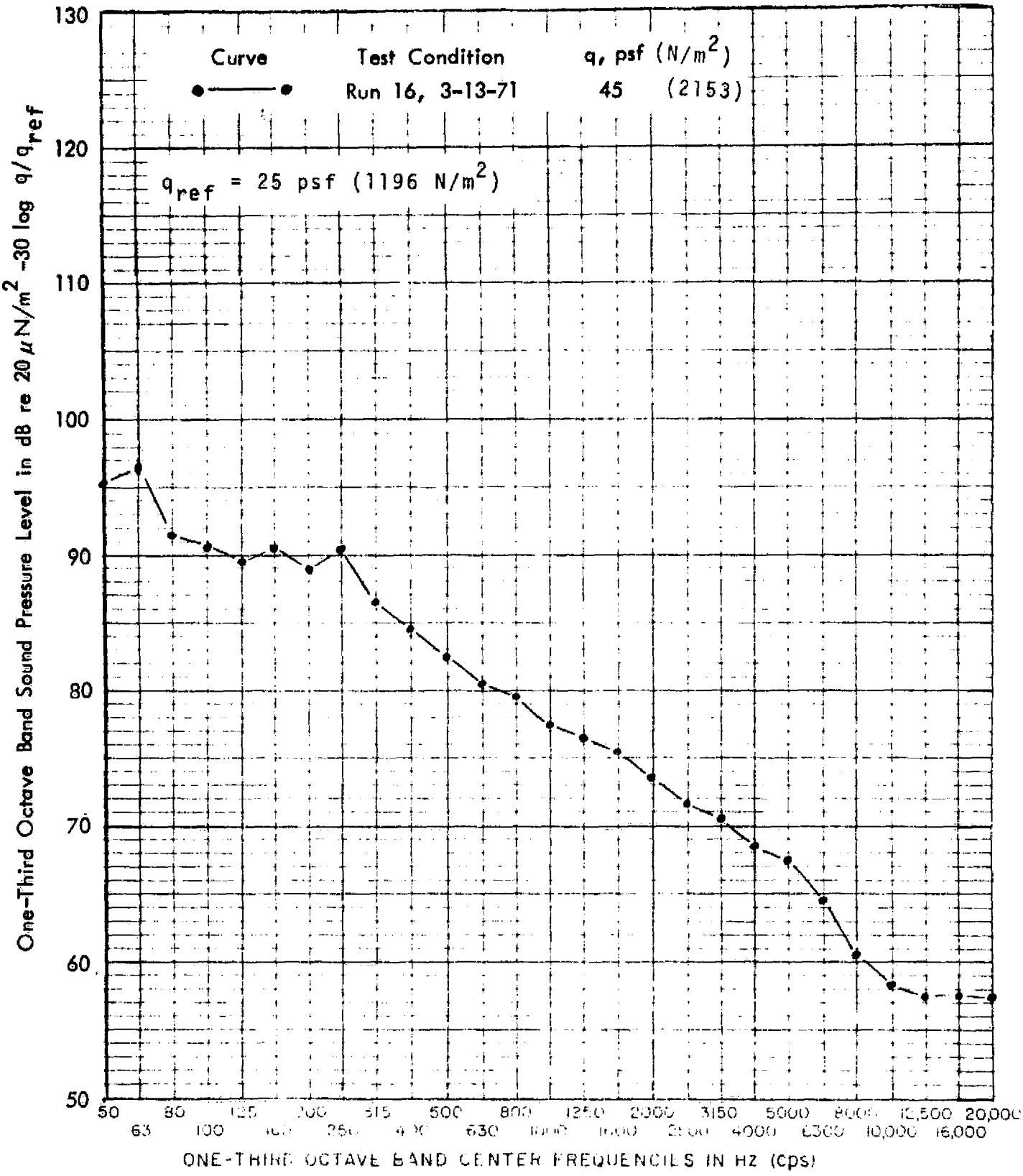

FIGURE 29. NORMALIZED PREPARATION ROOM, WIND-ON, MEASURED ONE-THIRD OCTAVE BAND SOUND PRESSURE LEVELS

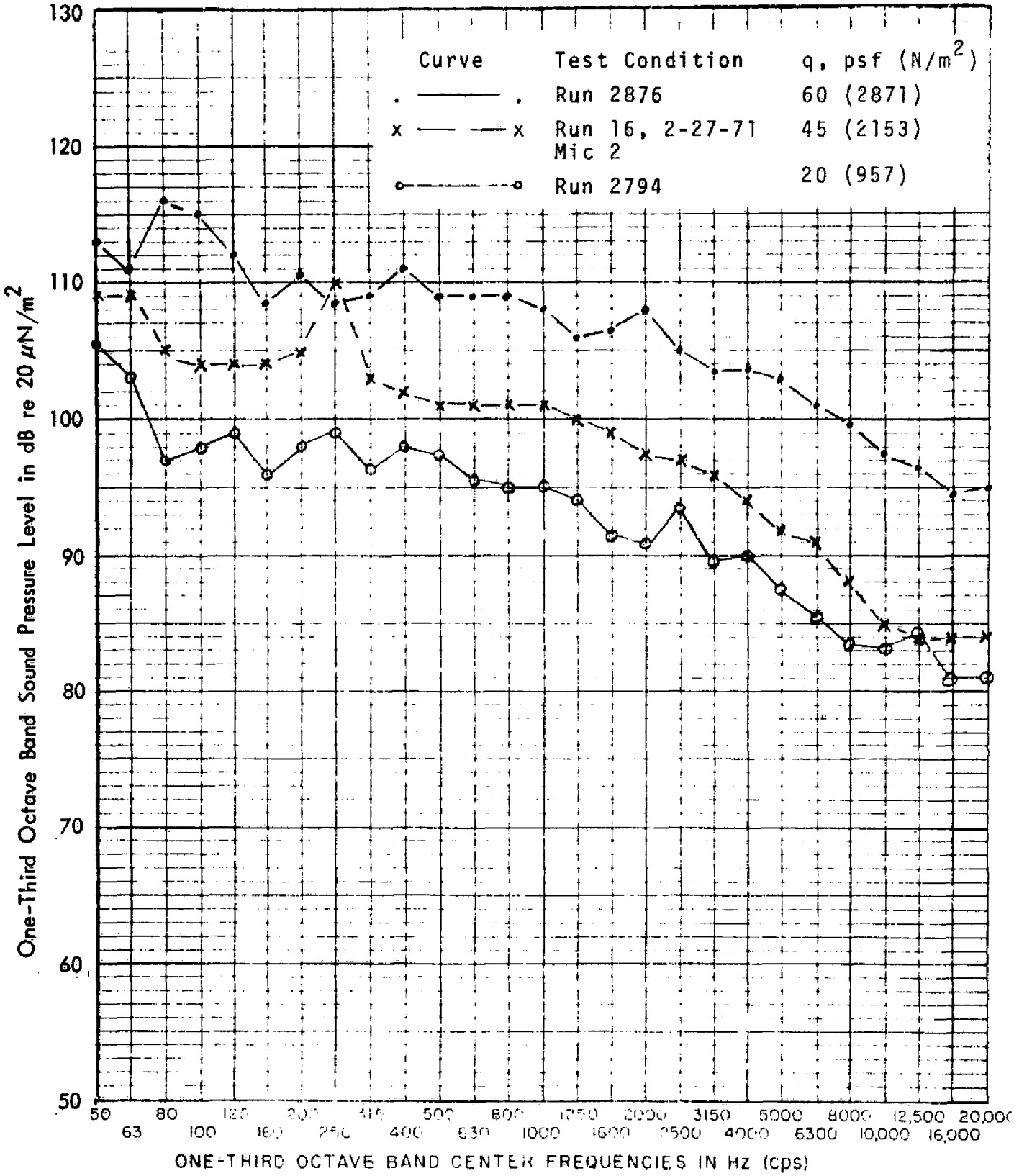

FIGURE 30. TEST SECTION MICROPHONE INDICATED SOUND PRESSURE LEVEL, ONE-QUARTER INCH MICROPHONE WITH NOSE CONE

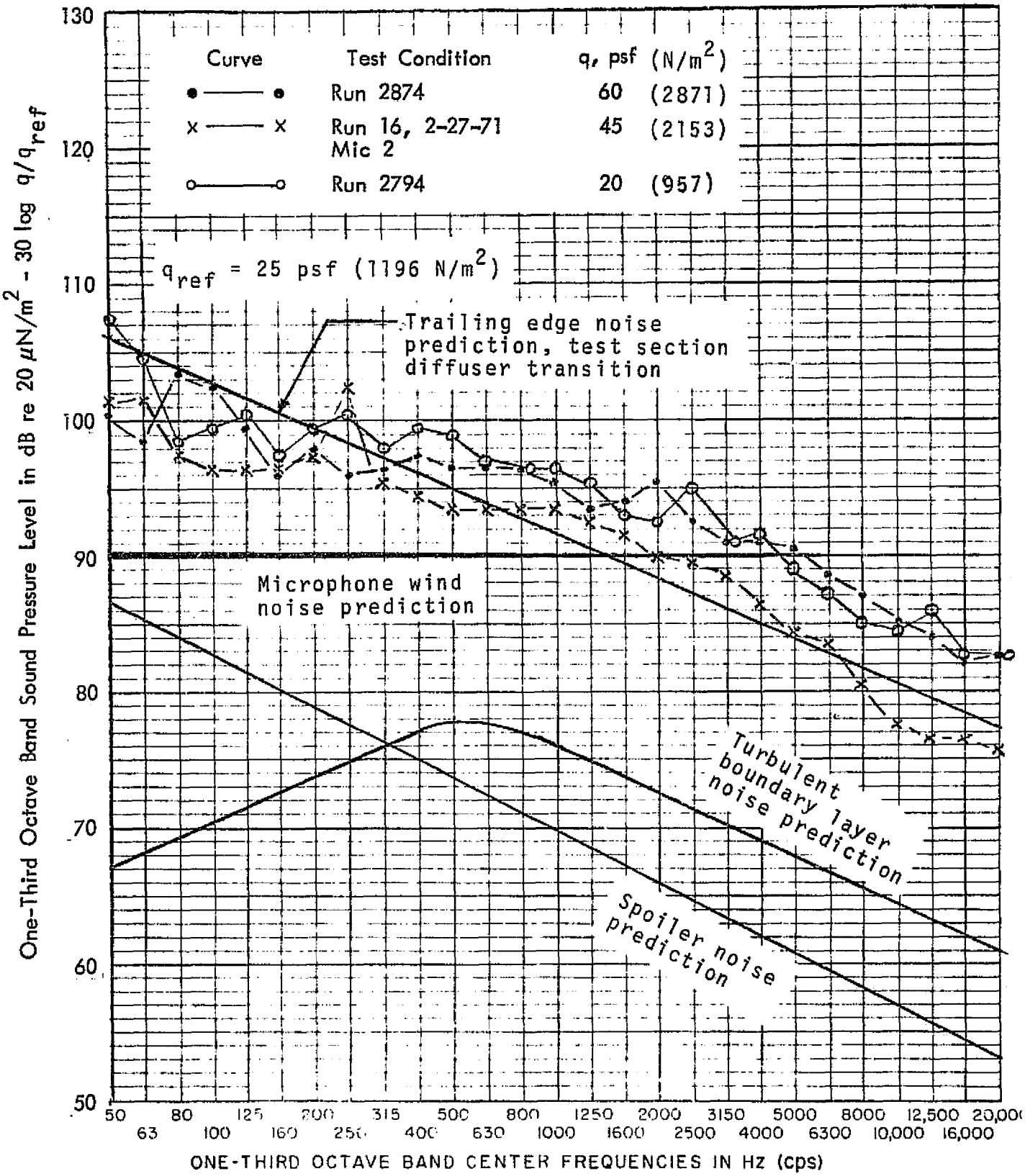

FIGURE 31. NORMALIZED TEST SECTION INDICATED SOUND PRESSURE LEVELS, ONE-QUARTER INCH MICROPHONE WITH NOSE CONE

C-2

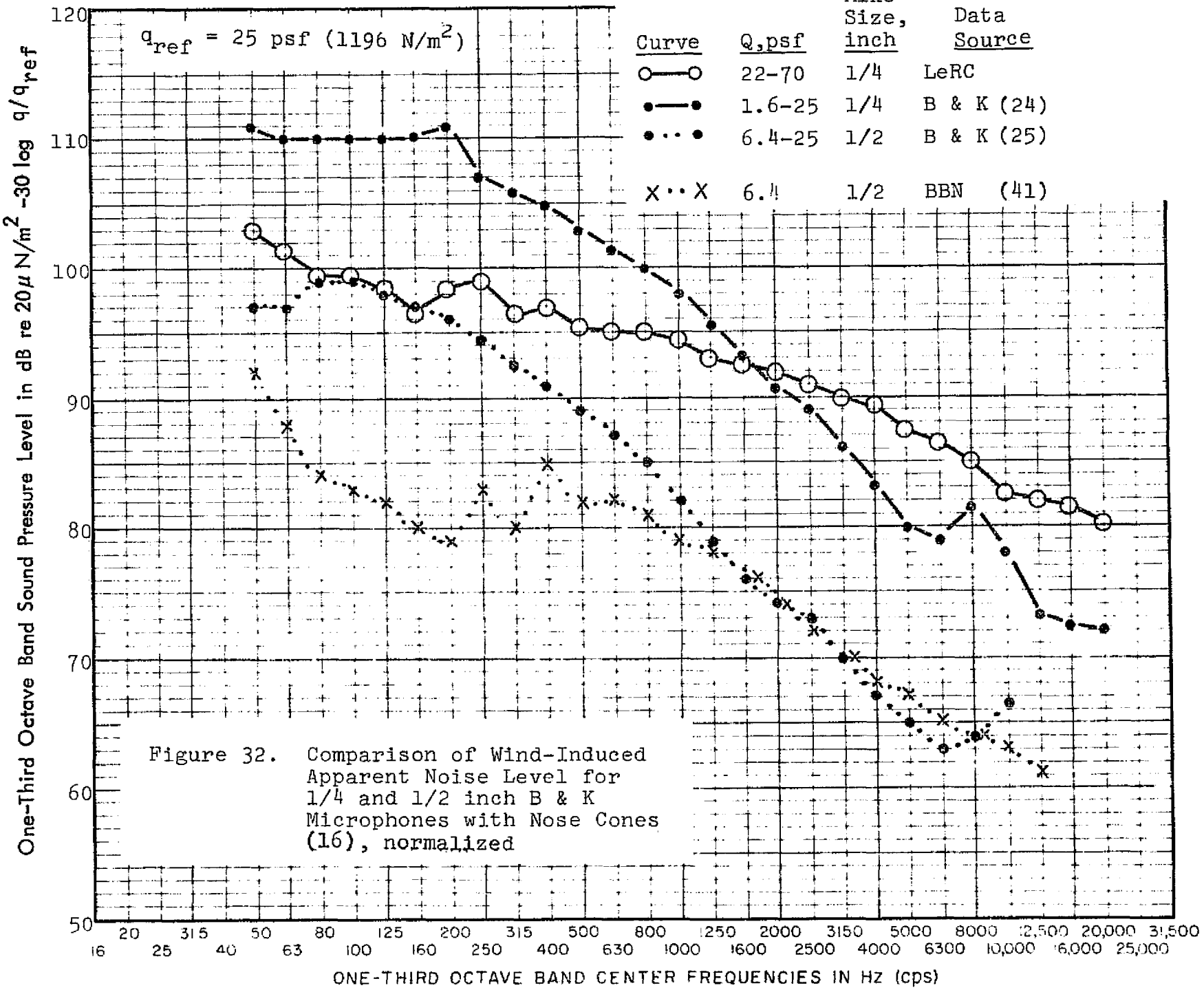

Figure 32. Comparison of Wind-Induced Apparent Noise Level for 1/4 and 1/2 inch B & K Microphones with Nose Cones (16), normalized

BOLT BERANEK & NEWMAN INC

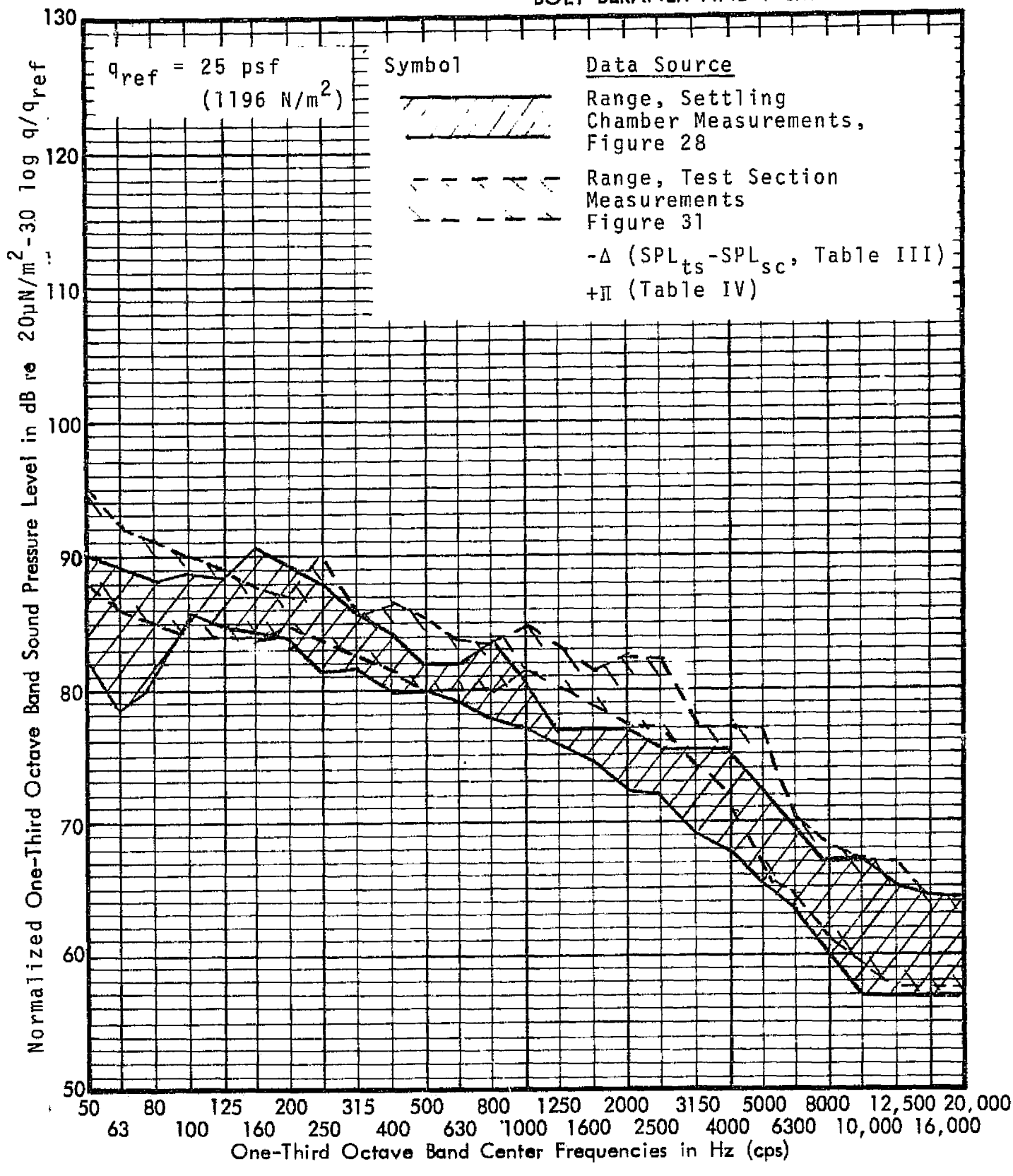

Figure 33. COMPARISON OF NORMALIZED SETTLING CHAMBER WIND-ON MEASURED SOUND PRESSURE LEVELS AND ESTIMATED LEVELS BASED TEST SECTION MICROPHONE MEASUREMENTS.